Eindhoven University of Technology

Master Thesis

Observer-based control for string stable CACC within heterogeneous vehicle platoons

Mechanical Engineering

Dynamics and Control

DC 2020.055

Author:
Max Bolderman, 0895067

Supervisors:
Dr. Ir. Erjen Lefeber
Dr. Ir. Jeroen Ploeg
Prof. dr. Henk Nijmeijer

May 31, 2020

Summary

The ever growing demand for mobility negatively affects road throughput, and thereby increases economical costs. Cooperative Adaptive Cruise Control (CACC) employs wireless inter-vehicle communication in combination with onboard sensors, such as radar and Inertial Measurement Unit (IMU), and thereby achieving string stable vehicle following behaviour at close inter-vehicle distances. String stability concerns the attenuation of signals upstream a platoon of vehicles, and, in combination with short inter-vehicle distances, drastically improves road throughput as well as driver comfort.

Due to the high potential of CACC, a large amount of contributions has been published in literature. One relatively new approach, denoted as a-CACC, proposes to communicate actual acceleration rather than the commonly used desired acceleration, denoted as u-CACC. Doing so eliminates the need for knowledge of the predecessor's dynamical behaviour. Based on this novel approach, this thesis contains the following three contributions.

String stability is known to be an important requirement for a CACC framework, but the design is often performed by means of a trial-and-error process. This raises the desire for a string stability condition which explicitly shows the effect of controller gains, communication delay, and inter-vehicle distance. By re-evaluation of a string stability definition, this thesis presents an elegant sufficient condition for string stability when employing a-CACC.

Secondly, u-CACC has a degraded version, denoted as u-dCACC, to cope with communication impairments. This thesis proposes such a fallback scenario for a-CACC, denoted as a-dCACC. This allows the use of the same controller when communication is compromised, and therefore eliminates the need for tuning another CACC controller.

Some literature proposes the use of observers, but this is predominantly focussed on how to cope with a (temporary) loss of communication. Unavailability of (accurate) onboard measurements therefore remains unstudied. Acceleration measurements, for example, are bound to exhibit a low signal-to-noise ratio when platoons are converging to a constant velocity. Additionally, current CACC controllers require relative velocity, which can not be obtained when using a lidar. To solve this, observer-based CACC is proposed in this thesis. Initially, a general observer-based framework is proposed, which can be used in situations varying from the use of only a low-pass filter on measurements, up until a full-state observer. Afterwards, this general framework is adopted to a special case in which only relative position and global velocity are measured. Afterwards, a stepwise manual tuning procedure is presented.

Finally, the resulting observer-based CACC controller is verified within a complex simulation environment, where it is implemented in discrete time, with sensor signals exhibiting measurement noise, and vehicle actuators experience a delay.

Acknowledgements

Before starting this thesis, I would like to take this opportunity to show my gratitude and appreciation towards my supervisors Erjen Lefeber and Jeroen Ploeg.
Erjen, not only as my supervisor during this graduation project, but also as a teacher for multiple courses (four, specifically), I have learned a lot from you. Your inexhaustible enthusiasm and never-ending knowledge have both motivated and amazed me.
Jeroen, you were both my supervisor as well as my boss at 2GetThere. Your enthusiasm and optimism, even during tough times, have helped me incredible both personal, as well as professional. Not to mention the amusing and often insightful coffee breaks, which were plentiful.
I would also like to thank Henk Nijmeijer for our monthly meetings, in which you always provided a stream of new ideas and possible solutions.
Finally, I would like to thank everyone at 2GetThere for the opportunity to work on this project. The skilled co-workers and pleasant atmosphere definitely contributed to this project.

As the last months of my graduation project consisted of working from home, I also take this opportunity to thank my father Teus, mother Tanja, brother Luuk, and girlfriend Sanne, for the help remaining motivated and creating a pleasant working environment.

Contents

Nomenclature

Abbreviations

ACC	Adaptive Cruise Control
ADAS	Advanced Driver Assistance System
CACC	Cooperative Adaptive Cruise Control
CC	Cruise Control
dCACC	Degraded Cooperative Adaptive Cruise Control
GAS	Global Asymptotic Stability
IMU	Inertial Measurement Unit
ISS	Input-to-State Stability
SSCS	String Stability Complementary Sensitivity

Symbols

A	System matrix
a	Acceleration
B	Input matrix
C	Output matrix
d	Relative position, distance to predecessor
e	Tracking error
Γ	String stability complementary sensitivity
h	Desired inter-vehicle time gap
j	Imaginary unit
L	Observer gains
λ	Eigenvalues
q	Rear bumper position
s	Laplace variable
S_I	Set of all vehicles within a platoon of length I
t	Time
τ	Driveline time constant
θ	Wireless communication delay
u	Desired acceleration
v	Velocity
ξ	a-CACC feedback controller
ζ	u-CACC feedback controller

Miscellaneous

$\mathbb{N}$	Set of all natural numbers
$\mathbb{R}$	Set of all real numbers
$E\{\cdot\}$	Expected value
$\cdot_i$	Vehicle index
$\cdot_a$	Using a-CACC
$\cdot_c$	Using u-CACC
$\cdot_o$	Using observer-based CACC
$\cdot_s$	Using Singer acceleration model
$\cdot_{saf}$	Safety margin
x^T	Transpose of x
$\dot{x}$	Time derivative of x
$\hat{x}$	Estimate of x
$\tilde{x}$	Estimation error of x
$\lvert \cdot \rvert$	Complex magnitude
$\lVert\cdot\rVert_{\mathcal{L}_p}$	Signal-p norm
$\lVert\cdot\rVert_{\mathcal{H}_\infty}$	System-∞ norm

Chapter 1

Introduction

Five different levels of autonomous driving are defined by SAE International [6], ranging from the baseline level 0 for no automation, up until level 5 for a full-time performing automated driving system. To climb the ladder of autonomous driving, different Advanced Driver Assistance Systems (ADAS) have been designed. These ADAS all serve the common goals summarized as: enhance traffic safety, decrease economical costs and environmental pollution, and improve driver comfort [2].

Human failure, such as fatigue, inattention, drowsiness, or intoxication, is estimated to be the cause of 90 percent of all traffic accidents [20]. Direct consequences of these accidents are 1.5 million yearly injuries just in Europe. Bluntly said, this directly costs 70 billion Euro on medical treatment alone, where the cost of the resulting traffic congestions is estimated to be a multiple of this number [2].

For the Paris Agreement [22], parties of the United Nations made an agreement to combat climate change. Greenhouse gas emissions, such as carbondioxide, should be reduced to restrict global temperature rise within a maximum of 2° Celsius. Within the Netherlands, 19 percent of all greenhouse gas emissions are caused by inland mobility [4]. Moreover, traffic congestions are shown to increase these emissions [8].

One specific ADAS, referred to as Cooperative Adaptive Cruise Control (CACC), possesses large potential to increase traffic throughput, and thereby directly cutting economical costs. The main idea and benefits of CACC are explained in Section 1.1, after which current challenges within the field of CACC are appointed in Section 1.2. Based on the stated challenges, the research objectives and contributions of this thesis are introduced in Section 1.3. Finally, Section 1.4 presents the outline of this thesis.

1.1 Cooperative Adaptive Cruise Control

In the year 1950, Ralph Teetor invented a longitudinal vehicle velocity controller [21], which is nowadays commonly referred to as Cruise Control (CC). CC aims to enhance driver comfort by regulating the vehicle velocity towards a desired value.

Its successor, Adaptive Cruise Control (ACC), maintains a desired distance to its predecessor in addition [11]. To do so, ACC uses onboard sensors, such as a radar, to measure relative distance and velocity. Since it is mainly focussed on comfort, safe following behaviour of ACC is achieved only for large inter-vehicle distances [7]. For example, string stability, which is the attenuation of signals in upstream direction within a vehicle platoon, is only achieved for inter-vehicle time gaps larger than 3 s [12]. String unstable following behaviour is often observed for human drivers in the form of phantom traffic jams. An increase in traffic throughput is achieved by string stable following behaviour in combination with short inter-vehicle distances. To achieve shorter inter-vehicle distances, and thereby exploiting the above mentioned benefits, CACC was proposed as a solution by the California Path program [18]. In addition to onboard measurements, CACC employs wireless inter-vehicle communication. In [12], it was shown that CACC could achieve string stability for inter-vehicle time gaps of less than 0.5 s in practical situations.

The design of a CACC controller is often specified by two control objectives. First, the tracking error, defined as the difference between actual and desired inter-vehicle distance, should be Globally Asymptotically Stable (GAS) when the predecessor vehicle follows a constant velocity, i.e., zero acceleration.
The second control objective is string stability, which is elaborated upon in Section 2.2. A commonly used string stability definition is $\mathcal{L}_p$ string stability [16], which basically states that the $\mathcal{L}_p$-norm of a signal must not increase over vehicle index i, see Appendix A.1 for the definitions of norms.
Since string stability does not exclude the possibility of collisions, some literature extends this control objective. For example in [17], where a model-based predictive controller is designed, which guarantees the avoidance of rear end collisions.

1.2 Challenges in CACC

The CACC controller most common in literature uses the wireless communication link to transfer desired acceleration, and is proposed in [14]. Throughout this thesis it is denoted as u-CACC and it is elaborated upon in Section 2.3. By communicating the desired acceleration, u-CACC requires the following vehicle to have information about the dynamical behaviour of the predecessor [10]. These dynamics may include confidential manufacturer information, from which it can be concluded that u-CACC is not directly adoptable to heterogeneous vehicle platoon.
A different approach, denoted as a-CACC, is taken in [10]. With a-CACC, the actual acceleration is communicated, and thereby the necessity to posses knowledge of the dynamical behaviour of the predecessor is eliminated. Therefore, a-CACC is directly adoptable to heterogeneous vehicle platoons as is elaborated upon in Section 2.4.
In situations of wireless communication impairments, [15] proposes degraded CACC (dCACC) as a fallback scenario for u-CACC. With respect to regular ACC, u-dCACC achieves string stability at denser packed platoons [15]. Such a fallback scenario does not yet exist for a-CACC, without requiring the switch to a completely different controller (e.g., u-dCACC).
Another challenge is the design of a CACC controller such that string stability is achieved. A string stability definition, denoted as $\mathcal{L}_p$ string stability, is proposed in [16], and is presented in Section 2.2. Predominantly, string stability is achieved by numerically evaluating the string stability criterion while increasing the inter-vehicle distance. No analytical relation between inter-vehicle distance, communication delay, and controller gains is obtained. Tuning controller gains, aiming for a desired inter-vehicle distance, therefore remains troublesome and non-intuitive. Therefore, an analytical expression, directly stating the effect of controller gains and communication delay on the minimal string stable inter-vehicle distance, is of large

interest.
Finally, observers were used in the CACC controller in for example [15], and [23]. However, observers in these cases were used to cope with a (temporary) loss in inter-vehicle communication, while still assuming perfect full-state onboard measurements. Unavailability of (accurate) measurements could therefore negatively affect current existing CACC frameworks. The acceleration for example, was already stated to experience a rather low signal-to-noise ratio when converging towards a constant velocity. Not to speak of the relative velocity, which is not measured at all when using a lidar.

1.3 Research objectives and contributions

In line with the previously mentioned challenges within the field of CACC, the research objective of this thesis is defined as:

Design an observer-based CACC framework for platoons that are heterogeneous with respect to their driveline dynamics, only requiring measurements of relative position and global velocity, extended with a manual tuning procedure to achieve string stable following behaviour for a predefined inter-vehicle time gap.

To accomplish this research objective, different contributions are contained within this thesis. These are, in order:

1. An analytical sufficient string stability condition for a-CACC, directly stating the effect of controller gains, communication delay, and inter-vehicle time gap.
2. A degraded form of a-CACC, denoted as a-dCACC, as a fallback scenario in the absence of wireless communication.
3. An observer-based CACC control framework. Starting with a general framework, extended with a proposed observer and controller combination only requiring measurements of relative position and global velocity. Afterwards, a manual tuning procedure achieving string stability is presented.

1.4 Outline

Following the research objective and contributions defined above, this thesis is organized as follows: Chapter 2 presents an overview of existing literature within the interest of this thesis. Contributions to a-CACC are presented in Chapter 3. More specifically, a sufficient string stability condition is derived in Section 3.1, and Section 3.2 presents a-dCACC with a comparison to u-dCACC. Based on these results, observer-based CACC is introduced in Chapter 4. The newly derived CACC controllers are verified by means of discrete-time simulations in Chapter 5. Finally, Chapter 6 summarizes the main conclusions and presents some recommendations and directions for further research.

Chapter 2

Literature review

The field of CACC encompasses numerous aspects, some of which are explicitly treated in this project, and others are briefly discussed for completeness. Accordingly, Section 2.1 is basically concerned with CACC in the widest sense, indicating otherwise implicitly made assumptions. Afterwards, a more detailed investigation on important literature used in this thesis is presented. More specifically, string stability is formalized in Section 2.2. Section 2.3 describes u-CACC, followed by a-CACC in Section 2.4. As a fallback scenario for u-CACC in case of communication impairment, u-dCACC is presented in Section 2.5.

2.1 Background

As stated previously, CACC is a longitudinal vehicle controller, aiming to regulate the inter-vehicle distance towards a desired value. The main aspects necessary to accomplish this goal are mentioned in this section.

The longitudinal vehicle model describes the dynamical behaviour of individual vehicles in longitudinal direction. The model used throughout this thesis is a linear, third order model

$$\begin{bmatrix} \dot{q}_i \\ \dot{v}_i \\ \dot{a}_i \end{bmatrix} = \begin{bmatrix} v_i \\ a_i \\ -\frac{1}{\tau_i} a_i + \frac{1}{\tau_i} u_i \end{bmatrix}, \quad i \in S_I, \tag{2.1}$$

with rear bumper position $q_i \in \mathbb{R}$, velocity $v_i \in \mathbb{R}$, and acceleration $a_i \in \mathbb{R}$, of vehicle i. The parameter $\tau_i \in \mathbb{R}^+$ is a time constant describing the, assumed to be, first order driveline dynamics. The vehicle input $u_i \in \mathbb{R}$ can be seen as the desired acceleration. The set $S_I = \{i \in \mathbb{N} \mid 1 \leq i \leq I\}$ contains all vehicles within the platoon of length I. The linear vehicle model (2.1) is sometimes obtained via a feedback linearization of a more general, nonlinear model [9], whereas others identify it by means of measurements in a certain operational area [12],[15]. Different vehicle models used throughout literature are summarized in [25], where differences arise in model order and choice of states.

When all vehicles, including their platoon controllers, within the platoon S_I are identical, it is so-called homogeneous. Heterogeneity in the platoon can have numerous causes, such as differences in vehicle driveline dynamics, maximal achievable acceleration, or platoon controllers. An overview of causes for heterogeneity can be found in [9]. This thesis focusses on vehicle platoons that are heterogeneous with respect to their driveline time constant τ_i.

The communication topology describes the wireless information flow within the platoon. A summary of different topologies is presented in [24]. This thesis follows the majority of literature and employs a predecessor-follower topology, such that information flows from vehicle i to vehicle $i+1$, where the vehicle index increases in upstream direction.

The desired inter-vehicle distance is chosen as the constant time gap policy, such that

$$d_i^r := r_i + h_i v_i, \qquad i \in S_I, \tag{2.2}$$

where $r_i \in \mathbb{R}^+$ is the standstill distance, and $h_i \in \mathbb{R}^+$ the inter-vehicle time gap. Most literature uses the constant time gap policy, as it possesses better string stability properties than the constant distance policy, i.e., $h_i = 0$ [3]. Other choices concerning the formation geometry are summarized in [5].

2.2 $\mathcal{L}_p$ string stability

An intuitive interpretation of string stability is formalized in [16]: *"as opposed to conventional stability notions for dynamical systems, that are basically concerned with the evolution of system states over time, string stability focuses on the propagation of system responses along a cascade of systems."*
Additionally, [16] introduces the $\mathcal{L}_p$ string stability definition. Consider the nonlinear cascaded state-space system

$$\begin{aligned} \dot{x}_0 &= f_r(x_0, u_r), \\ \dot{x}_i &= f_i(x_i, x_{i-1}), \\ y_i &= h_i(x), \quad i \in S_I, \end{aligned} \tag{2.3}$$

representing a general, possibly nonlinear, heterogeneous interconnected system. Here, $u_r \in \mathbb{R}^q$ is the external input, $x_i \in \mathbb{R}^n$, $i \in \{0\} \cup \{S_I\}$, is the state vector, and $y_i \in \mathbb{R}^l$, $i \in S_I$, is the output. Moreover, $f_r : \mathbb{R}^n \times \mathbb{R}^q \mapsto \mathbb{R}^n$, $f_i : \mathbb{R}^n \times \mathbb{R}^n \mapsto \mathbb{R}^n$, $i \in S_I$, and $h_i : \mathbb{R}^{nI} \mapsto \mathbb{R}^l$.

Definition 2.1. *($\mathcal{L}_p$ string stability, [16]) Consider the interconnected system (2.3). Let the lumped state vector be $x = \begin{bmatrix} x_0^T & x_1^T & \dots & x_I^T \end{bmatrix}^T$ and let $x^* = \begin{bmatrix} x_0^{*T} & x_0^{*T} & \dots & x_0^{*T} \end{bmatrix}$ denote the constant equilibrium solution of (2.3) for $u_r = 0$. The system (2.3) is $\mathcal{L}_p$ string stable if there exist class $\mathcal{K}$ functions α and β such that, for any initial state $x(0) \in \mathbb{R}^{(I+1)n}$ and any $u_r \in \mathcal{L}_p^q$*

$$\|y_i(t) - h_i(x^*)\|_{\mathcal{L}_p} \leq \alpha\left(\|u_r(t)\|_{\mathcal{L}_p}\right) + \beta\left(\|x(0) - x^*\|\right), \quad i \in S_I, \text{ and } I \in \mathbb{N}. \tag{2.4}$$

If, in addition, with $x(0) = x^*$, it also holds that

$$\|y_i(t) - h_i(x^*)\|_{\mathcal{L}_p} \leq \|y_{i-1}(t) - h_{i-1}(x^*)\|_{\mathcal{L}_p}, \quad i \in S_I \setminus \{1\}, \text{ and } I \in \mathbb{N}, \tag{2.5}$$

the system (2.3) is strictly $\mathcal{L}_p$ string stable with respect to its input $u_r(t)$.

A special case is when the cascaded system (2.3) is linear

$$\begin{aligned}\dot{x} = \begin{bmatrix}\dot{x}_0\\ \dot{x}_1\\ \vdots\\ \dot{x}_I\end{bmatrix} &= \begin{bmatrix}A_r & & & O\\ A_1 & A_0 & & \\ & \ddots & \ddots & \\ O & & A_1 & A_0\end{bmatrix}\begin{bmatrix}x_0\\ x_1\\ \vdots\\ x_I\end{bmatrix} + \begin{bmatrix}B_r\\ 0\\ \vdots\\ 0\end{bmatrix} u_r =: Ax + Bu_r,\\ y_i = C_i x, &\quad i \in S_I,\end{aligned} \tag{2.6}$$

for which [16] defines $\mathcal{L}_2$ string stability using the frequency domain. After applying the Laplace transformation, the linear cascaded system (2.6) can be rewritten to

$$y_i(s) = P_i(s)u_r(s) + O_i(s)x(0), \quad i \in S_I, \tag{2.7}$$

with $P_i(s) = C_i\,(sI - A)^{-1}\,B$ and $O_i(s) = C_i\,(sI - A)^{-1}$. Assumed is that the pair (C_i, A) is such that unstable (including marginally stable) modes are unobservable by a specific choice of C_i, such that the input-output behaviour is asymptotically stable. With initial condition $x(0) = 0$, it directly follows that

$$y_i(s) = P_i(s)P_{i-1}^{-1}(s)y_{i-1}(s) =: \Gamma_i(s)y_{i-1}(s), \quad i \in S_I, \tag{2.8}$$

where $\Gamma_i(s)$ is the String Stability Complementary Sensitivity (SSCS). Assuming functional controllability of (2.8), essentially $P_{i-1}^{-1}(s)$ exisits, [16] states the following theorem regarding the linear unidirectional cascade of systems (2.6).

Theorem 2.1. *($\mathcal{L}_2$ string stability, [16]) Let* (2.6) *represent a linear unidirectionally interconnected system for which the input-output behaviour is described in* (2.7)*. Assume that the pair (C_i, A) is such that unstable and marginally stable modes are unobservable and that $P_i(s)$ is square and nonsingular, for all $i \in \mathbb{N}$. Then, the system* (2.6) *is $\mathcal{L}_2$ string stable if*

1. *$\|P_1(j\omega)\|_{\mathcal{H}_\infty}$ exists.*
2. *$\|\Gamma_i(j\omega)\|_{\mathcal{H}_\infty} \leq 1, \quad i \in \mathbb{N} \setminus \{1\}$.*

with $\Gamma_i(s)$ as in (2.8)*. Moreover, the system is strictly $\mathcal{L}_2$ string stable if and only if conditions 1. and 2. hold.*

2.3 u-CACC

In [14], u-CACC is introduced and it is used in [12] to develop a CACC framework, after which it was implemented and tested on a homogeneous platoon consisting of Toyota Prius III Executives. The constant time gap distance policy is employed, in combination with the assumption of a homogeneous platoon, such that $\tau_i = \tau \;\; \forall\, i$. Furthermore, the tracking error e_i is defined as the difference between realized d_i and desired d_i^r bumper-to-bumper distance, such that

$$\begin{aligned} e_i :=& d_i - d_i^r,\\ =& q_{i-1} - q_i - L_i - d_i^r, \qquad i \in S_I,\end{aligned} \tag{2.9}$$

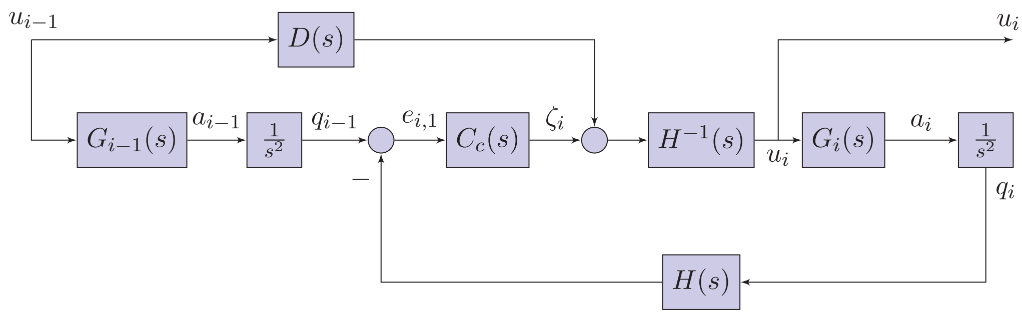

Figure 2.1: Block diagram of u-CACC (2.12) for a possibly heterogeneous vehicle platoon. Here $D(s) := e^{-\theta s}$ is the communication delay, $C_c(s) := k_p + k_d s + k_{dd} s^2$ the controller, $H(s) := hs + 1$ the spacing policy, and $G(s) = \frac{1}{\tau s+1}$ the vehicle model.

with $L_i \in \mathbb{R}^+$ the length of vehicle i. Then, u-CACC uses the tracking error coordinates

$$\begin{aligned} e_{i,1} &:= q_{i-1} - q_i - hv_i, \\ e_{i,2} &:= \dot{e}_{i,1} = v_{i-1} - v_i - ha_i, \\ e_{i,3} &:= \dot{e}_{i,2} = a_{i-1} - \left(1 - \frac{h}{\tau}\right) a_i - \frac{h}{\tau} u_i, \qquad i \in S_I, \end{aligned} \tag{2.10}$$

where $L_i = r = 0$ is taken without loss of generality, i.e., a coordinate transformation. Using the error coordinates (2.10), and longitudinal vehicle model (2.1), gives the uncontrolled dynamics

$$\begin{bmatrix} \dot{e}_{i,1} \\ \dot{e}_{i,2} \\ \dot{e}_{i,3} \end{bmatrix} = \begin{bmatrix} e_{i,2} \\ e_{i,3} \\ -\frac{1}{\tau} e_{i,3} + \frac{1}{\tau} u_{i-1} - \frac{1}{\tau} u_i - \frac{h}{\tau} \dot{u}_i \end{bmatrix}, \qquad i \in S_I. \tag{2.11}$$

Choose the control law

$$\dot{u}_i = -\frac{1}{h} u_i + \frac{1}{h} \underbrace{\begin{bmatrix} k_p & k_d & k_{dd} \end{bmatrix} \begin{bmatrix} e_{i,1} \\ e_{i,2} \\ e_{i,3} \end{bmatrix}}_{=:\zeta_i} + \frac{1}{h} u_{i-1}, \quad i \in S_I, \tag{2.12}$$

where the desired acceleration u_{i-1} is obtained via wireless inter-vehicle communication. Then, the closed loop platoon dynamics are given as

$$\begin{bmatrix} \dot{e}_{i,1} \\ \dot{e}_{i,2} \\ \dot{e}_{i,3} \\ \dot{u}_i \end{bmatrix} = \underbrace{\begin{bmatrix} 0 & 1 & 0 & 0 \\ 0 & 0 & 1 & 0 \\ -\frac{k_p}{\tau} & -\frac{k_d}{\tau} & -\frac{k_{dd}+1}{\tau} & 0 \\ \frac{k_p}{h} & \frac{k_d}{h} & \frac{k_{dd}}{h} & -\frac{1}{h} \end{bmatrix}}_{=:A_u} \begin{bmatrix} e_{i,1} \\ e_{i,2} \\ e_{i,3} \\ u_i \end{bmatrix} + \underbrace{\begin{bmatrix} 0 \\ 0 \\ 0 \\ \frac{1}{h} \end{bmatrix}}_{=:B_u} u_{i-1}, \qquad i \in S_I, \tag{2.13}$$

which is Input-to-State Stable (ISS) with respect to u_{i-1} for $k_p > 0$, $k_{dd} > -1$, and $k_d > \frac{k_p \tau}{1+k_{dd}}$. This approach can be extended to vehicle platoons that are heterogeneous with respect to their drivelines. Then, the error coordinates in which the system is presented are given as

$$\begin{aligned} e_{i,1} &:= q_{i-1} - q_i - hv_i, \\ e_{i,2} &:= v_{i-1} - v_i - ha_i, \\ e_{i,3} &:= a_{i-1} - \left(1 - \frac{h}{\tau_i}\right) a_i - \frac{h}{\tau_i} u_i, \qquad i \in S_I. \end{aligned} \tag{2.14}$$

Using the error coordinates (2.14), and longitudinal vehicle model (2.1), gives the uncontrolled dynamics

$$\begin{bmatrix} \dot{e}_{i,1} \\ \dot{e}_{i,2} \\ \dot{e}_{i,3} \end{bmatrix} = \begin{bmatrix} e_{i,2} \\ e_{i,3} \\ -\frac{1}{\tau_{i-1}} \left(a_{i-1} - u_{i-1}\right) + \frac{1}{\tau_i} \left(1 - \frac{h}{\tau_i}\right) \left(a_i - u_i\right)) - \frac{h}{\tau_i} \dot{u}_i \end{bmatrix}, \qquad i \in S_I. \tag{2.15}$$

To obtain closed loop dynamics similar to the homogeneous setting, choose the controller

$$\dot{u}_i = -\frac{1}{h} u_i + \underbrace{\frac{1}{h} \begin{bmatrix} k_p & k_d & k_{dd} \end{bmatrix} \begin{bmatrix} e_{i,1} \\ e_{i,2} \\ e_{i,3} \end{bmatrix}}_{=:\zeta_i} + \frac{1}{h} \left(1 - \frac{\tau_i}{\tau_{i-1}}\right) a_{i-1} + \frac{1}{h} \frac{\tau_i}{\tau_{i-1}} u_{i-1}, \qquad i \in S_I, \tag{2.16}$$

which gives the closed loop dynamics

$$\begin{bmatrix} \dot{e}_{i,1} \\ \dot{e}_{i,2} \\ \dot{e}_{i,3} \\ \dot{u}_i \end{bmatrix} = \begin{bmatrix} 0 & 1 & 0 & 0 \\ 0 & 0 & 1 & 0 \\ -\frac{k_p}{\tau_i} & -\frac{k_d}{\tau_i} & -\frac{k_{dd}+1}{\tau_i} & 0 \\ \frac{k_p}{h} & \frac{k_d}{h} & \frac{k_{dd}}{h} & -\frac{1}{h} \end{bmatrix} \begin{bmatrix} e_{i,1} \\ e_{i,2} \\ e_{i,3} \\ u_i \end{bmatrix} + \begin{bmatrix} 0 & 0 \\ 0 & 0 \\ 0 & 0 \\ \frac{1}{h}\left(1 - \frac{\tau_i}{\tau_{i-1}}\right) & \frac{1}{h}\frac{\tau_i}{\tau_{i-1}} \end{bmatrix} \begin{bmatrix} a_{i-1} \\ u_{i-1} \end{bmatrix}, \qquad i \in S_I. \tag{2.17}$$

The heterogeneous controller (2.16) clearly depends on the driveline time constant of the predecessor τ_{i-1}. This immediately raises the question whether τ_{i-1} can be used in the controller, since this parameter may contain classified information describing the predecessor vehicle driveline. Furthermore, the platoon can comprise different vehicles in different orders, causing varying τ_{i-1} in different situations. Another implication of the heterogeneous controller (2.16) is the need to communicate both a_{i-1} and u_{i-1}. Appendix B derives a controller that only requires u_{i-1} to be communicated. This is based on the idea that u_i is chosen such that $e_{i,3}$ follows dynamics $\dot{e}_{i,3} = -\frac{1}{\tau_{i-1}} e_{i,3} - \frac{1}{\tau_{i-1}} \zeta_i$ rather than $\dot{e}_{i,3} = -\frac{1}{\tau_i} e_{i,3} - \frac{1}{\tau_i} \zeta_i$, which was achieved using controller (2.16).
The block diagram in Figure 2.1 visualizes u-CACC (2.12) for a heterogeneous vehicle platoon. Here, $D(s) := e^{-\theta s}$ is added as a communication delay of $\theta \in \mathbb{R}^+$, $C_c(s) := k_p + k_d s + k_{dd} s^2$ is the controller, $H(s) := hs + 1$ is the spacing policy with time gap $h \in \mathbb{R}^+$, and $G_i(s) := \frac{1}{\tau_i s + 1}$ is the vehicle model. From the block diagram it is possible to compute the SSCS

$$\Gamma_u^{\mathrm{CACC}}(s) := \frac{a_i(s)}{a_{i-1}(s)} = \frac{1}{H(s)} \frac{G_i(s)}{G_{i-1}(s)} \frac{D(s)s^2 + G_{i-1}(s) C_c(s)}{s^2 + G_i(s) C_c(s)}. \tag{2.18}$$

Basic simulation results of u-CACC, as visualized in the block diagram of Figure 2.1, for a homogeneous platoon of length $I = 6$, are shown in Figure 2.2. This basic simulation uses

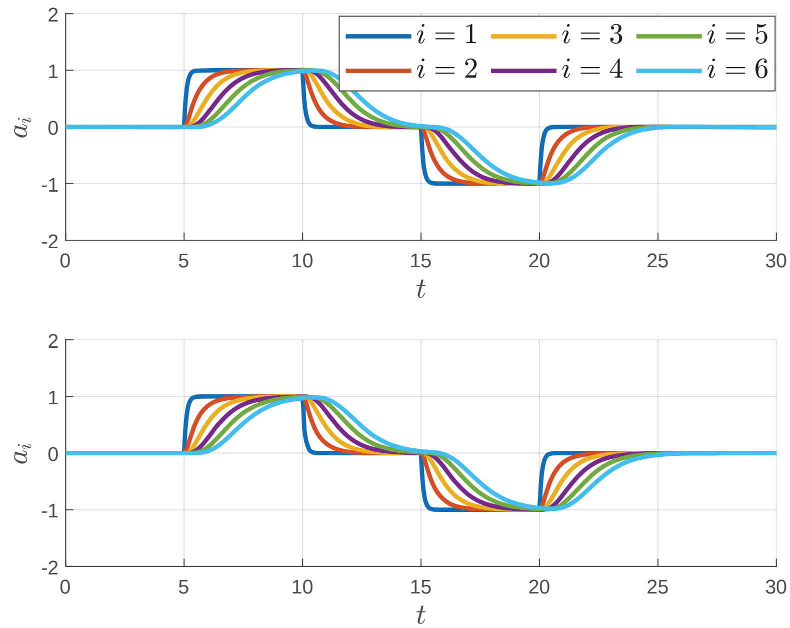

Figure 2.2: Basic simulation results showing acceleration a_i over time t for a platoon of $I = 6$ vehicles employing u-CACC (top) and a-CACC (bottom), using $k_p = 0.2$, $k_d = 0.7$, $k_{dd} = 0$, $\tau = 0.1\ s$, $h = 0.5\ s$, $\theta = 0.02\ s$, and input $u_1(t)$ given in (2.19).

the parameters $k_p = 0.2$, $k_d = 0.7$, $k_{dd} = 0$, $\tau = 0.1\ s$, $\theta = 0.02\ s$, $h = 0.5\ s$, and input

$$u_1(t) = \begin{cases} 1, & \text{if} \quad 5 \leq t \leq 10, \\ -1, & \text{if} \quad 15 \leq t \leq 20, \\ 0, & \text{else}. \end{cases} \tag{2.19}$$

The controller gains are tuned for minimal settling time while minimizing jerk, based on practical experiments [14]. This basic simulation forms the basis for the verification of u-CACC in the complex simulations presented in Chapter 5.

2.4 a-CACC

Recently, a-CACC is proposed in [10]. It starts by defining the error coordinates

$$\begin{aligned} e_{i,1} &:= q_{i-1} - q_i - hv_i, \\ e_{i,2} &:= \dot{e}_{i,1} = v_{i-1} - v_i - ha_i, \\ \varepsilon_i &:= v_{i-1} - v_i, \quad i \in S_I. \end{aligned} \tag{2.20}$$

Choose the control law

$$u_i = \frac{\tau_i}{h} \underbrace{\begin{bmatrix} k_p & k_d \end{bmatrix} \begin{bmatrix} e_{i,1} \\ e_{i,2} \end{bmatrix}}_{=:\xi_i} + \left(1 - \frac{\tau_i}{h}\right) a_i + \frac{\tau_i}{h} a_{i-1}, \quad i \in S_I, \tag{2.21}$$

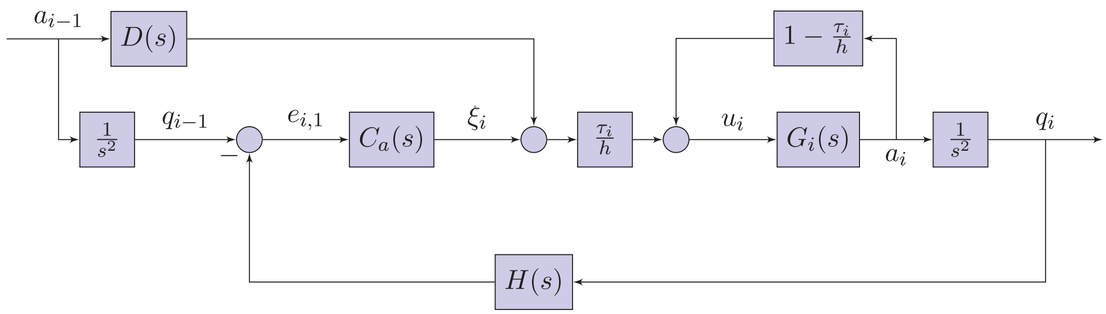

Figure 2.3: Block diagram of a-CACC (2.21) for a possibly heterogeneous platoon. Here $D(s) := e^{-\theta s}$ is the communcation delay, $C_a(s) := k_p + k_d s$ the controller, $H(s) := hs + 1$ the spacing policy, and $G_i(s) := \frac{1}{\tau_i s+1}$ the vehicle model.

with acceleration a_{i-1} obtained via wireless inter-vehicle communication. Then, using the linear vehicle model (2.1) gives the closed loop platoon dynamics

$$\begin{bmatrix} \dot{e}_{i,1} \\ \dot{e}_{i,2} \\ \dot{\varepsilon}_i \end{bmatrix} = \underbrace{\begin{bmatrix} 0 & 1 & 0 \\ -k_p & -k_d & 0 \\ 0 & \frac{1}{h} & -\frac{1}{h} \end{bmatrix}}_{=:A_a} \begin{bmatrix} e_{i,1} \\ e_{i,2} \\ \varepsilon_i \end{bmatrix} + \underbrace{\begin{bmatrix} 0 \\ 0 \\ 1 \end{bmatrix}}_{=:B_a} a_{i-1}, \quad i \in S_I, \tag{2.22}$$

which is ISS with respect to a_{i-1} for $k_p > 0$ and $k_d > 0$. Important to see is the fact that, for hetereogeneous platoons, u-CACC requires τ_{i-1} in the control law (2.16), whereas a-CACC (2.21) does not. Moreover, it was shown in [10] that a-CACC achieves dynamics of $\begin{bmatrix} e_{i,1} & e_{i,2} & e_{i,3} \end{bmatrix}^T$ identical to u-CACC by choosing

$$\dot{\xi}_i = -\frac{1}{\tau_i}\xi_i + \frac{1}{\tau_i}\begin{bmatrix} k_p & k_d & k_{dd} \end{bmatrix} \begin{bmatrix} e_{i,1} \\ e_{i,2} \\ e_{i,3} \end{bmatrix}, \qquad i \in S_I. \tag{2.23}$$

Furthermore, the a-CACC controller (2.21) with ξ_i chosen as (2.23) does not require knowledge of τ_{i-1}.

A block diagram of the platoon employing the a-CACC controller (2.21) is presented in Figure 2.3, from which the SSCS can be determined as

$$\Gamma_a^{\text{CACC}}(s) := \frac{a_i(s)}{a_{i-1}(s)} = \frac{1}{H(s)} \frac{D(s)s^2 + C_a(s)}{s^2 + C_a(s)}, \tag{2.24}$$

with feedback controller $C_a(s) := k_p + k_d s$. As a direct effect of the input-output linearisation, and communication of a_{i-1} in controller (2.21), the SSCS (2.24) does no longer depend on the predecessor as well as its own vehicle dynamics.

Basic simulation results of a-CACC, as visualized in the block diagram of Figure 2.3, for a homogeneous platoon of $I = 6$ vehicles, are shown in Figure 2.2. This basic simulation uses parameters $k_p = 0.2$, $k_d = 0.7$, $\tau = 0.1$ s, $\theta = 0.02$ s, $h = 0.5$ s, and again input

$$u_1(t) = \begin{cases} 1, & \text{if} \quad 5 \leq t \leq 10, \\ -1, & \text{if} \quad 15 \leq t \leq 20, \\ 0, & \text{else.} \end{cases} \tag{2.25}$$

It was shown in [10], that these controller gains resulted in similar settling time and maximal jerk as u-CACC as a response to a step-input. The $\mathcal{L}_2$-norms of the acceleration signals for both u-CACC and a-CACC are presented in Table 2.1. It can be seen that a-CACC performs slightly better in terms of attenuation of the acceleration $\mathcal{L}_2$-norm. Even though the controller gains are tuned to create a fair situation for the given τ, h, and θ, the comparison depends on $u_1(t)$. The basic simulation forms the basis for the verification of a-CACC in the complex simulation environment presented in Chapter 5.

Table 2.1: $\mathcal{L}_2$-norms of acceleration signals for u-CACC and a-CACC resulting from the basic simulation with input $u_1(t)$ (2.19), $k_p = 0.2$, $k_d = 0.7$, $k_{dd} = 0$, $\tau = 0.1\ s$, $h = 0.5\ s$, and $\theta = 0.02\ s$.

Vehicle	**u-CACC**	**a-CACC**
$i = 1$	3.13	3.13
$i = 2$	3.00	2.99
$i = 3$	2.92	2.90
$i = 4$	2.86	2.84
$i = 5$	2.81	2.78
$i = 6$	2.76	2.73

2.5 Degraded CACC

Inherent to CACC is its vulnerability to communication impairments, in which case it would effectively degrade to conventional ACC. To remain string stable in such a scenario, the minimum required time gap h easily increases from 0.25 s to more than 3 s [15].
Rather than having ACC as a fallback scenario, [15] proposes degraded CACC for u-CACC, from here on denoted as u-dCACC. Rather than relying on wireless communication, u-dCACC uses onboard sensors, such as radar and IMU, to measure relative position $q_{i-1} - q_i$, relative velocity $v_{i-1} - v_i$, and global acceleration a_i. Now, u-dCACC uses the controller

$$\dot{u}_i = -\frac{1}{h}u_i + \frac{1}{h}\begin{bmatrix} k_p & k_d & k_{dd} \end{bmatrix}\begin{bmatrix} e_{i,1} \\ e_{i,2} \\ e_{i,3} \end{bmatrix} + \frac{1}{h}\hat{a}_{i-1}, \qquad i \in S_I, \tag{2.26}$$

with $\hat{a}_{i-1} \in \mathbb{R}$ the estimated predecessor acceleration. In order to estimate $\hat{a}_{i-1}$, it is assumed for the predecessor to follow the Singer acceleration model

$$\dot{a}_{i-1} = -\alpha a_{i-1} + u_{i-1}, \qquad i \in S_I, \tag{2.27}$$

with $\alpha := \frac{1}{\tau_m}$, and τ_m the so-called maneuver time constant, essentially describing the time period of an acceleration manoeuvre [19]. The input u_{i-1} is unknown within vehicle i. Parameter α is basically meant for tuning, and, as a rule of thump, should be taken in the range

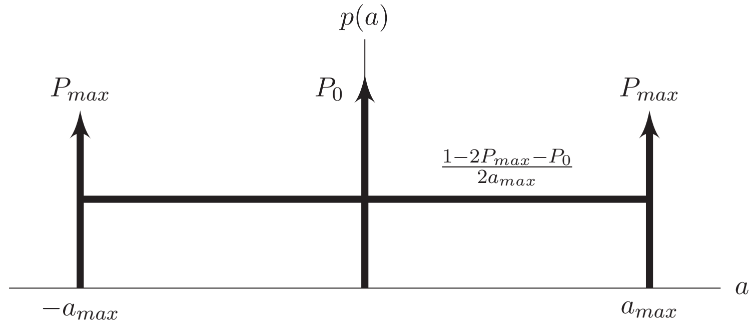

Figure 2.4: Probability density function of the predecessor acceleration a_{i-1}.

$0.5 \leq \alpha \leq 1.5$ for road vehicles [15]. Finally, the estimate $\hat{a}_{i-1}$ is the output of the observer

$$\begin{aligned}
\begin{bmatrix} \dot{\hat{q}}_{i-1} \\ \dot{\hat{v}}_{i-1} \\ \dot{\hat{a}}_{i-1} \end{bmatrix} &= \underbrace{\begin{bmatrix} 0 & 1 & 0 \\ 0 & 0 & 1 \\ 0 & 0 & -\alpha \end{bmatrix}}_{=:A_s} \begin{bmatrix} \hat{q}_{i-1} \\ \hat{v}_{i-1} \\ \hat{a}_{i-1} \end{bmatrix} + \underbrace{\begin{bmatrix} l_{11} & l_{12} \\ l_{21} & l_{22} \\ l_{31} & l_{32} \end{bmatrix}}_{=:L_s} \begin{bmatrix} q_{i-1} - \hat{q}_{i-1} \\ v_{i-1} - \hat{v}_{i-1} \end{bmatrix}, \\
\begin{bmatrix} \hat{q}_{i-1} \\ \hat{v}_{i-1} \end{bmatrix} &= \underbrace{\begin{bmatrix} 1 & 0 & 0 \\ 0 & 1 & 0 \end{bmatrix}}_{=:C_s} \begin{bmatrix} \hat{q}_{i-1} \\ \hat{v}_{i-1} \\ \hat{a}_{i-1} \end{bmatrix}, \qquad i \in S_I.
\end{aligned} \tag{2.28}$$

The observer (2.28) uses q_{i-1} and v_{i-1} to update the estimate, even though these are not directly measured. In [15], this is solved by rewriting the observer (2.28) using the Laplace transform to obtain

$$\begin{aligned}
\hat{a}_{i-1}(s) &= \underbrace{\begin{bmatrix} 0 & 0 & 1 \end{bmatrix} (sI - A_s + L_s C_s)^{-1} L_s}_{=:\begin{bmatrix} T_{qa(s)} & T_{va}(s) \end{bmatrix}} \begin{bmatrix} q_{i-1}(s) \\ v_{i-1}(s) \end{bmatrix} \\
&= \underbrace{\begin{bmatrix} T_{qa}(s) & T_{va}(s) \end{bmatrix}}_{=:T(s)} \left(\begin{bmatrix} q_{i-1}(s) - q_i(s) \\ v_{i-1}(s) - v_i(s) \end{bmatrix} + \begin{bmatrix} q_i(s) \\ v_i(s) \end{bmatrix} \right) \\
&= T(s) \begin{bmatrix} q_{i-1}(s) - q_i(s) \\ v_{i-1}(s) - v_i(s) \end{bmatrix} + \underbrace{\left(\frac{T_{qa}(s)}{s^2} + \frac{T_{va}(s)}{s} \right)}_{=:T_{aa}(s)} a_i(s), \qquad i \in S_I,
\end{aligned} \tag{2.29}$$

showing that only $q_{i-1} - q_i$, $v_{i-1} - v_i$, and a_i are required for measurement.
Additionally, [15] proposes the use of an optimal Kalman filter gain for L_s, assuming the predecessor acceleration to be a zero mean uncorrelated random process (white noise), and to have a probability density function $p(a)$ as shown in Figure 2.4. Specifically, the predecessor experiences a maximal acceleration of a_{max} (or deceleration $-a_{max}$) with probability P_{max}, zero acceleration with a probability P_0, and is uniformly distributed in between. Results are presented below, for the derivation the reader is referred to Appendix C. The observer gains are computed as

$$L = PC^T R^{-1}, \tag{2.30}$$

where P is the solution of the continuous-time algebraic Riccati equation

$$A_sP + PA_s^T - PC_s^TR^{-1T}C_sP + Q = 0. \tag{2.31}$$

The process noise covariance matrix Q, and measurement noise covariance matrix R, are given as

$$\begin{aligned} Q &= \begin{bmatrix} 0 & 0 & 0 \\ 0 & 0 & 0 \\ 0 & 0 & \frac{2}{3}\alpha a_{max}^2 \left(1 + 4P_{max} - P_0\right) \end{bmatrix}, \\ R &= \begin{bmatrix} \sigma_q^2 & 0 \\ 0 & \sigma_v^2 \end{bmatrix}, \end{aligned} \tag{2.32}$$

where σ_q^2 and σ_v^2 denote the variance of the measurement noise on the indirect measurements of q_{i-1} and v_{i-1}, respectively.
Finally, the SSCS of u-dCACC is given as

$$\Gamma_u^{\text{dCACC}}(s) = \frac{1}{H(s)} \frac{G_i(s)\left(T_{aa}(s)s^2 + C_c(s)\right)}{s^2 + G_i(s)C_c(s)}, \tag{2.33}$$

with $T_{aa}(s)$ given in (2.29), and $H_i(s)$, $G_i(s)$, and $C_c(s)$ as given in (2.18). The SSCS of u-dCACC (2.33) clearly shows that string stability is no longer affected by the predecessor dynamics. Since τ_{i-1} is not used in the u-dCACC controller (2.26), it is applicable to vehicle platoons with heterogeneous driveline dynamics.

2.6 Summary

This chapter started with a broad exploration on the different aspects encompassed within the field of CACC, indicating and explaining otherwise implicitly made assumptions. Briefly summarized, this thesis assumes third order linear longitudinal vehicle dynamics, predecessor-follower communication, and a constant time gap distance policy. Additionally, heterogeneity with respect to drivelines is considered throughout this thesis.
Afterwards, important contributions were presented. More specifically, Section 2.2 introduced $\mathcal{L}_p$ string stability, and Sections 2.3 and 2.4 introduced u-CACC and a-CACC, respectively. Degraded CACC was formally introduced in Section 2.5.
Most importantly, the background presented here, forms a rigorous basis for the continuation of this thesis.

Chapter 3

Contributions to *a*-CACC

It has been shown that a-CACC, introduced in [10], possesses large potential, especially regarding heterogeneous vehicle platoons. Moreover, in [10] it was shown that the class of u-CACC controllers is contained within the class of a-CACC controllers. Finally, it was shown in [10] that similar performance is achieved when using u-CACC and a-CACC for homogeneous vehicle platoons.
Since a-CACC appeared recently, it is not yet explored thoroughly and some additions can be made. Correspondingly, this chapter presents two important contributions to a-CACC. Section 3.1 derives an analytical sufficient string stability condition, directly stating the effect of controller gains and communication delay on the minimal string stable inter-vehicle time gap. Afterwards, Section 3.2 proposes a-dCACC as a fallback scenario of a-CACC in case of communication impairments. Finally, a short summary of this chapter is presented in Section 3.3.

3.1 Sufficient condition for string stability

The $\mathcal{L}_2$ string stability definition is presented in Theorem 2.1, and consists of two conditions. The first condition is satisfied by assuming the platoon leader to employ (GAS) CC and choosing acceleration output [16].
The second condition requires the $\mathcal{H}_\infty$-norm of the SSCS to be less than or equal to one. Analysis of this condition is more troublesome, and does not give a direct effect of the controller gains on the minimal string stable time gap h for a given communication delay θ. In literature, string stability is predominantly tested by means of iterations over either time gap h or communication delay θ for fixed controller gains. Achieving string stability for a desired time gap h therefore remains a process of trial-and-error. A sufficient string stability condition, providing an intuitive feeling of tuning parameters as well as a method for tuning controller gains, is derived in this section.

The remaining string stability condition, adopted to a-CACC, is given as

$$\|\Gamma_a^{\text{CACC}}(j\omega)\|_{\mathcal{H}_\infty} = \left\| \frac{a_i(j\omega)}{a_{i-1}(j\omega)} \right\|_{\mathcal{H}_\infty} \leq 1, \quad \forall \quad i \in S_I, \quad I \in \mathbb{N} \setminus \{1\}, \tag{3.1}$$

with $\Gamma_a^{\text{CACC}}(s)$ the a-CACC SSCS (2.24). Using the definition of the $\mathcal{H}_\infty$-norm as given in Appendix A.1, and the fact that $\Gamma(s)$ is single-input single-output, makes it possible to rewrite condition (3.1) into

$$\left|\Gamma_a^{\mathrm{CACC}}(j\omega)\right| \;\leq\; 1, \quad \forall \quad \omega \in \mathbb{R}. \tag{3.2}$$

The following proposition presents the sufficient string stability condition by using the rewritten string stability definition (3.2).

Proposition 3.1. *(Sufficient condition for string stability) Consider a vehicle platoon employing the a-CACC controller*

$$u_i = \frac{\tau_i}{h}\begin{bmatrix}k_p & k_d\end{bmatrix}\begin{bmatrix}e_{i,1}\\ e_{i,2}\end{bmatrix} + \left(1-\frac{\tau_i}{h}\right)a_i + \frac{\tau_i}{h}a_{i-1}, \qquad i \in S_I, \tag{3.3}$$

with $k_p, k_d > 0$. The SSCS is given as

$$\Gamma_a^{\mathrm{CACC}}(s) = \frac{1}{H(s)}\frac{s^2 D(s) + C_a(s)}{s^2 + C_a(s)}, \tag{3.4}$$

with spacing policy $H(s) := hs+1$, communication delay $D(s) := e^{-\theta s}$, and feedback controller $C_a(s) := k_p + k_d s$. Then, the platoon is string stable if

$$h \;\geq\; \frac{1}{k_d}\sqrt{\theta\left(2k_d + \theta k_p\right)}. \tag{3.5}$$

Proof. The complex magnitude in (3.2) is positive by definition. Therefore, the string stability condition (3.2) can be rewritten as

$$\left|\Gamma_a^{\mathrm{CACC}}(j\omega)\right|^2 \;\leq\; 1, \quad \forall \quad \omega \in \mathbb{R}. \tag{3.6}$$

Substituting the a-CACC SSCS (3.4) in the condition (3.6) gives the necessary and sufficient string stability condition

$$\frac{1}{\left|h\omega j+1\right|^2}\frac{\left|-\omega^2 e^{-\theta\omega j} + k_p + k_d\omega j\right|^2}{\left|-\omega^2 + k_p + k_d\omega j\right|^2} \;\leq\; 1, \quad \forall \quad \omega \in \mathbb{R}. \tag{3.7}$$

Using Euler's formula, i.e., $e^{-\theta\omega j} = \cos(\theta\omega) - \sin(\theta\omega)j$, and rewriting condition (3.7) while using $\frac{f(\omega)}{g(\omega)} \leq 1 \;\Rightarrow\; g(\omega) - f(\omega) \geq 0$ for positive $f(\omega), g(\omega)$, gives

$$\begin{aligned} &\left|k_p - \omega^2\cos(\theta\omega) + \left(k_d\omega + \omega^2\sin(\theta\omega)\right)j\right|^2 \;\leq\; \left|h\omega j+1\right|^2\left|k_p - \omega^2 + k_d\omega j\right|^2, \\ \Rightarrow\; &h^2\omega^4 + h^2\left(k_d^2 - 2k_p\right)\omega^2 - 2k_d\sin(\theta\omega)\omega + h^2k_p^2 + 2k_p\left(\cos(\theta\omega)-1\right) \;\geq\; 0, \quad \forall \quad \omega \in \mathbb{R}. \end{aligned} \tag{3.8}$$

Appendix A.2 presents polynomial bounds on both the sine and cosine functions using their Taylor approximations. Accordingly, choose the first two terms of the Taylor approximation to get $\omega\sin(\theta\omega) \;\leq\; \theta\omega^2$ and $\cos(\theta\omega) \;\geq\; 1 - \frac{1}{2}\theta^2\omega^2$. Substitute these bounds in (3.8), to obtain the sufficient string stability condition

$$h^2\omega^4 + \left(h^2(k_d^2 - 2k_p) - 2k_d\theta - k_p\theta^2\right)\omega^2 + h^2k_p^2 \geq 0, \quad \forall \quad \omega \in \mathbb{R}. \tag{3.9}$$

Define $a := h^2$, $b := h^2\left(k_d^2 - 2k_p\right) - 2k_d\theta - k_p\theta^2$, $c := h^2k_p^2$, and $x := \omega^2$. Then, sufficient string stability condition (3.9) can be written as

$$ax^2 + bx + c \geq 0, \quad \forall \quad x \geq 0. \tag{3.10}$$

Inequality (3.10) is satisfied for $a, b, c \geq 0$ or $a, c \geq 0 \wedge b^2 - 4ac \leq 0$. This implies that (3.10), which is a parabola opening upward for $a \geq 0$, has no zero-crossings, such that it is non-negative anywhere. Combining both conditions gives

$$\begin{aligned} a \geq 0, \quad &\Rightarrow \quad h^2 \geq 0, \\ \wedge\, c \geq 0, \quad &\Rightarrow \quad h^2 k_p^2 \geq 0, \\ \wedge\, b \geq -2\sqrt{ac} \quad &\Rightarrow \quad h^2 k_d^2 - 2k_d\theta - k_p\theta^2 \geq 0, \end{aligned} \tag{3.11}$$

from which the sufficient string stability condition (3.5) directly follows. □

Instead of using the bounds $\omega \sin(\theta\omega) \leq \theta\omega^2$, and $\cos(\theta\omega) \geq 1 - \frac{1}{2}\theta^2\omega^2$, it is also possible to use $\sin(\theta\omega) \leq 1$ and $\cos(\theta\omega) \geq -1$. This enables the derivation of a string stable time gap h independent of communication delay θ, which is described in the following remark.

Remark 3.1. *First, note that necessary string stability condition* (3.8) *is identical for positive and negative* ω *(the function is even). Therefore, it is only required to evaluate condition* (3.8) *for* $\omega \geq 0$*, and substitute the new bounds on the sine and cosine function, to get*

$$\begin{aligned} &\underbrace{h^2}_{=:a}\omega^4 + \underbrace{h^2(k_d^2 - 2k_p)}_{=:b}\omega^2 \underbrace{-2k_d}_{=:c}\omega + \underbrace{h^2k_p^2 - 4k_p}_{=:d} \;\geq\; 0, \quad \forall \quad \omega \geq 0, \\ &\Rightarrow a\omega^4 + b\omega^2 + c\omega + d \;\geq\; 0, \quad \forall \quad \omega \geq 0. \end{aligned} \tag{3.12}$$

Sufficient for condition (3.12) *is* $a, b, d \geq 0 \wedge c^2 - 4bd \leq 0$*. Then, string stability for all possible* θ *is achieved when*

$$\begin{aligned} a \;&\geq\; 0 \;\Rightarrow\; h^2 \geq 0, \\ \wedge\, b \;&\geq\; 0 \;\Rightarrow\; k_d^2 - 2k_p \geq 0, \\ \wedge\, d \;&\geq\; 0 \;\Rightarrow\; h^2 \geq \frac{4}{k_p}, \\ \wedge\, c^2 \;&\leq 4bd \;\Rightarrow\; h^2\left(h^2k_p^2 - 4k_p\right) - \frac{k_d^2}{k_d^2 - 2k_p} \geq 0 \\ &\qquad\;\;\Rightarrow\; h^2 \geq \frac{1}{k_p}\left(2 + \sqrt{4 + \frac{k_d^2}{k_d^2 - 2k_p}}\right) \geq \frac{4}{k_p}. \end{aligned} \tag{3.13}$$

Note that all conditions in (3.13) *are satisfied when the second and last condition are met.*

Conservatism of the sufficient string stability condition (3.5) is not yet examined. Therefore, a comparison between the sufficient condition (3.5) and the time gap that is numerically determined using $\left\|\Gamma_a^{\mathrm{CACC}}\right\|_{\mathcal{H}_\infty} \leq 1$, is presented in Figure 3.1 using the practical parameters $k_p = 0.2$ and $k_d = 0.7$. For $\theta \leq 1$ s, the required time gap h for the sufficient condition (3.5) remains within 2 percent from the numerically determined time gap h.
The resemblance between the sufficient string stability condition (3.5) and the numerical results indicate its potential for manually tuning the controller gains. Remember that no direct effect of k_p, k_d, θ, and h on string stability is obtained from the string stability definition.

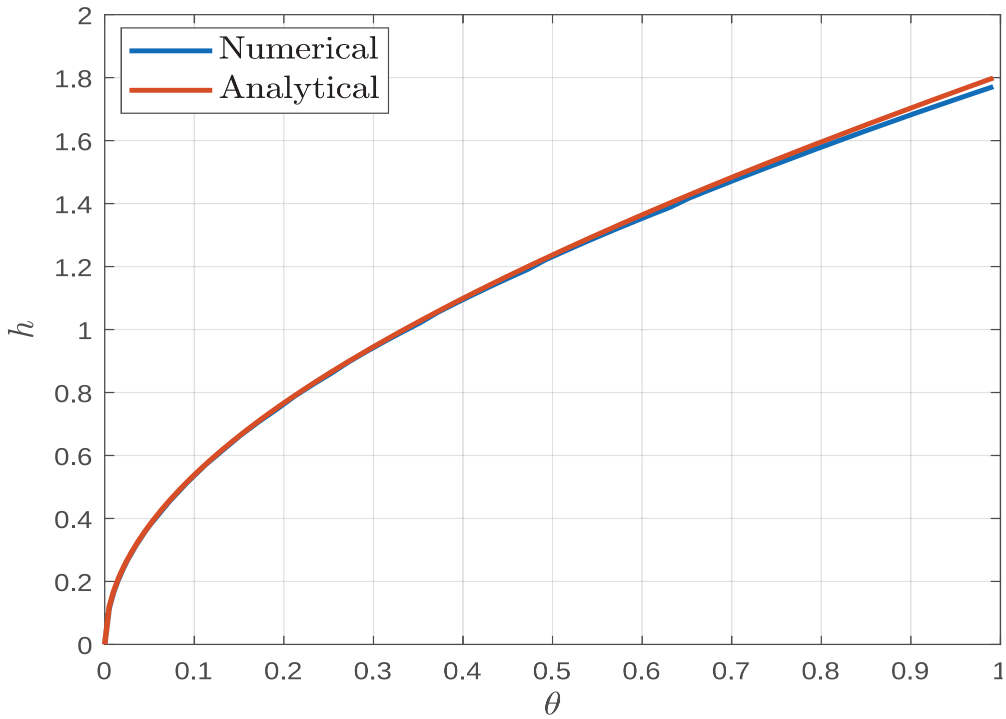

Figure 3.1: Minimal string stable time gap h for given communication delay θ, determined numerically using the string stability definition (3.1) and using the analytical sufficient string stability condition (3.5) for $k_p = 0.2$, and $k_d = 0.7$.

Table 3.1: Parameter values for practical application of dCACC.

Parameter	Value
h	$0.5\ s$
τ_i	$0.1\ s$
k_p	0.2
k_d	0.7
k_{dd}	0
α	$1.25\ s^{-1}$
a_{max}	$3\ \frac{m}{s^2}$
P_{max}	0.01
P_0	0.1
σ_q^2	$0.029\ m^2$
σ_v^2	$0.017\ \frac{m^2}{s^2}$

3.2 Degraded a-CACC

In Section 2.5, u-dCACC [15] has been formerly introduced. This section introduces the degraded version of a-CACC denoted with a-dCACC, after which it is compared to u-dCACC. To do so, the problem statement of dCACC is presented in Section 3.2.1, followed by an

explanation in Section 3.2.2 as to why u-dCACC solves this problem. Finally, Section 3.2.3 proposes a-dCACC, elaborated upon by a comparison with u-dCACC in Section 3.2.4.
Unless specifically stated otherwise, this section uses the parameters as presented in Table 3.1.

3.2.1 Problem statement

Inherent to CACC is its vulnerability to communication impairments, in which case it would effectively degrade to conventional ACC, and thereby drastically increases the minimal string stable inter-vehicle time gap h [15]. CACC can essentially be regarded as a feedback controller (ACC) extended with a feedforward term obtained via wireless communication (C). Rather than having ACC as a fallback scenario, onboard measurements can be used to estimate the global acceleration of the predecessor a_{i-1}, such that inter-verhicle communication is no longer required.
To do so, the predecessor is assumed to follow the linear longitudinal vehicle dynamics

$$\begin{bmatrix} \dot{q}_{i-1} \\ \dot{v}_{i-1} \\ \dot{a}_{i-1} \end{bmatrix} = \begin{bmatrix} 0 & 1 & 0 \\ 0 & 0 & 1 \\ 0 & 0 & -\frac{1}{\tau_{i-1}} \end{bmatrix} \begin{bmatrix} q_{i-1} \\ v_{i-1} \\ a_{i-1} \end{bmatrix} + \begin{bmatrix} 0 \\ 0 \\ \frac{1}{\tau_{i-1}} \end{bmatrix} u_{i-1}, \qquad i \in S_I, \tag{3.14}$$

where the predecessor driveline time constant τ_{i-1} is unknown. From practical constraints, the predecessor has bounded velocity v_{i-1}, acceleration a_{i-1}, and input u_{i-1}, such that

$$\begin{aligned} |v_{i-1}(t)| \;&=\; \left| \int^t a_{i-1}(t)dt \right| \;\leq\; v_{max} < \infty, \quad \forall \quad t, \\ |a_{i-1}(t)| \;&\leq\; a_{max} < \infty, \quad \forall \quad t, \\ |u_{i-1}(t)| \;&\leq u_{max} < \infty, \quad \forall \quad t, \qquad i \in S_I. \end{aligned} \tag{3.15}$$

Onboard sensors provide measurements of relative position $q_{i-1} - q_i$ and velocity $v_{i-1} - v_i$ (e.g., radar), global velocity v_i (e.g., wheel encoder), and global acceleration a_i (e.g., IMU).
Now, determine a controller, only relying on these measurements, achieving the following two control objectives:

1. Stable tracking dynamics; the velocity v_i, acceleration a_i, and input u_i should remain bounded when v_{i-1}, a_{i-1}, and u_{i-1} are bounded. Additionally, when the predecessor vehicle follows a constant velocity, i.e., $a_{i-1} = 0$, the tracking error should be GAS: $\lim_{t\to\infty} e_{i,1} = 0$.
2. String stable following behaviour; acceleration signals should not increase over vehicle index i in terms of their $\mathcal{L}_2$-norm. Therefore, the acceleration should satisfy $\|a_i\|_{\mathcal{L}_2} \leq \|a_{i-1}\|_{\mathcal{L}_2}$.

In order to improve over ACC, which only uses feedback and is known for its large minimal string stable inter-vehicle time gap h, the designed controller should combine both feedback as well as feedforward.

3.2.2 *u*-dCACC

This section elaborates upon u-dCACC [15] as introduced in Section 2.5, and shows that it satisfies the problem statement presented in Section 3.2.1. To ease reading this section, the tracking error coordinates

$$
\begin{aligned}
e_{i,1} &:= q_{i-1} - q_i - hv_i, \\
e_{i,2} &:= \dot{e}_{i,1} = v_{i-1} - v_i - ha_i, \\
e_{i,3} &:= \dot{e}_{i,2} = a_{i-1} - \left(1 - \frac{h}{\tau_i}\right) a_i - \frac{h}{\tau_i} u_i, \qquad i \in S_I,
\end{aligned}
\tag{3.16}
$$

and the control law

$$
\dot{u}_i = -\frac{1}{h} u_i + \frac{1}{h} \begin{bmatrix} k_p & k_d & k_{dd} \end{bmatrix} \begin{bmatrix} e_{i,1} \\ e_{i,2} \\ e_{i,3} \end{bmatrix} + \frac{1}{h} \hat{a}_{i-1}, \qquad i \in S_I, \tag{3.17}
$$

are restated. The predecessor acceleration a_{i-1} is estimated using the observer

$$
\begin{aligned}
\begin{bmatrix} \dot{\hat{q}}_{i-1} \\ \dot{\hat{v}}_{i-1} \\ \dot{\hat{a}}_{i-1} \end{bmatrix} &= \underbrace{\begin{bmatrix} 0 & 1 & 0 \\ 0 & 0 & 1 \\ 0 & 0 & -\alpha \end{bmatrix}}_{=:A_s} \begin{bmatrix} \hat{q}_{i-1} \\ \hat{v}_{i-1} \\ \hat{a}_{i-1} \end{bmatrix} + \underbrace{\begin{bmatrix} l_{11} & l_{12} \\ l_{21} & l_{22} \\ l_{31} & l_{33} \end{bmatrix}}_{=:L_s} \begin{bmatrix} q_{i-1} - \hat{q}_{i-1} \\ v_{i-1} - \hat{v}_{i-1} \end{bmatrix}, \\
\begin{bmatrix} \hat{q}_{i-1} \\ \hat{v}_{i-1} \end{bmatrix} &= \underbrace{\begin{bmatrix} 1 & 0 & 0 \\ 0 & 1 & 0 \end{bmatrix}}_{=:C_s} \begin{bmatrix} \hat{q}_{i-1} \\ \hat{v}_{i-1} \\ \hat{a}_{i-1} \end{bmatrix}, \qquad i \in S_I.
\end{aligned}
\tag{3.18}
$$

To overcome the need to measure q_{i-1} and v_{i-1}, a trick is presented in Section 2.5 such that only measurements of $q_{i-1} - q_i$, $v_{i-1} - v_i$, and a_i are required.

Define the observer error variables $\tilde{q}_{i-1} := q_{i-1} - \hat{q}_{i-1}$, $\tilde{v}_{i-1} := v_{i-1} - \hat{v}_{i-1}$, and $\tilde{a}_{i-1} := a_{i-1} - \hat{a}_{i-1}$. Then, the closed loop dynamics of u-dCACC can be derived using longitudinal vehicle dynamics (3.14), tracking error coordinates (3.16), and controller (3.17) with observer (3.18), resulting in

$$
\underbrace{\left[\begin{array}{c} \dot{e}_{i,1} \\ \dot{e}_{i,2} \\ \dot{e}_{i,3} \\ \dot{u}_i \\ \hline \dot{\tilde{q}}_{i-1} \\ \dot{\tilde{v}}_{i-1} \\ \dot{\tilde{a}}_{i-1} \end{array}\right]}_{=:\dot{x}_{i,c}} = \left[\begin{array}{cccc|ccc} 0 & 1 & 0 & 0 & 0 & 0 & 0 \\ 0 & 0 & 1 & 0 & 0 & 0 & 0 \\ -\frac{k_p}{\tau} & -\frac{k_d}{\tau} & -\frac{k_{dd}+1}{\tau} & 0 & 0 & 0 & -\frac{1}{h} \\ \frac{k_p}{h} & \frac{k_d}{h} & \frac{k_{dd}}{h} & -\frac{1}{h} & 0 & 0 & \frac{1}{h} \\ \hline 0 & 0 & 0 & 0 & -l_{11} & 1 - l_{12} & 0 \\ 0 & 0 & 0 & 0 & -l_{21} & -l_{22} & 1 \\ 0 & 0 & 0 & 0 & -l_{31} & -l_{32} & -\alpha \end{array}\right] \left[\begin{array}{c} e_{i,1} \\ e_{i,2} \\ e_{i,3} \\ u_i \\ \hline \tilde{q}_{i-1} \\ \tilde{v}_{i-1} \\ \tilde{a}_{i-1} \end{array}\right] + \left[\begin{array}{cc} 0 & 0 \\ 0 & 0 \\ -\frac{1}{h} & \frac{1}{\tau} \\ -\frac{1}{h} & 0 \\ \hline 0 & 0 \\ 0 & 0 \\ \alpha - \frac{1}{\tau} & \frac{1}{\tau} \end{array}\right] \begin{bmatrix} a_{i-1} \\ u_{i-1} \end{bmatrix}. \tag{3.19}
$$

The matrices A_u and $A_s - L_s C_s$ are recognized on the diagonal of the system matrix in (3.19), such that it is Hurwitz for $k_p > 0$, $k_{dd} > -1$, $k_d > \frac{k_p \tau}{1+k_{dd}}$, and L_s chosen such that $A_s - L_s C_s$ has eigenvalues located in the left half-plane (separation principle). Since the pair (A_s, C_s) is observable, the eigenvalues of $A_s - L_s C_s$ can be placed in the complex left half-plane by properly choosing L_s. Therefore, $x_{i,c}$ in (3.19) is ISS with respect to $\begin{bmatrix} a_{i-1} & u_{i-1} \end{bmatrix}^T$.

In particular, bounded a_{i-1}, and u_{i-1} give bounded $x_{i,c}$, and a_{i-1} and u_{i-1} converging to zero gives $x_{i,c}$ converging to zero. Using the inverse tracking error coordinate transformation

$$\begin{aligned} q_i &= -e_{i,1} + he_{i,2} + \frac{h^2\tau_i}{h-\tau_i}e_{i,3} + q_{i-1} - hv_{i-1} - \frac{h^2\tau_i}{h-\tau_i}a_{i-1} + \frac{h^3}{h-\tau_i}u_i, \\ v_i &= -e_{i,2} - \frac{h\tau_i}{h-\tau_i}e_{i,3} + v_{i-1} + \frac{h\tau_i}{h-\tau_i}a_{i-1} - \frac{h^2}{h-\tau_i}u_i, \\ a_i &= \frac{\tau_i}{h-\tau_i}e_{i,3} - \frac{\tau_i}{h-\tau_i}a_{i-1} + \frac{h}{h-\tau_i}u_i, \quad i \in S_I, \end{aligned} \tag{3.20}$$

and control law (3.17), it is possible to draw the same conclusion for v_i, a_i, and u_i. Therefore, control objective 1 is satisfied.

Numerically computing the $\mathcal{H}_\infty$-norm of the u-dCACC SSCS

$$\Gamma_u^{\text{dCACC}}(s) = \frac{1}{H(s)} \frac{G_i(s)\left(T_{aa}(s)s^2 + C_c(s)\right)}{s^2 + G_i(s) + C_c(s)}, \tag{3.21}$$

with $T_{aa}(s)$ in (2.29), for the parameters in Table 3.1 yields string instability. Iteratively increasing the time gap h appears to give string stability for a minimal time gap of $h = 1.75$ s, and thereby satisfying control objective 2.

3.2.3 a-dCACC

Instead of using u-dCACC, it is also possible to extend a-CACC with a degraded version a-dCACC. To ease reading this section, the tracking error coordinates

$$\begin{aligned} e_{i,1} &:= q_{i-1} - q_i - hv_i, \\ e_{i,2} &:= v_{i-1} - v_i - ha_i, \\ \varepsilon_i &:= v_{i-1} - v_i, \qquad i \in S_I, \end{aligned} \tag{3.22}$$

are restated. Now, a-dCACC uses the controller

$$u_i = \frac{\tau_i}{h}\begin{bmatrix} k_p & k_d \end{bmatrix}\begin{bmatrix} e_{i,1} \\ e_{i,2} \end{bmatrix} + \left(1 - \frac{\tau_i}{h}\right)a_i + \frac{\tau_i}{h}\hat{a}_{i-1}, \qquad i \in S_I, \tag{3.23}$$

where $\hat{a}_{i-1}$ is generated from the observer (3.18). Then, a-dCACC is a solution to the problem statement in Section 3.2.1, as is elaborated upon in this section.

Define the observer error variables $\tilde{q}_{i-1} := q_{i-1} - \hat{q}_{i-1}$, $\tilde{v}_{i-1} := v_{i-1} - \hat{v}_{i-1}$, and $\tilde{a}_{i-1} := a_{i-1} - \hat{a}_{i-1}$. Then, the closed loop dynamics of a-dCACC can be derived using the longitudinal vehicle dynamics (3.14), tracking error coordinates (3.22), and controller (3.23) with observer (3.18), resulting in

$$\underbrace{\begin{bmatrix} \dot{e}_{i,1} \\ \dot{e}_{i,2} \\ \dot{\varepsilon}_i \\ \hline \dot{\tilde{q}}_{i-1} \\ \dot{\tilde{v}}_{i-1} \\ \dot{\tilde{a}}_{i-1} \end{bmatrix}}_{=:\dot{x}_{i,a}} = \left[\begin{array}{ccc|ccc} 0 & 1 & 0 & 0 & 0 & 0 \\ -k_p & -k_d & 0 & 0 & 0 & 1 \\ 0 & \frac{1}{h} & -\frac{1}{h} & 0 & 0 & 0 \\ \hline 0 & 0 & 0 & -l_{11} & 1-l_{12} & 0 \\ 0 & 0 & 0 & -l_{21} & -l_{22} & 1 \\ 0 & 0 & 0 & -l_{31} & -l_{32} & -\alpha \end{array}\right] \begin{bmatrix} e_{i,1} \\ e_{i,2} \\ \varepsilon_i \\ \hline \tilde{q}_{i-1} \\ \tilde{v}_{i-1} \\ \tilde{a}_{i-1} \end{bmatrix} + \left[\begin{array}{cc} 0 & 0 \\ 0 & 0 \\ 1 & 0 \\ \hline 0 & 0 \\ 0 & 0 \\ \alpha - \frac{1}{\tau_{i-1}} & \frac{1}{\tau_{i-1}} \end{array}\right] \begin{bmatrix} a_{i-1} \\ u_{i-1} \end{bmatrix}. \tag{3.24}$$

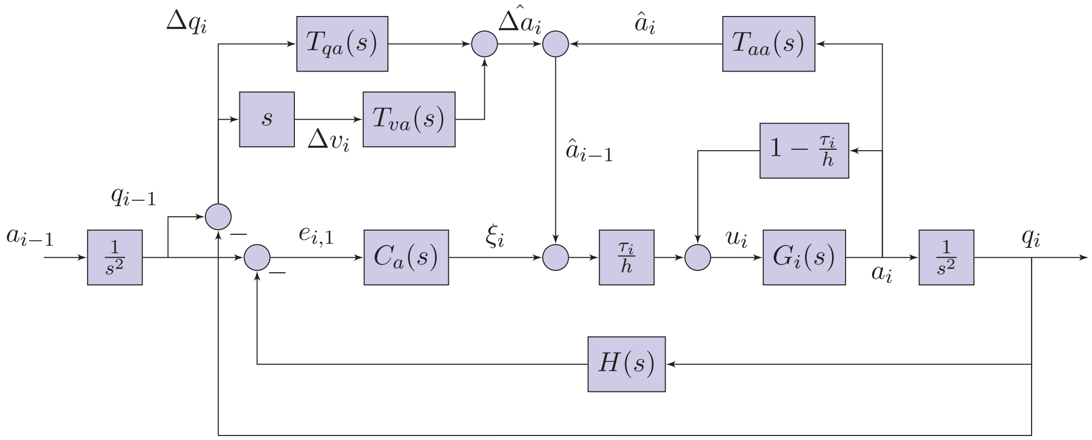

Figure 3.2: Block diagram of the system employing a-dCACC (3.23). Here, $H(s) := hs+1$, $C(s) := k_p + k_d s$, $G_i(s) := \frac{1}{\tau_i s+1}$, and $T_{qa}(s)$, $T_{va}(s)$ and $T_{aa}(s)$ are given in (2.29).

The matrices A_a and $A_s - L_s C_s$ are recognized on the diagonal of the system matrix, from which follows that it is Hurwitz for $k_p, k_d > 0$, and L_s chosen such that $A_s - L_s C_s$ has eigenvalues located in the left half-plane (separation principle). Since the pair (A_s, C_s) is observable, the eigenvalues of $A_s - L_s C_s$ can be placed in the complex left half-plane by properly choosing L_s. Therefore, $x_{i,a}$ in (3.24) is ISS with respect to $\begin{bmatrix} a_{i-1} & u_{i-1} \end{bmatrix}^T$. In particular, bounded a_{i-1} and u_{i-1} give bounded $x_{i,a}$, and a_{i-1} and u_{i-1} converging to zero gives $x_{i,a}$ converging to zero. Using the inverse tracking error coordinate transformation

$$\begin{aligned} q_i &= -e_{i,1} + h\varepsilon_i + q_{i-1} - hv_{i-1}, \\ v_i &= -\varepsilon_i + v_{i-1}, \\ a_i &= \frac{1}{h}\left(\varepsilon_i - e_{i,2}\right), \quad i \in S_I. \end{aligned} \tag{3.25}$$

and control law (3.23), it is possible to draw the same conclusion for v_i, a_i, and u_i, and thereby satisfying control objective 1.

A block diagram of the system employing a-dCACC is presented in Figure 3.2, from which the a-dCACC SSCS can be determined as

$$\Gamma_a^{\text{dCACC}}(s) = \frac{1}{H(s)} \frac{T_{aa}(s)s^2 + C_a(s)}{s^2 + C_a(s)}, \tag{3.26}$$

with observer transfer function $T_{aa}(s)$ given in (2.29), distance policy $H(s) := hs+1$, and controller $C_a(s) := k_p + k_d s$. Note that, in comparison with the u-dCACC SSCS (3.21), the a-dCACC SSCS (3.26) is not affected by the vehicle model $G_i(s)$. This is caused by the input-output linearisation in the controller (3.23).
Numerically computing the $\mathcal{H}_\infty$-norm of the a-dCACC SSCS (3.26), while iteratively increasing time gap h using the parameters in Table 3.1, appears to give string stability for $h > 1.74$ s, and thereby satisfying control objective 2.

3.2.4 Comparison u-dCACC and a-dCACC

There are now two different approaches to cope with communication impairments; u-dCACC and a-dCACC. Using the parameters given in Table 3.1, they are shown to achieve string stable following behaviour for $h > 1.75\ s$ and $h > 1.74\ s$, respectively. Intuitively, a-dCACC seems more logical, since the acceleration a_{i-1} is replaced with an estimated acceleration $\hat{a}_{i-1}$, whereas u-dCACC replaces the desired acceleration u_{i-1} with an estimated acceleration $\hat{a}_{i-1}$. This section performs a comparison between u-dCACC and a-dCACC.

In order to create a fair comparison, the parameters as presented in Table 3.1 are chosen. In [10], it was shown that these parameters resulted in comparable settling time and maximal jerk as a response to a step input for u-CACC and a-CACC. A similar result is observed for u-dCACC and a-dCACC, as is summarized in Table 3.2. Correspondingly, this section retains the same parameters. Tree main differences between u-dCACC and a-dCACC are observed, which are elaborated upon below.

Table 3.2: Settling time and maximal jerk as a response to a step input, using the parameters in Table 3.1.

Approach	Settling time	Maximal jerk
u-CACC	1.85 s	1.35 $\frac{m}{s^3}$
a-CACC	1.82 s	1.35 $\frac{m}{s^3}$
u-dCACC	6.5 s	1.19 $\frac{m}{s^3}$
a-dCACC	6.9 s	1.19 $\frac{m}{s^3}$

Proposition 3.2. *(Frequency domain comparison) Consider the u-dCACC SSCS* (3.21) *and a-dCACC SSCS* (3.26)*, where both use the same predecessor acceleration observer, i.e., $T_{aa}(s)$ is identical in both methods. Then, for:*

- $0 <\mid \omega \mid< \sqrt{2\frac{k_d}{\tau_i}}$*; a-dCACC outperforms u-dCACC in terms of acceleration attenuation.*
- $\mid \omega \mid> \sqrt{2\frac{k_d}{\tau_i}}$*; u-dCACC outperforms a-dCACC in terms of acceleration attenuation.*

Proof. The above can be proven by computation of the squared complex magnitudes of the SSCS functions. First, the a-dCACC SSCS (3.26) gives

$$\mid \Gamma_a^{\text{dCACC}}(j\omega) \mid^2 = \frac{\mid -T_{aa}(j\omega)\omega^2 + k_p + k_d\omega j \mid^2}{\mid h\omega j + 1 \mid^2 \underbrace{\mid -\omega^2 + k_p + k_d\omega j \mid^2}_{=:f(\omega)}}, \tag{3.27}$$

with $f(\omega) := \omega^4 + \left(k_d^2 - 2k_p\right) + k_p^2$. The u-dCACC SSCS (3.21) gives

$$\mid \Gamma_u^{\text{dCACC}}(j\omega) \mid^2 = \frac{\mid -T_{aa}(j\omega)\omega^2 + k_p + k_d\omega j \mid^2}{\mid h\omega j + 1 \mid^2 \underbrace{\mid -\omega^2 + k_p - \left(\tau_i\omega^3 - k_d\omega\right) j \mid^2}_{=:f(\omega)+\Delta(\omega)}}, \tag{3.28}$$

with

$$\Delta(\omega) := \tau_i^2\omega^6 - 2\tau_i k_d\omega^4 = \tau_i^2\omega^4\left(\omega + \sqrt{2 + \frac{k_d}{\tau_i}}\right)\left(\omega - \sqrt{2\frac{k_d}{\tau_i}}\right). \tag{3.29}$$

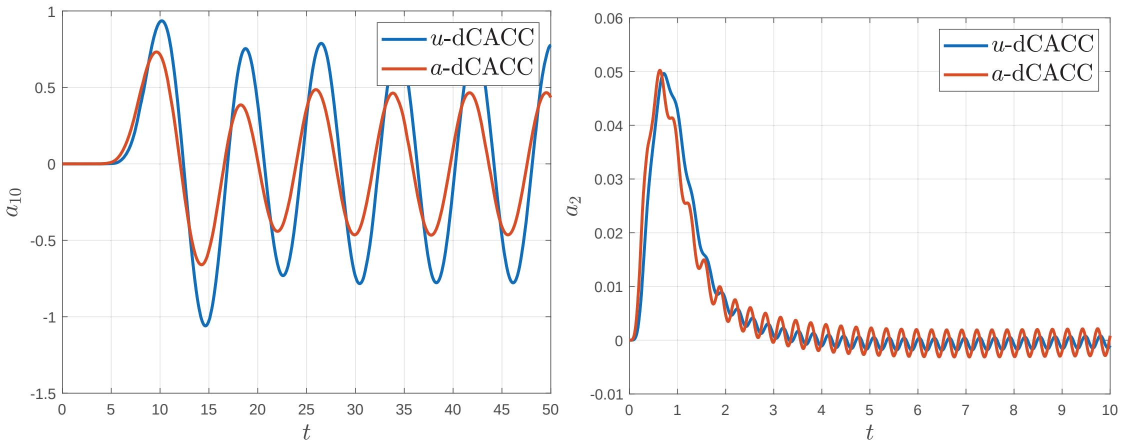

Figure 3.3: Simulation results of u-dCACC (2.26) and a-dCACC (3.23) with input $u_1(t) = \sin(\omega t)$ where $\omega = 0.8\ \frac{rad}{s}$ (left) and $\omega = 20\ \frac{rad}{s}$ (right), with parameters as presented in Table 3.1.

Besides the term $\Delta(\omega)$, both squared complex magnitudes are identical. Correspondingly, for $\Delta(\omega) < 0$ (or similarly $0 <\mid \omega \mid< \sqrt{2\frac{k_d}{\tau_i}}$) it can be seen that $\mid \Gamma_a^{\text{dCACC}}(j\omega) \mid < \mid \Gamma_u^{\text{dCACC}}(j\omega) \mid$. Moreover, for $\Delta(\omega) > 0$ (or similarly $\mid \omega \mid> \sqrt{2\frac{k_d}{\tau_i}}$) it can be seen that $\mid \Gamma_u^{\text{dCACC}}(j\omega) \mid < \mid \Gamma_a^{\text{dCACC}}(j\omega) \mid$. Then, since $a_i(s) = \Gamma(s)a_{i-1}(s)$, the above proposition is proven. $\square$

With an eye on driver comfort and fuel consumption, more attenuation is better. Depending on the dominant frequencies of disturbances, either one approach is preferred as is illustrated in Figure 3.3 for the harmonic input signal $u_1(t) = \sin(\omega t)$ with $\omega = 0.8\ \frac{rad}{s} < \sqrt{2\frac{k_d}{\tau_i}}$ and $\omega = 20\ \frac{rad}{s} > \sqrt{2\frac{k_d}{\tau_i}}$. Vehicle indices $i = 10$ and $i = 2$ are chosen such that the difference in attenuation is shown clearly. Since high frequencies are highly damped compared to the lower frequences (note the difference in vehicle index i and the y-scale in Figure 3.3), the a-dCACC is preferred over u-dCACC.

Even though the above investigates signal attenuation, it does not provide any information regarding string stability. Therefore, a comparison is desired between u-dCACC and a-dCACC in terms of their minimal required string stable time gap. To do so, the controller gains are fixed to the values presented in Table 3.1, since it was stated that these specific values contributed to a fair comparison. Additionally, the effect of the tuning parameters α, a_{max}, P_{max}, and P_0 on the minimal required string stable time gap h is examined.
A comparison of the minimal string stable time gap h for different values of tuning parameter α is shown in Figure 3.4. A significant difference in the advantage of a-dCACC is seen for $\alpha < 0.5\ s^{-1}$. However, α should be chosen in the range $0.5 \leq \alpha \leq 1.5$ as a rule of thumb [15], for which no significant difference is observed. Changing other observer tuning parameters $a_{max} \in [0, 5]$, $P_{max} \in \left[0, \frac{1-P_0}{2}\right]$, or $P_0 \in [0, 1 - 2P_{max}]$ does not show a significant difference either.
A significant difference in minimal string stable time gap h is observed for changing driveline time constant τ_i, and visualized in Figure 3.5. This clearly shows that a-dCACC, in contrast

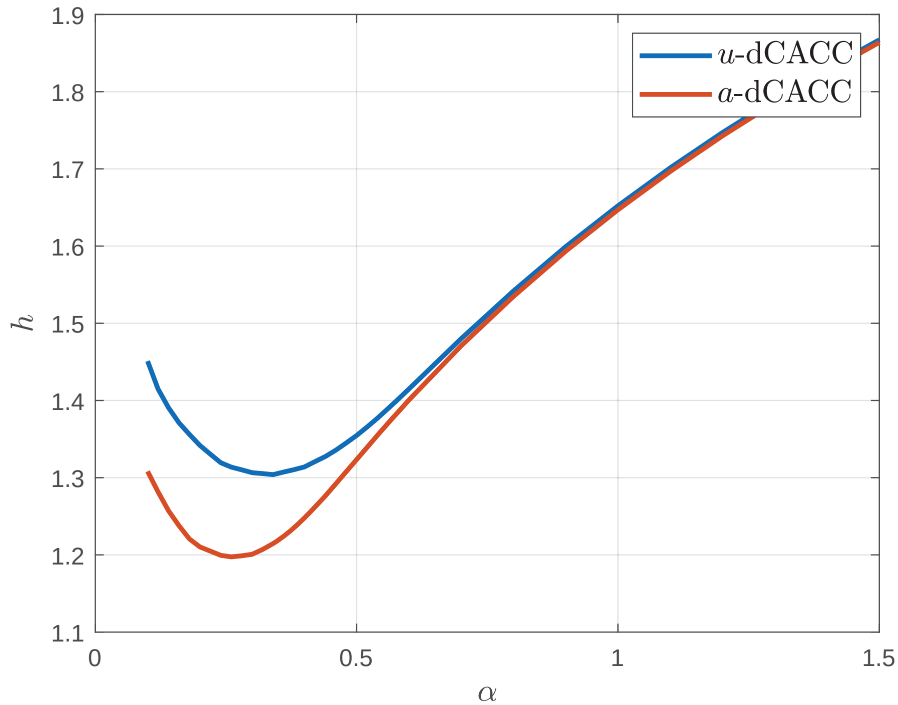

Figure 3.4: Minimal required string stable time gap h as a function of α, for u-dCACC (2.26) and a-dCACC (3.23), using parameters presented in Table 3.1.

to u-dCACC, does not lose performance for increasing driveline time constant τ_i. Actually, this is not a fair comparison, since controller gains for u-dCACC should be tuned accordingly. However, it does indicate that a-dCACC is wider applicable, since controller gains can be tuned completely independent on vehicle dynamics.

Combining the above three remarks concludes a preference in using a-dCACC rather than u-dCACC. Despite only minor differences, each difference is beneficial for a-dCACC. Moreover, a-dCACC provides a method to cope with communication impairments when employing a-CACC without requiring the need to change to a completely different controller.

3.3 Summary

As a reaction to the newly proposed a-CACC, two contributions were proposed in this chapter. The first major contribution is an analytical sufficient string stability condition enabling manual controller gain tuning guaranteeing string stability. Usefulness of this condition is shown later when it also appears in the string stability analysis of the observer-based CACC framework.
Secondly, a degraded version of a-CACC is proposed as a fallback scenario in case of communication impairments. This a-dCACC provided minor benefits compared to u-dCACC in terms of signal attenuation, string stability, and adaptability. However, it does eliminate the necessity to switch to a completely different controller in case of communication impairments when employing a-CACC.

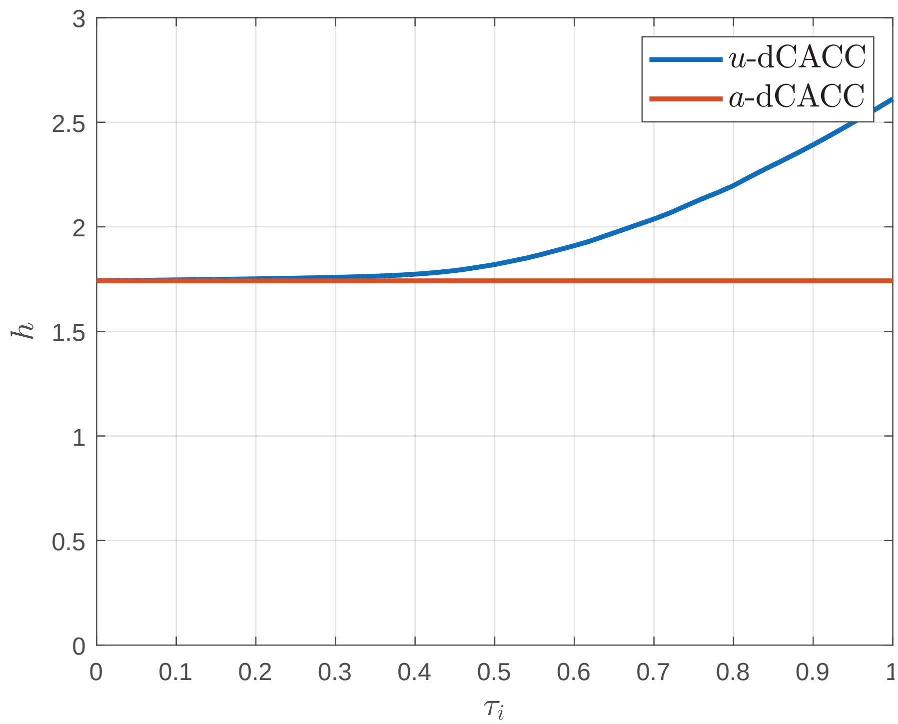

Figure 3.5: Minimal required string stable time gap h as a function of τ_i, for both u-dCACC (2.26) as well as a-dCACC (2.21) using the parameters presented in Table 3.1.

Chapter 4

CACC using observer-based control

In [10], it was shown that u-CACC is a specific class of a-CACC. Additionally, Section 3.2 presented a-dCACC to cope with communication impairments. Most important however, was the analytical sufficient string stability condition presented in Section 3.1, enabling manual controller tuning for a-CACC. Therefore, a-CACC is used within this section as a basis for the design of observer-based CACC.

Section 2.4 introduced a-CACC. Briefly restating, it defines the tracking error variables

$$\begin{aligned} e_{i,1} &:= q_{i-1} - q_i - hv_i, \\ e_{i,2} &:= v_{i-1} - v_i - ha_i, \\ \varepsilon_i &:= v_{i-1} - v_i, \qquad i \in S_I, \end{aligned} \tag{4.1}$$

and controller

$$u_i = \frac{\tau_i}{h} \underbrace{\begin{bmatrix} k_p & k_d \end{bmatrix} \begin{bmatrix} e_{i,1} \\ e_{i,2} \end{bmatrix}}_{=:\xi_i} + \left(1 - \frac{\tau_i}{h}\right) a_i + \frac{\tau_i}{h} a_{i-1}, \quad \forall \quad i \in S_I, \tag{4.2}$$

where a_{i-1} is obtained via wireless inter-vehicle communication.
The control law (4.2) clearly uses the states $e_{i,1}$, $e_{i,2}$, a_i, and a_{i-1} in the determination of the desired input. However, a vehicle might not be able to measure $e_{i,1}$, $e_{i,2}$, or a_i. Furthermore, situations exist in which $e_{i,1}$, $e_{i,2}$, a_i or a_{i-1} exhibit a rather low signal-to-noise ratio. Certainly, when reaching an equilibrium velocity for the entire platoon, essentially $a_i = 0$, the acceleration signals a_i and a_{i-1} are bound to be dominated by measurement noise. When using a lidar, and therefore not measuring relative velocity, it is even impossible to obtain $e_{i,2}$.

The above problem is solved in this chapter by proposing observer-based CACC. Note that observer-based CACC is inherently different to dCACC, which uses an observer to cope with communication impairments, whereas observer-based CACC uses observers to cope with inaccuracy or unavailability of onboard measurements while still employing inter-vehicle communication. To do so, Section 4.1 describes the problem statement, after which a general observer-based control framework is described in Section 4.2. A specific observer and controller combination is proposed in Section 4.3 for the scenario in which only relative position $q_{i-1} - q_i$ and global velocity v_i are measured. A thorough analysis on string stability, featuring a relation with a-CACC and a stepwise manual tuning procedure is presented in Section 4.4. Finally, Section 4.5 summarizes the main results of this chapter.

4.1 Problem statement

Essential to a-CACC are the (indirect) measurements of the variables $e_{i,1}$, $e_{i,2}$, a_i, and communication of a_{i-1}. Additionally, u-CACC requires knowledge of $e_{i,3}$ and u_{i-1}. Situations exist in which one is unable to (accurately) measure these states, for example a low signal-to-noise ratio of the acceleration when the platoon is at constant velocity, such that $a_i = 0$. Moreover, some vehicles do not feature the required sensors at all. A lidar for example is unable to directly measure relative velocity.
To solve this problem, it is assumed for all vehicles within the platoon to follow the linear longitudinal vehicle dynamics

$$\begin{bmatrix} \dot{q}_i \\ \dot{v}_i \\ \dot{a}_i \end{bmatrix} = \begin{bmatrix} v_i \\ a_i \\ -\frac{1}{\tau_i} a_i + \frac{1}{\tau_i} u_i \end{bmatrix}, \qquad i \in S_I, \tag{4.3}$$

where parameter τ_i is unknown within vehicles other than i.
Additionally, from practical constraints it is known that the predecessor velocity v_{i-1}, acceleration a_{i-1}, and input u_{i-1} are bounded, thus

$$\begin{aligned} |v_{i-1}(t)| &\leq v_{max} < \infty, \quad \forall\, t, \\ |a_{i-1}(t)| &\leq a_{max} < \infty, \quad \forall\, t, \\ |u_{i-1}(t)| &\leq u_{max} < \infty, \quad \forall\, t, \quad i \in S_I. \end{aligned} \tag{4.4}$$

Due to the possible inaccuracy or unavailability of other measurements, only the onboard sensors providing measurements of relative position $q_{i-1} - q_i$ (e.g., lidar) and global velocity v_i (e.g., wheel encoder) can be used. The input u_i is perfectly known within vehicle i. In addition, wireless inter-vehicle communication subject to a communication delay θ is available. Now, determine a controller achieving the following two control objectives:

1. Stable tracking dynamics; the velocity v_i, acceleration a_i, and input u_i should remain bounded when v_{i-1}, a_{i-1}, and u_{i-1} are bounded. Additionally, when the predecessor vehicle follows a constant velocity, i.e., $a_{i-1} = 0$, the tracking error should be GAS: $\lim_{t\to\infty} e_{i,1} = 0$.
2. String stable following behaviour; acceleration signals should not increase over vehicle index i in terms of their $\mathcal{L}_2$-norm. Therefore, the acceleration should satisfy $\|a_i\|_{\mathcal{L}_2} \leq \|a_{i-1}\|_{\mathcal{L}_2}$.

4.2 General framework

The first step is made by changing the controller (4.2) such that it only requires estimated states, i.e.,

$$u_i = \frac{\tau_i}{h}\xi_i + \left(1 - \frac{\tau_i}{h}\right)\hat{a}_i + \frac{\tau_i}{h}\hat{a}_{i-1}, \qquad i \in S_I. \tag{4.5}$$

A block diagram of a vehicle employing the observer-based controller (4.5) is shown in Figure 4.1. The acceleration a_i is estimated using $\hat{a}_i(s) = O_i(s)u_i(s)$, with $O_i(s)$ the acceleration observer transfer function. Similarly, the predecessor $i-1$ estimates its acceleration as $\hat{a}_{i-1}(s) = O_{i-1}(s)u_{i-1}(s)$, and sends it to vehicle i with a delay of θ. Finally, an observer-based feedback controller $C_o(s)$ is introduced, such that $\xi_i(s) = C_o(s)e_{i,1}(s) =$

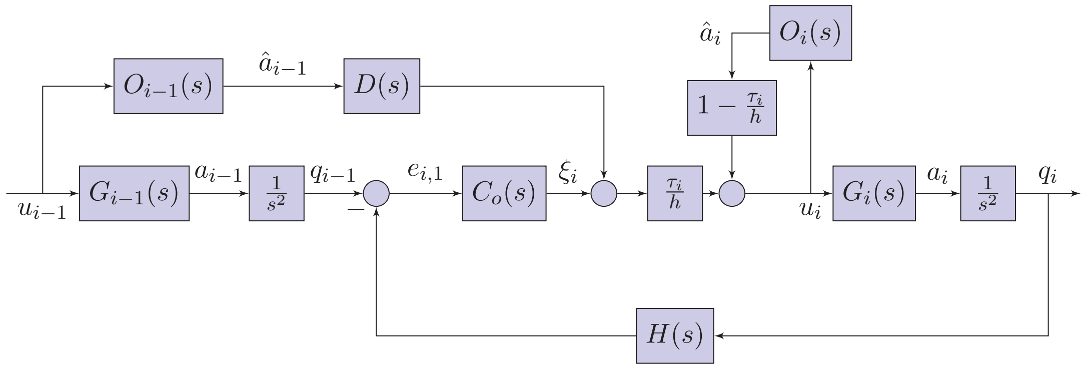

Figure 4.1: Block diagram of the general observer-based CACC framework (4.5) for a possibly heterogeneous vehicle platoon. Here, $O_i(s)$ is the acceleration observer transfer function, and $C_0(s)$ the observer-based feedback controller.

$C_o(s)\,(q_{i-1}(s) - q_i(s) - hv_i(s))$. Specific observers for $O_i(s)$, $O_{i-1}(s)$, and $C_o(s)$ are proposed in Section 4.3, requiring measurements of only relative position and global velocity.

Generality of the block diagram in Figure 4.1 can be seen by substituting specific choices for $O_{i-1}(s)$, $O_i(s)$, and $C_o(s)$. Two examples are:

- Perfect full-state measurements; then $O_{i-1}(s) = G_{i-1}(s)$, $O_i(s) = G_i(s)$, and $C_o(s) = C_a(s)$. Correspondingly, the general observer-based CACC block diagram in Figure 4.1 reduces to the block diagram of a-CACC in Figure 2.3.
- Filtered measurements; rather than using an observer, use for example a low-pass filter $F_{lp}(s) = \frac{1}{\frac{1}{\omega_c}s+1}$ with cutoff frequency ω_c to attenuate high frequent measurement noise. For example, to filter acceleration measurements choose $O_i(s) = F_{lp}(s)G_i(s)$, such that $\hat{a}_i(s) = F_{lp}(s)G_i(s)u_i(s) = F_{lp}(s)a_i(s)$ is the filtered acceleration measurement.

When using observers for $O_{i-1}(s)$, $O_i(s)$, and $C_o(s)$, it is no longer necessary to filter the measurements.
The SSCS of this general observer-based CACC can be derived from the block diagram in Figure 4.1 and is given as

$$\Gamma_{\mathrm{o}}(s) = \frac{G_i(s)}{G_{i-1}(s)} \frac{s^2 D(s) O_{i-1}(s) + C_o(s) G_{i-1}(s)}{s^2\left(\frac{h}{\tau_i} + O_i(s)(1-\frac{h}{\tau_i})\right) + H(s) C_o(s) G_i(s)}. \tag{4.6}$$

A downside to this general framework is the required knowledge of both the predecessor vehicle dynamics $G_{i-1}(s)$, and the predecessor acceleration observer $O_{i-1}(s)$ in order to analyse string stability using the SSCS (4.6).
For now, due to the absence of specific choices for $O_{i-1}(s)$, $O_i(s)$, and $C_o(s)$, no string stability analysis can be performed. However, the SSCS (4.6) does provide a rigorous basis for analysis on further work, as becomes clear in the next section.

4.3 Specific application

Where Section 4.2 showed a general observer-based control structure, this section proposes specific choices for $O_{i-1}(s)$, $O_i(s)$, and $C_o(s)$ based purely on measurements of relative position $q_{i-1} - q_i$, and global velocity v_i.
For completeness, the linear vehicle model

$$\begin{bmatrix} \dot{q}_i \\ \dot{v}_i \\ \dot{a}_i \end{bmatrix} = \begin{bmatrix} 0 & 1 & 0 \\ 0 & 0 & 1 \\ 0 & 0 & -\frac{1}{\tau_i} \end{bmatrix} \begin{bmatrix} q_i \\ v_i \\ a_i \end{bmatrix} + \begin{bmatrix} 0 \\ 0 \\ \frac{1}{\tau_i} \end{bmatrix} u_i, \qquad i \in S_I, \tag{4.7}$$

the a-CACC tracking error coordinates

$$\begin{aligned} e_{i,1} &:= q_{i-1} - q_i - hv_i, \\ e_{i,2} &:= v_{i-1} - v_i - ha_i, \\ \varepsilon_i &:= v_{i-1} - v_i, \qquad i \in S_I, \end{aligned} \tag{4.8}$$

and the tracking error dynamics

$$\begin{bmatrix} \dot{e}_{i,1} \\ \dot{e}_{i,2} \\ \dot{\varepsilon}_i \end{bmatrix} = \begin{bmatrix} 0 & 1 & 0 \\ 0 & 0 & 0 \\ 0 & \frac{1}{h} & -\frac{1}{h} \end{bmatrix} \begin{bmatrix} e_{i,1} \\ e_{i,2} \\ \varepsilon_i \end{bmatrix} + \begin{bmatrix} 0 \\ -1 \\ 0 \end{bmatrix} \xi_i + \begin{bmatrix} 0 \\ 0 \\ 1 \end{bmatrix} a_{i-1}, \qquad i \in S_I, \tag{4.9}$$

are restated. A practical choice of auxiliary input ξ_i is for example the PD controller $\xi_i := k_p e_{i,1} + k_d e_{i,2}$, such that the closed loop tracking error dynamics are

$$\begin{bmatrix} \dot{e}_{i,1} \\ \dot{e}_{i,2} \\ \dot{\varepsilon}_i \end{bmatrix} = \underbrace{\begin{bmatrix} 0 & 1 & 0 \\ -k_p & -k_d & 0 \\ 0 & \frac{1}{h} & -\frac{1}{h} \end{bmatrix}}_{=:A_a} \begin{bmatrix} e_{i,1} \\ e_{i,2} \\ \varepsilon_i \end{bmatrix} + \begin{bmatrix} 0 \\ 0 \\ 1 \end{bmatrix} a_{i-1}, \qquad \in S_I. \tag{4.10}$$

The general observer-based CACC controller (4.5) is used as a basis. In order to obtain estimated accelerations $\hat{a}_i$, and $\hat{a}_{i-1}$, and estimated tracking errors $\hat{e}_{i,1}$, and $\hat{e}_{i,2}$, two observers are proposed.

Proposition 4.1. *(Acceleration observer) Consider the linear vehicle model* (4.7) *with measurements of v_i. The input u_i is perfectly known, and the driveline time constant τ_i is determined a priori. Then, estimate the acceleration using the linear observer*

$$\begin{aligned} \hat{a}_i &= \begin{bmatrix} 0 & 1 \end{bmatrix} \begin{bmatrix} \hat{v}_i \\ \hat{a}_i \end{bmatrix}, \\ \begin{bmatrix} \dot{\hat{v}}_i \\ \dot{\hat{a}}_i \end{bmatrix} &= \begin{bmatrix} 0 & 1 \\ 0 & -\frac{1}{\tau_i} \end{bmatrix} \begin{bmatrix} \hat{v}_i \\ \hat{a}_i \end{bmatrix} + \begin{bmatrix} 0 \\ \frac{1}{\tau_i} \end{bmatrix} u_i + \begin{bmatrix} l_1^a \\ l_2^a \end{bmatrix} (v_i - \hat{v}_i), \qquad i \in S_I, \end{aligned} \tag{4.11}$$

with l_1^a, and l_2^a the observer gains. Combining the acceleration observer (4.11) *with the linear vehicle model* (4.7)*, and defining the observer error variables $\tilde{v}_i := v_i - \hat{v}_i$, and $\tilde{a}_i := a_i - \hat{a}_i$ gives observer error dynamics*

$$\begin{bmatrix} \dot{\tilde{v}}_i \\ \dot{\tilde{a}}_i \end{bmatrix} = \underbrace{\begin{bmatrix} -l_1^a & 1 \\ -l_2^a & -\frac{1}{\tau_i} \end{bmatrix}}_{=:A^a} \begin{bmatrix} \tilde{v}_i \\ \tilde{a}_i \end{bmatrix}, \qquad i \in S_I. \tag{4.12}$$

Computing the eigenvalues λ^a of the system matrix A^a gives $\lambda^a = \frac{-l_1^a - \frac{1}{\tau_i} \pm \sqrt{(l_1 + \frac{1}{\tau_i})^2 - 4(l_2 + \frac{l_1}{\tau_i})}}{2}$, from which it can be concluded that the acceleration observer error dynamics (4.12) *are GAS for $l_1^a > -\frac{1}{\tau_i}$, and $l_2^a > -\frac{l_1^a}{\tau_i}$.*
The acceleration observer (4.11) *can be rewritten using the Laplace transform*

$$\begin{aligned}\hat{a}_i(s) &= \begin{bmatrix}0 & 1\end{bmatrix}\left(sI - \begin{bmatrix}-l_1^a & 1\\ -l_2^a & -\frac{1}{\tau_i}\end{bmatrix}\right)^{-1}\left(\begin{bmatrix}0\\ \frac{1}{\tau_i}\end{bmatrix}u_i(s) + \begin{bmatrix}l_1^a\\ l_2^a\end{bmatrix}v_i(s)\right)\\ &= \frac{1}{\tau_i s^2 + (1 + l_1^a\tau_i)s + l_1^a + l_2^a\tau_i}\left((l_1^a + s)u_i(s) + (l_2^a\tau_i s)v_i(s)\right)\\ &= \frac{1}{\tau_i s^2 + (1 + l_1^a\tau_i)s + l_1^a + l_2^a\tau_i}\left((l_1^a + s) + (l_2^a\tau_i s)\frac{G_i(s)}{s}\right)u_i(s) = \frac{1}{\tau_i s + 1}u_i(s), \quad i \in S_I.\end{aligned} \tag{4.13}$$

Then, $O_i(s)$ is given as

$$O_i(s) := \frac{\hat{a}_i(s)}{u_i(s)} = \frac{1}{\tau_i s + 1} =: \hat{G}_i(s), \qquad i \in S_I. \tag{4.14}$$

Note that $\hat{G}_i(s) = G_i(s)$, because it is assumed that both τ_i and the vehicle model $G_i(s)$ are perfectly known. The choice however, is made to keep the notation of $\hat{G}_i(s)$, such that it can be used to test the effect of a difference in τ_i or $G_i(s)$ later.

Proposition 4.2. *(Observer-based PD controller) Consider the tracking error dynamics* (4.9) *with measurements of $q_{i-1} - q_i$ and v_i, such that $e_{i,1} := q_{i-1} - q_i - hv_i$ is measured indirectly. Instead of the previously used PD controller $\xi_i = k_p e_{i,1} + k_d e_{i,2}$, generate ξ_i with the observer*

$$\begin{aligned}\xi_i &= \begin{bmatrix}k_p & k_d\end{bmatrix}\begin{bmatrix}\hat{e}_{i,1}\\ \hat{e}_{i,2}\end{bmatrix},\\ \begin{bmatrix}\dot{\hat{e}}_{i,1}\\ \dot{\hat{e}}_{i,2}\end{bmatrix} &= \begin{bmatrix}0 & 1\\ 0 & 0\end{bmatrix}\begin{bmatrix}\hat{e}_{i,1}\\ \hat{e}_{i,2}\end{bmatrix} + \begin{bmatrix}0\\ -1\end{bmatrix}\xi_i + \begin{bmatrix}l_1^e\\ l_2^e\end{bmatrix}(e_{i,1} - \hat{e}_{i,1}), \qquad i \in S_I,\end{aligned} \tag{4.15}$$

where l_1^e, and l_2^e are the observer gains. Combining the observer (4.15) *with the tracking error dynamics* (4.9)*, and defining the observer error variables $\tilde{e}_{i,1} := e_{i,1} - \hat{e}_{i,1}$, and $\tilde{e}_{i,2} := e_{i,2} - \hat{e}_{i,2}$ gives observer error dynamics*

$$\begin{bmatrix}\dot{\tilde{e}}_{i,1}\\ \dot{\tilde{e}}_{i,2}\end{bmatrix} = \underbrace{\begin{bmatrix}-l_1^e & 1\\ -l_2^e & 0\end{bmatrix}}_{=:A^e}\begin{bmatrix}\tilde{e}_{i,1}\\ \tilde{e}_{i,2}\end{bmatrix}, \qquad i \in S_I. \tag{4.16}$$

Computing the eigenvalues λ^e of the system matrix A^e gives $\lambda^e = \frac{-l_1^e \pm \sqrt{{l_1^e}^2 - 4l_2^e}}{2}$, from which it can be concluded that the tracking observer error dynamics (4.12) *are GAS for $l_1^e > 0$, and $l_2^e > 0$.*
Laplace transformation of the observer-based PD controller (4.15) *gives*

$$C_o(s) := \frac{\xi_i(s)}{e_{i,1}(s)} = \frac{k_p l_2^e + (k_p l_1^e + k_d l_2^e)\,s}{s^2 + (k_d + l_1^e)s + l_1^e k_d + l_2^e + k_p} =: \frac{k_p + k_d s + k_p c_2 s}{1 + c_1 s^2 + (k_d c_1 + c_2)s + k_d c_2 + k_p c_1}, \tag{4.17}$$

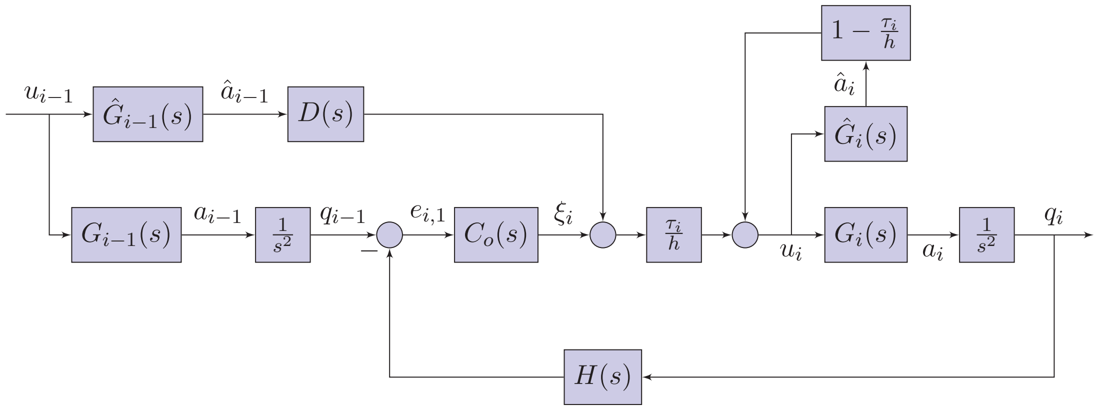

Figure 4.2: Block diagram of observer-based CACC (4.18), with acceleration observer (4.11), and observer-based PD controller $C_o(s)$ (4.15) for a possibly heterogeneous platoon. Here, $D(s) := e^{-\theta s}$, $H(s) := hs + 1$, $\hat{G}_i(s) = G_i(s) := \frac{1}{\tau_i s+1}$ the vehicle model.

with $c_1 := \frac{1}{l_2^e}$ and $c_2 := \frac{l_1^e}{l_2^e}$. Clearly, for $c_1, c_2 = 0$, $C_o(s)$ in (4.17) reduces to the regular PD controller $C_a(s) = k_p + k_d s$. Note however, that it is impossible to achieve $c_1, c_2 = 0$ using a bounded observer gain l_2^e.

Combining both observers, results in the proposition of the use of controller

$$u_i = \underbrace{\frac{\tau_i}{h}\begin{bmatrix}k_p & k_d\end{bmatrix}\begin{bmatrix}\hat{e}_{i,1} \\ \hat{e}_{i,2}\end{bmatrix}}_{=:\xi_i} + \left(1 - \frac{\tau_i}{h}\right)\hat{a}_i + \frac{\tau_i}{h}\hat{a}_{i-1}(t-\theta), \quad \forall \quad i \in S_I. \tag{4.18}$$

where $\hat{a}_i$ and $\hat{a}_{i-1}$ are generated onboard with observer (4.11) by vehicles i and $i-1$, respectively. The estimation $\hat{a}_{i-1}$ is achieved by wireless inter-vehicle communication experiencing a communication delay of θ. Additionally ξ_i is the output of observer (4.15), which estimates $\hat{e}_{i,1}$ and $\hat{e}_{i,2}$.

The observer-based CACC system using the acceleration observer (4.11), and observer-based PD controller (4.15) is schematically depicted with the block diagram in Figure 4.2. Using the block diagram, it is possible to derive the SSCS

$$\Gamma_o(s) := \frac{a_i(s)}{a_{i-1}(s)} = \frac{1}{H(s)}\frac{s^2 D(s) + C_o(s)}{s^2 + C_o(s)}, \tag{4.19}$$

with observer-based PD controller $C_o(s)$ given in (4.17), spacing policy $H(s) := hs + 1$, and communication delay $D(s) := e^{-\theta s}$. Here it is used that $\hat{G}_{i-1}(s) = G_{i-1}(s)$, and $\hat{G}_i(s) = G_i(s)$ when vehicles $i-1$, and i both use acceleration observer (4.11) to estimate their own acceleration.

The goal is now to show as to why the observer-based CACC controller (4.18) is a solution to the problem statement in Section 4.1. To do so, control objective 1 is proven below. Control objective 2 is relocated to the dedicated Section 4.4.

The control law (4.18) can be rewritten to

$$
\begin{aligned}
u_i &= \frac{\tau_i}{h}\begin{bmatrix} k_p & k_d \end{bmatrix}\begin{bmatrix} \hat{e}_{i,1} \\ \hat{e}_{i,2} \end{bmatrix} + \left(1 - \frac{\tau_i}{h}\right)\hat{a}_i + \frac{\tau_i}{h}\hat{a}_{i-1}(t-\theta), \qquad i \in S_I \\
&= \frac{\tau_i}{h}\begin{bmatrix} k_p & k_d \end{bmatrix}\left(\begin{bmatrix} e_{i,1} \\ e_{i,2} \end{bmatrix} - \begin{bmatrix} \tilde{e}_{i,1} \\ \tilde{e}_{i,2} \end{bmatrix}\right) + \left(1 - \frac{\tau_i}{h}\right)(a_i - \tilde{a}_i) + \frac{\tau_i}{h}\left(a_{i-1}(t-\theta) - \tilde{a}_{i-1}(t-\theta)\right).
\end{aligned}
\tag{4.20}
$$

Using the observer-based CACC controller (4.20), in combination with acceleration observer (4.11), tracking error observer (4.15), tracking error coordinates (4.1), and vehicle dynamics (4.7), results in the closed loop dynamics

$$
\underbrace{\left[\begin{array}{c} \dot{e}_{i,1} \\ \dot{e}_{i,2} \\ \dot{\varepsilon}_i \\ \hline \dot{\tilde{e}}_{i,1} \\ \dot{\tilde{e}}_{i,2} \\ \hline \dot{\tilde{v}}_i \\ \dot{\tilde{a}}_i \\ \hline \dot{\tilde{v}}_{i-1}(t-\theta) \\ \dot{\tilde{a}}_{i-1}(t-\theta) \end{array}\right]}_{=:\dot{x}_i}
=
\left[\begin{array}{ccc|cc|cc|cc}
0 & 1 & 0 & 0 & 0 & 0 & 0 & 0 & 0 \\
-k_p & -k_d & 0 & k_p & k_d & 0 & 1-\frac{\tau_i}{h} & 0 & 1 \\
0 & \frac{1}{h} & -\frac{1}{h} & 0 & 0 & 0 & 0 & 0 & 0 \\
\hline
0 & 0 & 0 & -l_1^e & 1 & 0 & 0 & 0 & 0 \\
0 & 0 & 0 & -l_2^e & 0 & 0 & 1-\frac{\tau_i}{h} & 0 & 1 \\
\hline
0 & 0 & 0 & 0 & 0 & -l_1^a & 1 & 0 & 0 \\
0 & 0 & 0 & 0 & 0 & -l_2^a & -\frac{1}{\tau_i} & 0 & 0 \\
\hline
0 & 0 & 0 & 0 & 0 & 0 & 0 & -l_1^a & 1 \\
0 & 0 & 0 & 0 & 0 & 0 & 0 & -l_2^a & -\frac{1}{\tau_i}
\end{array}\right]
\left[\begin{array}{c} e_{i,1} \\ e_{i,2} \\ \varepsilon_i \\ \hline \tilde{e}_{i,1} \\ \tilde{e}_{i,2} \\ \hline \tilde{v}_i \\ \tilde{a}_i \\ \hline \tilde{v}_{i-1}(t-\theta) \\ \tilde{a}_{i-1}(t-\theta) \end{array}\right]
$$

$$
+ \left[\begin{array}{ccc|cc|cc|cc} 0 & 0 & 1 & 0 & 0 & 0 & 0 & 0 & 0 \\ 0 & 1 & 0 & 0 & 1 & 0 & 0 & 0 & 0 \end{array}\right]^T \begin{bmatrix} a_{i-1} \\ a_{i-1} - a_{i-1}(t-\theta) \end{bmatrix}.
\tag{4.21}
$$

Here, A_a, A^e, and A^a (twice) are recognized on the diagonal of system matrix, concluding it to be Hurwitz for $k_p, k_d, l_1^e, l_2^e > 0$ $l_1^a > -\frac{1}{\tau_i}$, and $l_2^2 > -\frac{l_1^a}{\tau_i}$ (separation principle). Then, x_i is ISS with respect to $w_{i-1} := \begin{bmatrix} a_{i-1} & a_{i-1} - a_{i-1}(t-\theta) \end{bmatrix}^T$. In particular, bounded w_{i-1} give bounded x_i, and w_{i-1} converging to zero gives x_i converging to zero. Note that the assumed boundedness of a_{i-1} and u_{i-1} implies bounded w_i. Additionally, $|a_{i-1} - a_{i-1}(t-\theta)| \leq |a_{i-1}| + |a_{i-1}(t-\theta)|$, which converges to zero when a_{i-1} converges to zero.
Using the coordinate transformation (4.8), in combination with the control law (4.18) shows that v_i, a_i, and u_i remain bounded as well, and therefore objective 1 is satisfied.

Table 4.1: $\mathcal{L}_2$-norms of acceleration signals for different CACC controllers resulting from the basic simulation, using the parameters $k_p = 0.2$, $k_d = 0.7$, $l_1^a = l_2^a = 0$, $l_1^e = 2.8$, $l_2^e = 2.0$, $\tau = 0.1$ s, $\theta = 0.02$ s, $h = 0.5$ s, and input $u_1(t)$ as given in (4.22).

Vehicle	***u*-CACC**	***a*-CACC**	**Observer-based**
$i = 1$	3.13	3.13	3.13
$i = 2$	3.00	2.99	3.00
$i = 3$	2.92	2.90	2.93
$i = 4$	2.86	2.84	2.88
$i = 5$	2.81	2.78	2.84
$i = 6$	2.76	2.73	2.80

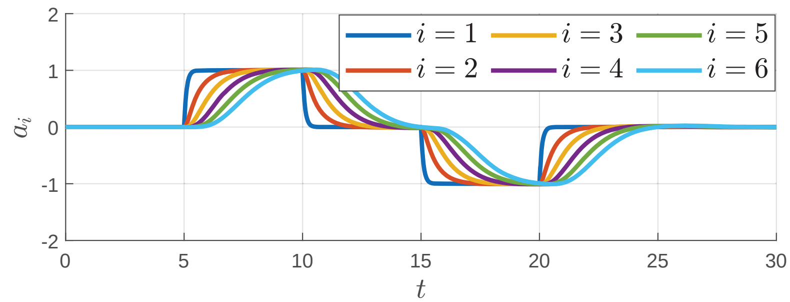

Figure 4.3: Basic simulation results showing acceleration a_i over time t for a platoon of $I = 6$ vehicles employing observer-based CACC, using $k_p = 0.2$, $k_d = 0.7$, $k_{dd} = 0$, $l_1^a = l_2^a = 0$, $l_1^e = 2.8$, $l_2^e = 2.0$, $h = 0.5\ s$, and $\theta = 0.02\ s$.

Basic simulation results of observer-based CACC, as visualized in the block diagram of Figure 4.2, for a homogeneous platoon of $I = 6$ vehicles, are shown in Figure 4.3. This basic simulation uses the parameters $k_p = 0.2$, $k_d = 0.7$, $l_1^a = l_2^a = 0$, $l_1^e = 2.8$, $l_2^e = 2.0$, $\tau = 0.1\ s$, $\theta = 0.02\ s$, $h = 0.5\ s$, and input

$$u_1(t) = \begin{cases} 1, & \text{if} \quad 5 \leq t \leq 10, \\ -1, & \text{if} \quad 15 \leq t \leq 20, \\ 0, & \text{else.} \end{cases} \tag{4.22}$$

Moreover, Table 4.1 shows the $\mathcal{L}_2$-norms of the acceleration using different CACC controllers. These controller gains achieve similar settling time and maximal jerk as a response to a step input for the different CACC controllers. As expected, observer-based CACC performs worse than u-CACC and a-CACC in terms of attenuation of the acceleration $\mathcal{L}_2$-norms. However, it does only require measurements of relative position $q_{i-1} - q_i$ and global velocity v_i. Note that, for the choice of $l_1^a = l_2^a = 0$, the acceleration observer (4.11) reduces to

$$\dot{\hat{a}}_i = -\frac{1}{\tau_i}\hat{a}_i + \frac{1}{\tau_i}u_i, \qquad i \in S_I. \tag{4.23}$$

The observer (4.23) in combination with the vehicle dynamics (4.7) gives the GAS observer error dynamics

$$\dot{\tilde{a}}_i := \dot{a}_i - \dot{\hat{a}}_i = -\frac{1}{\tau_i}\tilde{a}_i, \qquad i \in S_I. \tag{4.24}$$

Important to note here is that the choice of $l_1^a = l_2^a = 0$ causes the observer to be vulnerable to model inaccuracies. The reason for this choice becomes clear in Chapter 5, where observer-based CACC is implemented in a more complex simulation environment, which includes actuator delays.

4.4 String stability analysis

This section analyses string stability of observer-based CACC (4.18) using the string stability condition

$$|\Gamma(j\omega)| \ \leq \ 1, \quad \forall \quad \omega \in \mathbb{R}. \tag{4.25}$$

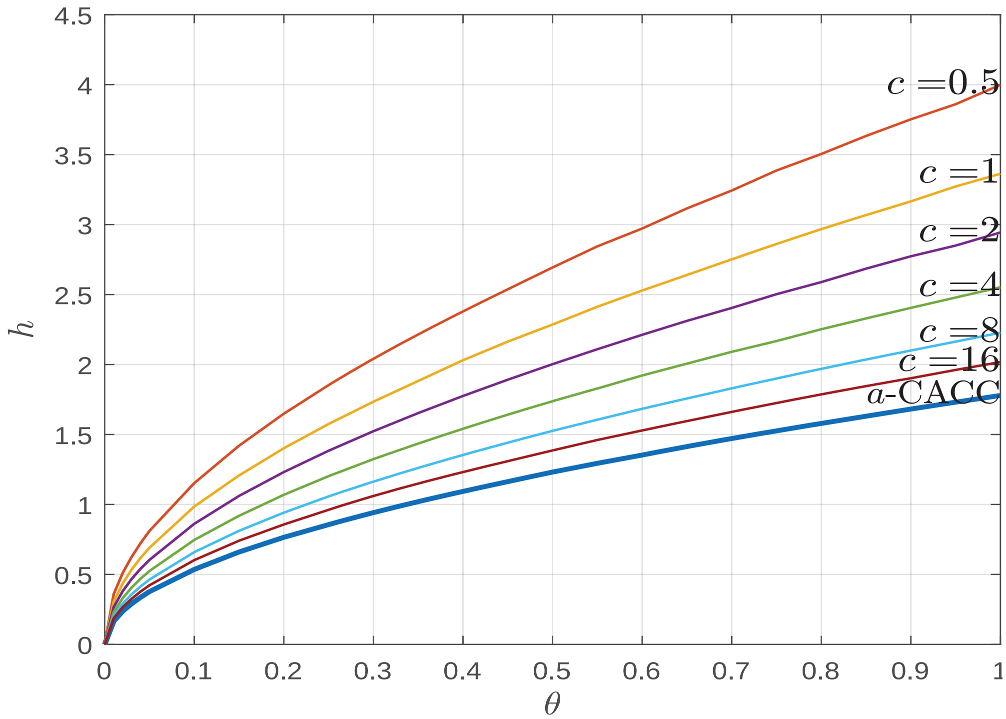

Figure 4.4: Iteratively determined minimal string stable time gap h as a function of communication delay θ, for a-CACC and observer-based CACC using $k_p = 0.2$ and $k_d = 0.7$. Observer gains are tuned to achieve $\frac{\mathrm{Re}\{\lambda_o\}}{\mathrm{Re}\{\lambda_a\}} = c$, and $\frac{\mathrm{Im}\{\lambda_o\}}{\mathrm{Im}\{\lambda_a\}} = 1$.

The observer-based CACC SSCS (4.19) gives the observer-based string stability condition

$$\left| \frac{1}{H(\omega j)} \frac{-\omega^2 D(\omega j) + C_o(\omega j)}{-\omega^2 + C_o(\omega j)} \right|^2 \leq 1, \quad \forall \quad \omega \in \mathbb{R}, \tag{4.26}$$

with $H(s) := hs + 1$, $D(s) := e^{-\theta s}$, and $C_o(s)$ the observer-based PD controller (4.17).

Figure 4.4 shows the iteratively determined minimal string stable time gap h using a-CACC and observer-based CACC with $k_p = 0.2$ and $k_d = 0.7$. Observer gains l_1^e and l_2^e are chosen such that the real part of the eigenvalues of the observer error dynamics (4.16) are a factor c of the a-CACC tracking error dynamics (4.9) eigenvalues. The computation of the observer gains l_1^e and l_2^e as a function of factor c is derived in the following remark.

Remark 4.1. *(Observer tuning) The eigenvalues λ_a of the tracking error dynamics* (4.9) *are*

$$\begin{aligned} &\det\left(\begin{bmatrix} 0 & 1 \\ -k_p & -k_d \end{bmatrix} - \lambda_a I \right) = 0, \\ &\Rightarrow \lambda_a = -\frac{1}{2}k_d \pm \frac{1}{2}\sqrt{k_d^2 - 4k_p}. \end{aligned} \tag{4.27}$$

For the specific choices $k_p = 0.2$, and $k_d = 0.7$, $k_d^2 - 4k_p < 0$ resulting in complex eigenvalues

λ_a. *The eigenvalues* λ_o *of the observer error dynamics* (4.16) *are given as*

$$
\begin{aligned}
&\det\left(\begin{bmatrix} -l_1^e & 1 \\ -l_2^e & 0 \end{bmatrix} - \lambda_o I\right) = 0, \\
&\Rightarrow \lambda_o = -\frac{1}{2} l_1^e \pm \frac{1}{2}\sqrt{l_1^{e\,2} - 4 l_2^e},
\end{aligned}
\tag{4.28}
$$

and should satisfy $\mathrm{Re}\{\lambda_o\} = c\ \mathrm{Re}\{\lambda_a\}$ *and* $\mathrm{Im}\{\lambda_o\} = \mathrm{Im}\{\lambda_a\}$, *with* $c > 0$, *and* $\mathrm{Re}\{\cdot\}$ *and* $\mathrm{Im}\{\cdot\}$ *indicating the real and imaginary parts, respectively. Therefore, the observer gains are computed as*

$$
\begin{aligned}
\mathrm{Re}\{\lambda_o\} = c\mathrm{Re}\{\lambda_a\} \quad &\Rightarrow \quad l_1^e = c k_d, \\
\mathrm{Im}\{\lambda_o\} = \mathrm{Im}\{\lambda_a\} \quad &\Rightarrow \quad l_2^e = k_p - \frac{1}{4}\left(1 - c^2\right) k_d^2.
\end{aligned}
\tag{4.29}
$$

Figure 4.4 shows a loss in performance, i.e., a larger minimal string stable time gap h when employing observer-based CACC. However, this loss in performance reduces when placing the eigenvalues λ_o further in the complex left half-plane, or, similarly, choosing c larger. This immediately raises the question whether observer-based CACC can be tuned to achieve string stability for a comparable time gap h with respect to a-CACC. The following proposition provides an answer to this question.

Proposition 4.3. *(Sufficient string stability) Define* $h_{\min}^{\mathrm{nec}}$ *as the minimum value of* h *for which* $\left\|\Gamma_a^{\mathrm{CACC}}(j\omega)\right\|_{\mathcal{H}_\infty} \leq 1$ *is satisfied. Assume that* k_p *and* k_d *are chosen such that* $k_d^2 - 2k_p > 0$. *Additionally, choose* h *such that* $h^2 = h_{\min}^{\mathrm{nec}\,2} + h_{\mathrm{saf}}^2$, *with* h_{saf}^2 *a safety margin (or similarly choose* $h = h_{\min}^{\mathrm{nec}} + \delta$, *with margin* $\delta > 0$, *such that* $h_{\mathrm{saf}}^2 = 2\delta h_{\min}^{\mathrm{nec}} + \delta^2$*). Choose a safety factor* $c_{\mathrm{saf}} \geq 1$, *and choose the observer gains*

$$
\begin{aligned}
l_1^e &= c_{\mathrm{saf}}\left(c_{1,1} + c_{1,2}\sqrt{l_2^e}\right), \\
l_2^e &\geq \max_{n\in[2,3]}\left(\frac{c_{\mathrm{saf}} c_{1,2} c_{n,2} + \sqrt{c_{\mathrm{saf}}^2 c_{1,2}^2 c_{n,2}^2 + 4\left(c_{n,1} + c_{\mathrm{saf}} c_{1,1} c_{n,2}\right)}}{2}\right)^2,
\end{aligned}
\tag{4.30}
$$

with the coefficients defined as

$$
\begin{aligned}
c_{1,1} &:= \frac{1}{3} k_p \frac{\theta^3}{h^2}, \\
c_{1,2} &:= \sqrt{2 + \frac{1}{3} k_d \frac{\theta^3}{h^2}}, \\
c_{2,1} &:= \frac{2h^2\left(k_d^2 - 2k_p\right) + k_d^2\theta^2}{h_{\mathrm{saf}}^2}, \\
c_{2,2} &:= \frac{k_d\theta^2 + h_{\mathrm{saf}}\sqrt{k_p + 3k_d\frac{h^2}{\theta^3}}\,\theta}{h_{\mathrm{saf}}^2}, \\
c_{3,1} &:= \frac{\left(2h^2 + \theta^2\right) k_p^2}{\left(k_d^2 - 2k_p\right) h_{\mathrm{saf}}^2}, \\
c_{3,2} &:= \frac{2k_d^2\theta + k_p k_d\theta^2 + h_{\mathrm{saf}}\sqrt{2\left(k_d^2 - 2k_p\right)\left(k_p k_d + 3k_p\frac{h^2}{\theta^3}\right)\theta}}{\left(k_d^2 - 2k_p\right) h_{\mathrm{saf}}^2}.
\end{aligned}
\tag{4.31}
$$

Then, for the chosen h, string stability is achieved using observer-based CACC.

The proof of Proposition 4.3 is relocated to Appendix D.

From Proposition 4.3 it can be seen that a platoon employing observer-based CACC can be made string stable, if it is string stable when employing a-CACC with a (possibly small) margin δ. The observer gains l_1^e and l_2^e approach infinity when δ approaches zero when using the conditions in Proposition 4.3. This might be due to the conservatism of the conditions in Proposition 4.3. Note that, for $l_1^e = 0$, and $l_2^e \to \infty$, it was shown in (4.17) that $C_o(s) = C_a(s)$, and therefore $\Gamma_{\mathrm{o}}(s) = \Gamma_a(s)$, such that observer-based CACC and a-CACC have identical string stable behaviour.

In the next part, a method is derived that uses Proposition 4.3 indirectly to manually tune controller and observer gains. Currently, it requires knowledge of $h_{\min}^{\mathrm{nec}}$, which cannot be determined analytically from the controller gains and communication delay. As a first step, it is shown that, when satisfying the string stability sufficient condition for a-CACC

$$h \geq \frac{1}{k_d}\sqrt{\theta\left(2k_d + \theta k_p\right)}, \tag{4.32}$$

it is possible to remain string stable using observer-based CACC with bounded observer gains. To do so, define $h_{\min}^{\mathrm{suf}}$ as the minimal time gap h for which the sufficient string stability condition (4.32) is satisfied, i.e., $h_{\min}^{\mathrm{suf}} := \frac{1}{k_d}\sqrt{\theta\left(2k_d + \theta k_p\right)}$. Now define $\epsilon := h_{\min}^{\mathrm{suf}} - h_{\min}^{\mathrm{nec}}$, for which it is known that $\epsilon \geq 0$ due to conservatism of the sufficient string stability condition (4.32). If it can be shown that $\epsilon > 0$, it is possible to choose $\delta = \epsilon > 0$ in Proposition 4.3, such that observer-based CACC (4.18) is string stable for $h_{\min}^{\mathrm{suf}}$ in combination with bounded gains. Below follows the proof that $\epsilon > 0$.

Proof. The sufficient string stability condition for a-CACC (4.32) was derived from inequality

$$\underbrace{h^2\omega^4 + \left[h^2(k_d^2 - 2k_p) - 2k_d\theta - k_p\theta^2\right]\omega^2 + h^2k_p^2}_{=:P_{suf}(\omega)} \geq 0, \qquad \forall \quad \omega \in \mathbb{R}. \tag{4.33}$$

Therefore, $h_{\min}^{\mathrm{suf}}$ is the minimal value of h for which (4.33) is satisfied. Additionally, $h_{\min}^{\mathrm{nec}}$ is the minimal value of h for which the necessary and sufficient string stability condition

$$\underbrace{h^2\omega^4 + h^2\left(k_d^2 - 2k_p\right)\omega^2 - 2k_d\sin(\theta\omega)\omega + h^2k_p^2 + 2k_p\left(\cos(\theta\omega) - 1\right)}_{=:P_{nec}(\omega)} \geq 0, \quad \forall \quad \omega \in \mathbb{R}, \tag{4.34}$$

is satisfied. For $\omega, \theta \neq 0$, strict inequalities $\cos(\theta\omega) > 1 - \frac{1}{2}\theta^2\omega^2$ and $\omega\sin(\theta\omega) < \theta\omega^2$ are obtained, and therefore

$$P_{nec}(\omega) > P_{suf}(\omega), \quad \forall \quad \omega \in \mathbb{R}\setminus\{0\},\ \theta > 0. \tag{4.35}$$

From the strict inequality (4.35), and the facts that $\theta > 0$ and $\Gamma_{\mathrm{o}}(j0) = \Gamma_a^{\mathrm{CACC}}(j0) = 1$, it directly follows that $h_{\min}^{\mathrm{nec}} < h_{\min}^{\mathrm{suf}}$, and, correspondingly, $\epsilon = h_{\min}^{\mathrm{nec}} - h_{\min}^{\mathrm{suf}} > 0$. □

Straightforwardly, it is also possible to choose $\delta > \epsilon$, such that string stability is achieved for $h = h_{\min}^{\mathrm{nec}} + \delta > h_{\min}^{\mathrm{nec}} + \epsilon = h_{\min}^{\mathrm{suf}}$. Based on this idea, a stepwise manual tuning procedure is proposed, which does not require numerically determined parameters, i.e., $h_{\min}^{\text{nec}}$ and ϵ. The tuning procedure is presented in the following remark, and substantiated with a visualization in Figure 4.5.

In order to achieve a string stable observer-based CACC controller (4.18), follow the manual stepwise tuning procedure:

1. Desired time gap h^{des} (yellow line, Figure 4.5); choose a desired time gap h^{des} for which string stability should be achieved using observer-based CACC. This can, for example, be done based on system requirements.
2. Controller gains k_p, k_d (red line, Figure 4.5); choose a margin $\Delta > 0$, such that $\Delta := h^{\text{des}} - h_{\min}^{\text{suf}}$. Substitute $h_{\min}^{\text{suf}}$ in sufficient string stability condition for a-CACC (4.32), and choose k_p and k_d, such that it is satisfied with equality. The larger the margin Δ is chosen, the smaller the observer gains can be.
3. Observer gains l_1^e, l_2^e (blue line, Figure 4.5); tune the observer gains using conditions (4.30) with $h_{\text{saf}}^2 = 2\Delta h_{min}^{saf} + \Delta^2$.

Then, string stability is guaranteed, because $\delta = \Delta + \epsilon > \Delta$. Essentially, the chosen margin

$$\begin{aligned} h_{\text{saf}}^2 &= 2\Delta h_{\min}^{\text{suf}} + \Delta^2 \\ &= 2\left(\delta - \epsilon\right)\left(h_{\min}^{\text{nec}} + \epsilon\right) + \left(\delta - \epsilon\right)^2 \\ &= 2\delta h_{\min}^{\text{nec}} + \delta^2 - \epsilon\left(\epsilon + 2h_{\min}^{\text{nec}}\right) < 2\delta h_{\min}^{\text{nec}} + \delta^2, \end{aligned} \tag{4.36}$$

is taken restrictive, since string stability was proven for the smaller $h_{\text{saf}}^2 = 2\delta h_{\min}^{\text{nec}} h_{\min}^{\text{nec}} + \delta^2$ in Proposition 4.3. Conservatism of both Proposition 4.3 and the choice of h_{saf}^2 causes string stability to be achieved for smaller values than h^{des}. The minimal time gap $h_{\text{min, observer}}^{\text{nec}}$ which achieves string stability using observer-based CACC, is numerically determined and shown with the purple line in Figure 4.5.

4.5 Summary

This chapter introduced observer-based CACC. First, the problem statement was presented in Section 4.1, followed by the introduction of a general observer-based CACC framework. This general framework can be used in situations varying from the use of a low-pass filter for noisy measurements, up until complete observer-based control. As a solution to the problem statement, a specific observer-controller combination was proposed in Section 4.3, which only required measurements of relative position and global velocity. A thorough analysis on string stability for observer-based CACC, recapitulating on a-CACC, was presented in Section 4.4. Noteworthy was the method to split the string stability definition in two separate parts; a-CACC, and an extra part induced by observer-based CACC. This enabled the derivation of a manual tuning procedure based on the sufficient string stability condition for a-CACC in combination with some additional conditions.

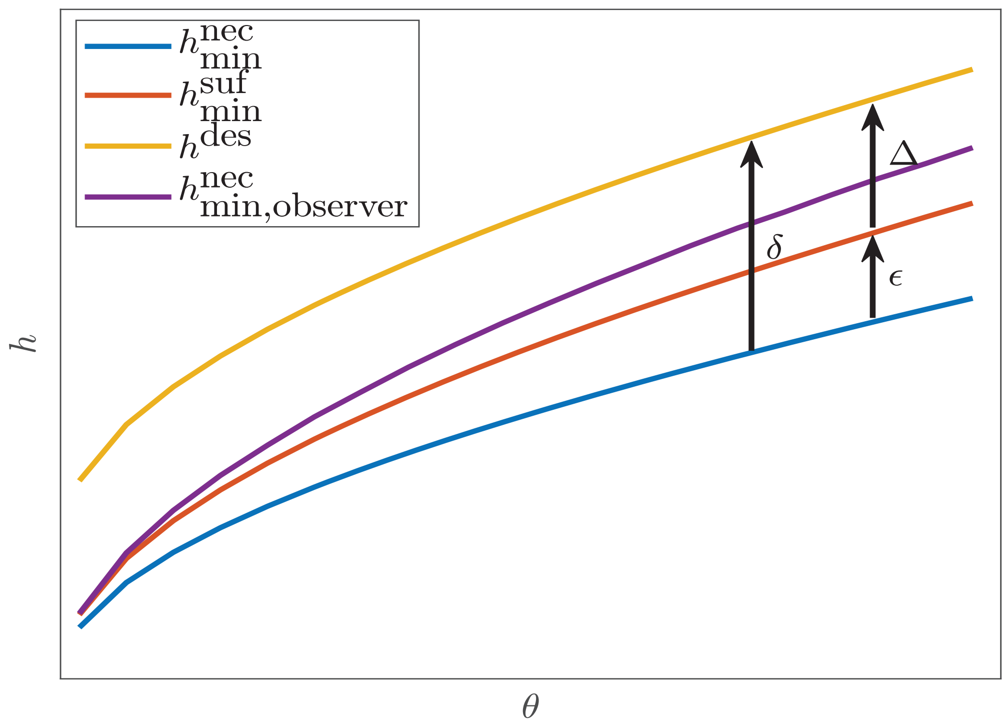

Figure 4.5: Visualization of the manual tuning procedure for observer-based CACC (4.18).

Chapter 5

Discrete-time CACC verification

Basic simulation results were previously shown in this report, u-CACC and a-CACC were presented in Figure 2.2, and Table 2.1, and observer-based CACC in Figure 4.3, and Table 4.1. In practical situations, the CACC controllers are implemented in discrete time, measurements are subject to noise, and vehicles exhibit an actuator delay. To test the usefulness of the CACC controllers under these conditions, u-CACC, a-CACC, and observer-based CACC are implemented in a more complex simulation environment, for a homogeneous platoon S_I of length $I = 6$.

This chapter focusses on the results of the complex simulation environment. More specifically, Section 5.1 introduces the complex simulation environment. Afterwards, simulation results are presented for vehicles with and without an actuator delay in Sections 5.2, and 5.3, respectively.

5.1 Simulation environment

Within the complex simulation environment, each vehicle is divided in different submodules, which are schematically depicted in Figure 5.1.

The Platooning Control System (PCS) contains the CACC controllers, and determines the desired acceleration u_i based on vehicle data, radar measurements, and predecessor vehicle data obtained via wireless communication. A clustering algorithm is implemented in the PCS, which couples the Vehicle-to-Vehicle (V2V) communication and radar measurements to a specific vehicle.

The V2V communication is mimicked in the V2V submodule, and experiences a communication delay θ. Both the desired acceleration u_{i-1}, and actual acceleration a_{i-1} can be communicated.

Radar measurements are mimicked in the Radar submodule, and exhibit measurement noise with variances $\sigma^2_{\Delta q}$, and $\sigma^2_{\Delta v}$ for relative position $q_{i-1} - q_i$, and relative velocity $v_{i-1} - v_i$, respectively. Moreover, the radar is able to run at a maximum frequency of 14 Hz.

The Vehicle submodule mimics the vehicle dynamics, and generates measurements of the velocity v_i, and acceleration a_i, which are subject to measurement noise with a variance of σ^2_v, and σ^2_a, respectively. The length of the vehicle is denoted with L_i. Moreover, the vehicle

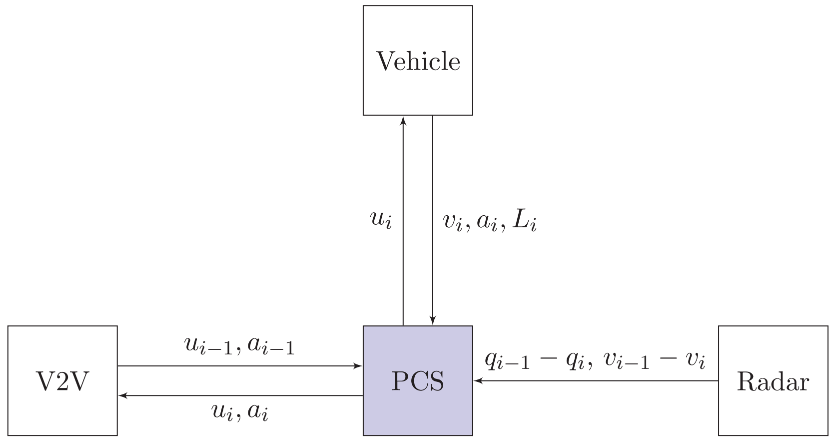

Figure 5.1: Overview of the complex simulation environment, with PCS the implementation of the CACC controller, and the modules V2V, Vehicle, and Radar mimicking the wireless communication, vehicle, and radar.

experiences an actuator delay ϕ, such that its dynamics are given as

$$\dot{a}_i(t) = -\frac{1}{\tau_i} a_i(t) + \frac{1}{\tau_i} u_i(t - \phi), \qquad i \in S_I. \tag{5.1}$$

Parameter values used within the simulations are summarized in Table 5.1, where T_s indicates the sampling time for each submodule. Since the actuator delay appears to drastically affect string stability, simulations are performed both with and without this actuator delay.

Table 5.1: Parameter values used within the complex simulation environment.

Submodule	**Parameter**	**Value**
PCS	k_p	0.2
	k_d	0.7
	k_{dd}	0
	l_1^a	0
	l_2^a	0
	l_1^e	2.8
	l_2^e	2.0
	h	0.5 s
	T_s	0.02 s
V2V	θ	0.02 s
	T_s	0.02 s
Radar	$\sigma^2_{\Delta q}$	0.1 m^2
	$\sigma^2_{\Delta v}$	0.15 m^2
	T_s	0.08 s
Vehicle	τ	0.1 s
	ϕ	0.2 s
	L_i	6 m
	T_s	0.02 s

Time simulations do not give a conclusive answer regarding string stability, because all possible input signals should be simulated to do so. This can be seen from the string stability Theorem 2.1, which requires that

$$\|\Gamma(j\omega)\|_{\mathcal{H}_\infty} \leq 1. \tag{5.2}$$

Note that the $\mathcal{H}_\infty$-norm is induced by the $\mathcal{L}_2$-norm of the input and output, such that

$$\|\Gamma(j\omega)\|_{\mathcal{H}_\infty} := \max_{a_{i-1}} \frac{\|a_i(t)\|_{\mathcal{L}_2}}{\|a_{i-1}(t)\|_{\mathcal{L}_2}}. \tag{5.3}$$

Assuming that acceleration signals are converged to zero when the simulation stops, it is possible to compute their $\mathcal{L}_2$-norms. To compute $\|\Gamma(j\omega)\|_{\mathcal{H}_\infty}$, all possible signals $a_{i-1}(t)$ must be simulated, which is impossible. Therefore, if $\|a_i(t)\|_{\mathcal{L}_2} < \|a_{i-1}(t)\|_{\mathcal{L}_2}$, it does not follow from (5.3) that $\|\Gamma(j\omega)\|_{\mathcal{H}_\infty} \leq 1$, and the system is not necessarily string stable.
Conversely, when $\|a_i(t)\|_{\mathcal{L}_2} > \|a_{i-1}(t)\|_{\mathcal{L}_2}$, it follows from (5.3) that $\|\Gamma(j\omega)\|_{\mathcal{H}_\infty} > 1$, and the system is string unstable. However, measurement noise is not taken into account in (5.3), such that it might hold that $\|\Gamma(j\omega)\|_{\mathcal{H}_\infty} \leq 1$ even though $\|a_i(t)\|_{\mathcal{L}_2} > \|a_{i-1}(t)\|_{\mathcal{L}_2}$.
Since no concrete statements can be made regarding string stability based on time-domain simulations, performance of the CACC controllers is discussed based on acceleration attenuation in terms of the $\mathcal{L}_2$-norm.

5.2 Without actuator delay

Simulation results for vehicles without actuator delay, i.e., $\phi = 0\ s$, are presented in Figure 5.2 for u-CACC and a-CACC (Figure 2.2 for the basic simulation), and in Figure 5.3 for observer-based CACC (Figure 4.3 for the basic simulation). Similar to the basic simulations, the platoon leader is subject to the input

$$u_1(t) = \begin{cases} 1, & \text{if} \quad 5 \leq t \leq 10, \\ -1, & \text{if} \quad 15 \leq t \leq 20, \\ 0, & \text{else.} \end{cases} \tag{5.4}$$

The transient behaviour of u-CACC, and a-CACC in Figure 5.2 is almost identical. For observer-based CACC, relatively large oscillations in the acceleration profiles in Figure 5.3 are observed. Jerk, essentially the differences of acceleration, is known cause driver discomfort [1], from which it can be stated that observer-based CACC is the least comfortable of the three. Ofcourse, it is unrealistic to expect observer-based CACC to outperform u-CACC and a-CACC while not using the same amount of measurements.

The $\mathcal{L}_2$-norms of the acceleration of all vehicles within the platoon S_I are computed and summarized in Table 5.2. The acceleration $\mathcal{L}_2$-norms resulting from the basic simulation presented in Table 4.1 are restated for comparison.
No large differences are seen when comparing the basic simulation results with the complex simulation results in Table 5.2.

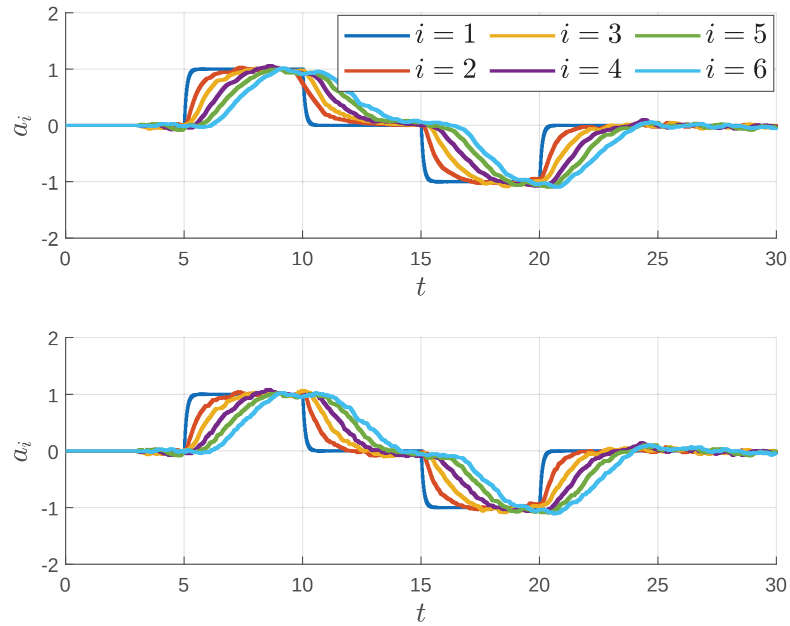

Figure 5.2: Complex simulation results showing acceleration a_i over time t for a platoon of $I = 6$ vehicles employing u-CACC (top) and a-CACC (bottom), without actuator delay, i.e., $\phi = 0\ s$, and other parameters summarized in Table 5.1.

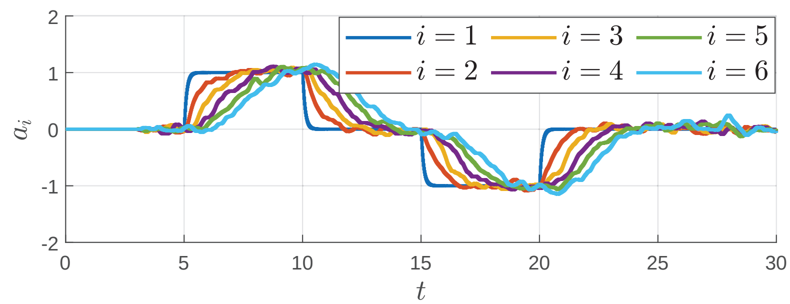

Figure 5.3: Complex simulation results showing acceleration a_i over time t for a platoon of $I = 6$ vehicles employing observer-based CACC, without actuator delay, i.e., $\phi = 0\ s$, and other parameters summarized in Table 5.1.

It seems that u-CACC is the least affected by the discrete-time implementation with measurement noise, see Table 5.2. This is partly caused by the fact that measurement noise is filtered by the dynamic u-CACC controller, which is, in Laplace domain, given as

$$u_i(s) = \frac{1}{hs+1}\left(\begin{bmatrix} k_p & k_d & k_{dd} \end{bmatrix} \begin{bmatrix} e_{i,1}(s) \\ e_{i,2}(s) \\ e_{i,3}(s) \end{bmatrix} + u_{i-1}(s)\right), \qquad i \in S_I. \tag{5.5}$$

Note that the term $\frac{1}{hs+1}$ can be regarded as a low-pass filter with cut-off frequency $\omega_c = \frac{1}{h}$. This filtering of high frequencies explains the relative insensitivity to measurement noise of u-CACC.

In comparison to u-CACC, less attenuation of acceleration $\mathcal{L}_2$-norms is achieved using a-CACC, see Table 5.2. This is caused by the fact that a-CACC passes measurement noise directly through to the desired acceleration u_i.

Observer-based CACC is the only CACC controller for which an amplification in acceleration $\mathcal{L}_2$-norm can be observed, see $\|a_6(t)\|_{\mathcal{L}_2} > \|a_5(t)\|_{\mathcal{L}_2}$ in Table 5.2.

Table 5.2: $\mathcal{L}_2$-norms of acceleration signals for different CACC controllers resulting from the basic and complex simulations without actuator delay, i.e., $\phi = 0$ s, and other parameters summarized in Table 5.1.

	***u*-CACC**		***a*-CACC**		**Observer-based**	
Vehicle	Basic	Complex	Basic	Complex	Basic	Complex
$i = 1$	3.13	3.13	3.13	3.13	3.13	3.13
$i = 2$	3.00	2.96	2.99	3.02	3.00	3.04
$i = 3$	2.92	2.91	2.90	2.99	2.93	3.00
$i = 4$	2.86	2.87	2.84	2.96	2.88	2.98
$i = 5$	2.81	2.82	2.78	2.92	2.84	2.95
$i = 6$	2.76	2.78	2.73	2.89	2.80	2.96

5.3 With actuator delay

In contrast to the previous section, this section focusses on vehicles experiencing an actuator delay ϕ. Because all other conditions are identical, differences with the previous section are caused by the actuator delay.

Acceleration responses to the input $u_1(t)$ (5.4) for a platoon of $I = 6$ homogeneous vehicles are presented in Figure 5.4 for u-CACC and a-CACC, and in Figure 5.5 for observer-based CACC. Again, the parameters summarized in Table 5.1 are used. From these acceleration responses, it can be seen that a-CACC is drastically affected by the actuator delay (Figure 5.4 with actuator delay, Figure 5.2 without actuator delay). Even though it was stated that no conclusions could be made regarding string stability, the extreme amplifications in upstream direction indicates that the actuator delay causes string instability when using a-CACC.
However, u-CACC and observer-bsed CACC are not visibly affected by the communication delay (Figures 5.4 and 5.5 with actuator delay, and Figures 5.2 and 5.3 without actuator delay).

The $\mathcal{L}_2$-norms of the acceleration signals for platoons employing u-CACC, a-CACC, and observer-based CACC are summarized in Table 5.3. It can again be seen that u-CACC and observer-based CACC are barely affected by the actuator delay. Furthermore, the amplification of acceleration signals using a-CACC is emphasized in Table 5.3.

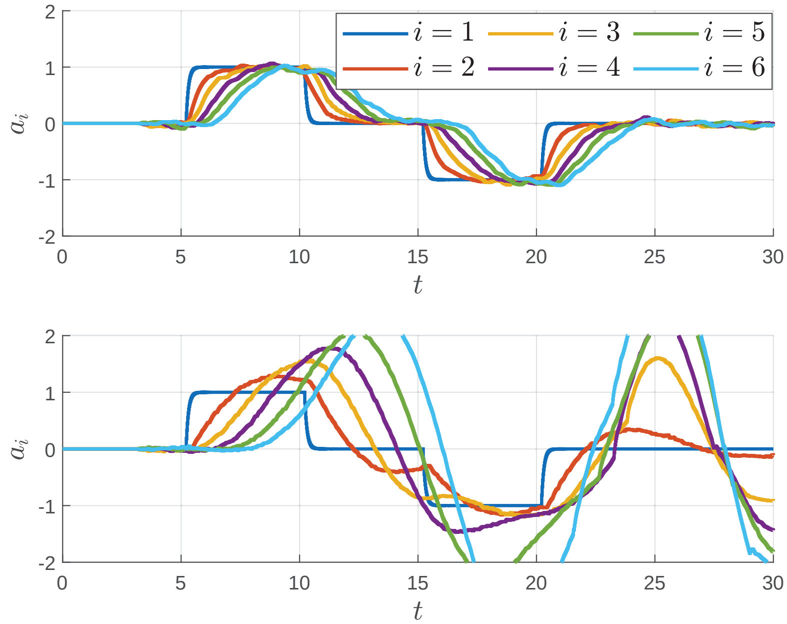

Figure 5.4: Complex simulation results showing acceleration a_i over time t for a platoon of $I = 6$ vehicles employing u-CACC (top) and a-CACC (bottom), using the parameters summarized in Table 5.1.

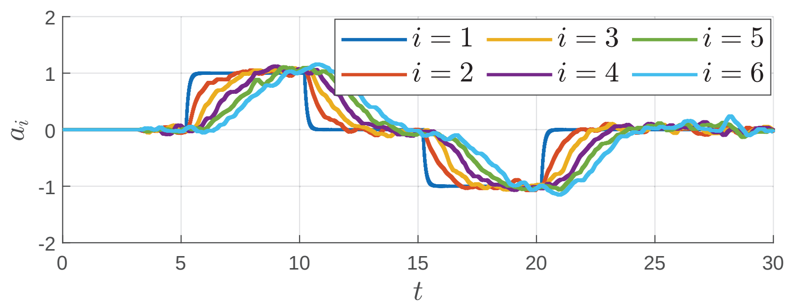

Figure 5.5: Complex simulation results showing acceleration a_i over time t for a platoon of $I = 6$ vehicles employing observer-based CACC, using the parameters summarized in Table 5.1.

The amplification of the $\mathcal{L}_2$-norm for a-CACC can be explained intuitively. Consider the predecessor vehicle to experience an input $u_{i-1}(t)$, which causes vehicle $i-1$ to accelerate at time $t+\phi$. This acceleration is communicated to vehicle i with delay θ, such that it is used in the input on time $t+\phi+\theta$. Correspondingly, $u_{i-1}(t+\phi+\theta)$ causes the vehicle i to exhibit an acceleration at time $t+2\phi+\theta$. Then, the acceleration of vehicle i lags $\phi+\theta$ behind the acceleration of vehicle $i-1$.

Since u-CACC communicates the input of vehicle $i-1$, it can be used in the input of vehicle i at time $t+\theta$. Correspondingly, vehicle $i-1$ starts accelerating at time $t+\phi$, whereas vehicle i starts accelerating at time $t+\phi+\theta$. The acceleration of vehicle i now only lags θ behind the acceleration of vehicle $i-1$.

Note however that this explanation only focusses on the effect of the feedforward term ob-

Table 5.3: $\mathcal{L}_2$-norms of acceleration signals for different CACC controllers resulting from the complex simulation with an actuator delay of $\phi = 0.2$ s, and other parameters summarized in Table 5.1.

	***u*-CACC**		***a*-CACC**		**Observer-based**	
Actuator delay	$\phi = 0$	$\phi = 0.2$	$\phi = 0$	$\phi = 0.2$	$\phi = 0$	$\phi = 0.2$
$i = 1$	3.13	3.13	3.13	3.13	3.13	3.13
$i = 2$	2.96	2.98	3.02	3.47	3.04	3.04
$i = 3$	2.91	2.94	2.99	4.69	3.00	3.01
$i = 4$	2.87	2.90	2.96	5.86	2.98	2.98
$i = 5$	2.82	2.84	2.92	7.12	2.95	2.96
$i = 6$	2.78	2.80	2.89	8.93	2.96	2.97

tained via wireless communication, and does not take feedback into account. A more thorough understanding of the effect of an actuator delay can be achieved by deriving the closed loop dynamics. The results are presented below, for the derivation the reader is referred to Appendix E.

The closed loop dynamics of u-CACC are given as

$$\begin{aligned}
\dot{e}_{i,1}(t) &= e_{i,2}(t), \\
\dot{e}_{i,2}(t) &= e_{i,3}(t), \\
\dot{e}_{i,3}(t) &= -\frac{1}{\tau}e_{i,3}(t) - \frac{1}{\tau}\begin{bmatrix} k_p & k_d & k_{dd} \end{bmatrix}\begin{bmatrix} e_{i,1}(t-\phi) \\ e_{i,2}(t-\phi) \\ e_{i,3}(t-\phi) \end{bmatrix} + \frac{1}{\tau}\left(u_{i-1}(t-\phi) - u_{i-1}(t-\phi-\theta)\right), \\
\dot{u}_i(t) &= -\frac{1}{h}u_i(t) + \frac{1}{h}\begin{bmatrix} k_p & k_d & k_{dd} \end{bmatrix}\begin{bmatrix} e_{i,1}(t) \\ e_{i,2}(t) \\ e_{i,3}(t) \end{bmatrix} + \frac{1}{h}u_{i-1}(t-\theta), \qquad i \in S_I.
\end{aligned} \tag{5.6}$$

Secondly, a-CACC has closed loop dynamics

$$\begin{aligned}
\dot{e}_{i,1}(t) &= e_{i,2}(t), \\
\dot{e}_{i,2}(t) &= -\begin{bmatrix} k_p & k_d \end{bmatrix}\begin{bmatrix} e_{i,1}(t-\phi) \\ e_{i,2}(t-\phi) \end{bmatrix} + a_{i-1}(t) - a_{i-1}(t-\phi-\theta) - \left(1 - \frac{h}{\tau}\right)\left(a_i(t) - a_i(t-\phi)\right), \\
\dot{\varepsilon}_i(t) &= \frac{1}{h}e_{i,2}(t) - \frac{1}{h}\varepsilon_i(t) + a_{i-1}(t), \qquad i \in S_I.
\end{aligned} \tag{5.7}$$

Finally, the closed loop dynamics of observer-based CACC are given as

$$\begin{aligned}
\dot{e}_{i,1}(t) &= e_{i,2}(t), \\
\dot{e}_{i,2}(t) &= -\begin{bmatrix} k_p & k_d \end{bmatrix}\begin{bmatrix} \hat{e}_{i,1}(t-\phi) \\ \hat{e}_{i,2}(t-\phi) \end{bmatrix} + a_{i-1}(t) - \hat{a}_{i-1}(t-\phi-\theta) - \left(1 - \frac{h}{\tau}\right)\left(a_i(t) - \hat{a}_i(t-\phi)\right), \\
\dot{\varepsilon}_i(t) &= \frac{1}{h}e_{i,2}(t) - \frac{1}{h}\varepsilon_i(t) + a_{i-1}(t), \qquad i \in S_I,
\end{aligned} \tag{5.8}$$

where estimated tracking errors $\hat{e}_{i,1}$, and $\hat{e}_{i,2}$ are generated by the observer

$$\begin{aligned}\xi_i &= \begin{bmatrix} k_p & k_d \end{bmatrix} \begin{bmatrix} \hat{e}_{i,1} \\ \hat{e}_{i,2} \end{bmatrix}, \\ \begin{bmatrix} \dot{\hat{e}}_{i,1} \\ \dot{\hat{e}}_{i,2} \end{bmatrix} &= \begin{bmatrix} 0 & 1 \\ 0 & 0 \end{bmatrix} \begin{bmatrix} \hat{e}_{i,1} \\ \hat{e}_{i,2} \end{bmatrix} + \begin{bmatrix} 0 \\ -1 \end{bmatrix} \xi_i + \begin{bmatrix} l_1^e \\ l_2^e \end{bmatrix} \left(e_{i,1} - \hat{e}_{i,1}\right), \qquad i \in S_I,\end{aligned} \tag{5.9}$$

and estimated accelerations $\hat{a}_i$, and $\hat{a}_{i-1}$ generated by the observer

$$\begin{aligned}\hat{a}_i &= \begin{bmatrix} 0 & 1 \end{bmatrix} \begin{bmatrix} \hat{v}_i \\ \hat{a}_i \end{bmatrix}, \\ \begin{bmatrix} \dot{\hat{v}}_i \\ \dot{\hat{a}}_i \end{bmatrix} &= \begin{bmatrix} 0 & 1 \\ 0 & -\frac{1}{\tau_i} \end{bmatrix} \begin{bmatrix} \hat{v}_i \\ \hat{a}_i \end{bmatrix} + \begin{bmatrix} 0 \\ \frac{1}{\tau_i} \end{bmatrix} u_i + \begin{bmatrix} l_1^a \\ l_2^a \end{bmatrix} \left(v_i - \hat{v}_i\right), \qquad i \in S_I,\end{aligned} \tag{5.10}$$

onboard of vehicles i, and $i-1$, respectively.

All three CACC controllers experience a delay of ϕ in the feedback loop. The main difference between the controllers is the disturbance acting on the closed loop. For u-CACC (5.6) this disturbance is $u_{i-1}(t-\phi) - u_{i-1}(t-\phi-\theta)$, which are θ out of phase. For a-CACC (5.7), the disturbances are $a_{i-1}(t) - a_{i-1}(t-\phi-\theta)$, and $a_i(t) - a_i(t-\phi)$, which are $\phi+\theta$ and ϕ out of phase, respectively. This explains as to why a-CACC experiences significantly more trouble in the presence of actuator delays.
Observer-based CACC (5.8) experiences disturbances $a_{i-1}(t) - \hat{a}_{i-1}(t-\phi-\theta)$, and $a_i(t) - \hat{a}_i(t-\phi)$. From the complex simulation results in Table 5.3, it was seen that the actuator delay ϕ barely affects the attenuation of its acceleration $\mathcal{L}_2$-norm. This is explained by the fact that the acceleration observer uses the non-delayed vehicle model without updating based on measurements, such that $\hat{a}_i(t-\phi)$ actually estimates $a_i(t)$. In Appendix E.3 it was proven that

$$\begin{aligned}&a_i(t) - \hat{a}_i(t-\phi) = e^{-\frac{1}{\tau}t} a_i(0), \\ &a_{i-1}(t) - \hat{a}_{i-1}(t-\phi-\theta) = e^{-\frac{1}{\tau}t} a_{i-1}(0) + \hat{a}_{i-1}(t-\phi) - \hat{a}_{i-1}(t-\phi-\theta), \qquad i \in S_I,\end{aligned} \tag{5.11}$$

in which $e^{-\frac{1}{\tau}t}$ converges to zero exponentially. The remaining disturbance $\hat{a}_{i-1}(t-\phi) - \hat{a}_{i-1}(t-\phi-\theta)$, lags just θ behind $\hat{a}_{i-1}(t-\phi)$.
The above is a result of the choice $l_1^a = l_2^a = 0$ for the acceleration observer gains. This choice however, implies that the observer relies completely on the vehicle model. Therefore, inaccuracies in the parameter τ or the vehicle model $G(s)$ can negatively affect the performance.
A short investigation on the effect of a parameter inaccuracy is performed, by assuming that τ is not perfectly known. To do so, both the observer-based CACC controller, and the acceleration observer use $\hat{\tau}$ as an approximation of τ. Simulation results are presented in Table 5.4 for an inaccuracy of 10 percent in the approximation of $\hat{\tau}$. Remarkably, $\hat{\tau} = 0.11\ s$ seems to result in more attenuation than using the correct value $\tau = 0.1\ s$.

Important to note is that the homogeneity assumption, made in the beginning of this chapter, also implies that the actuator delay ϕ is constant for all vehicles. When vehicles experience differences in actuator delay, u-CACC and observer-based CACC are negatively affected as well.

Even though a-CACC is at its current form negatively affected by the actuator delay, this is not unsolvable. Usage of the acceleration observer (5.10) with $l_1^a = l_2^a = 0$, onboard of vehicles $i-1$, and i for example, drastically improves the results already. Additionally, robustness can be improved by using a Smith predictor, which includes an update based on past measurements.

Table 5.4: $\mathcal{L}_2$-norms of acceleration signals for observer-based CACC using different values of $\hat{\tau}$ in the observer-based CACC controller (4.18), and acceleration observer (4.11).

Vehicle	$\hat{\tau} = \mathbf{0.1}$ **s**	$\hat{\tau} = \mathbf{0.09}$ **s**	$\hat{\tau} = \mathbf{0.11}$ **s**
$i = 1$	3.13	3.13	3.13
$i = 2$	3.04	3.04	3.04
$i = 3$	3.01	3.01	3.00
$i = 4$	2.98	2.99	2.98
$i = 5$	2.96	2.97	2.95
$i = 6$	2.97	2.99	2.96

5.4 Summary

In order to validate u-CACC, a-CACC, and observer-based CACC, simulations were performed which closely resemble practical applications. The main reason for verification of the CACC controllers was to investigate the effect of discrete-time implementation, measurement noise, and actuator delays.

A brief introduction to the simulation environment was given in Section 5.1. Afterwards, discrete-time implementation of the CACC controllers, in combination with sensor signals exhibiting measurement noise, was shown to be possible in Section 5.2.

Section 5.3 showed that adding an actuator delay ϕ resulted in large amplifications of acceleration in upstream direction when using a-CACC. Observer-based CACC was merely affected by the actuator delays, even though it was derived from a-CACC. This was shown to be caused by a trick in the acceleration observer, which used the non-delayed vehicle model without using measurements to update the estimation. Additionally, it was shown that, when parameter τ is not perfectly known, CACC is still possible.

Finally, in order for a-CACC to cope with actuator delays, it can be extended by using, for example, a Smith predictor to compensate the actuator delay on a low level.

Chapter 6

Conclusion and recommendations

The main conclusions of this thesis are presented in Section 6.1, followed up by a discussion on these conclusions and possible directions for further research in Section 6.2.

6.1 Conclusions

Cooperative Adaptive Cruise Control is basically a longitudinal vehicle controller using on-board measurements in combination with wireless inter-vehicle communication. As it allows for short inter-vehicle distances, a decrease in economical costs and environmental pollution can be achieved. Moreover, by excluding the need for a human driver, safety as well as passenger comfort can be improved.
For vehicle platoons that are heterogeneous with respect to their driveline dynamics, a-CACC enables platooning without requiring knowledge of these dynamics describing the preceding vehicle. An analytical sufficient string stability condition is derived, which directly states the effect of controller gains, communication delay, and time gap on string stability. By comparison with iteratively determined results, conservatism of this sufficient conditions was shown to be almost negligible
In order to cope with communication impairments, a-dCACC is proposed, such that string stable vehicle following behaviour is achieved for inter-vehicle time gaps significantly smaller than for ACC. The performance of a-dCACC has been shown to be at least comparable to u-dCACC. In contrast with u-dCACC, controller gains using a-dCACC can be tuned independent of the vehicle dynamics.
To enable platooning for vehicles that do not (accurately) measure relative position, relative velocity, global velocity, or global acceleration, observer-based CACC is proposed. String stable vehicle following behaviour using only relative position and global velocity while employing observer-based CACC, has been shown to be possible for short inter-vehicle distances.
Finally, simulation results showed that a-CACC drastically loses performance in the presence of actuator delays. These actuator delays barely affect observer-based CACC. This was caused by choosing the observer gains zero, and completely relying on the vehicle model for acceleration estimation. Inaccuracies, in terms of an incorrect approximation of the driveline dynamics, have been shown to barely affect observer-based CACC.

6.2 Recommendations

This thesis proposes two new CACC controllers, a-dCACC and observer-based CACC, which are analysed mathematically and tested using discrete-time simulations. Practical experiments however, have not been performed. The first direction for further research is therefore a real-time implementation and verification of the controllers. Since the complex simulation environment allows real-time implementation, observer-based CACC can be directly used within practical settings. Therefore, a test case should be devised, after which observer-based CACC can be tested. Even though not mentioned in this report, a-dCACC is also implemented in the complex simulation environment, such that it is ready for testing as well.

Moreover, a comparison between observer-based CACC and a-CACC would be a great addition. What is the effect of measurement noise, and what is the actual loss in string stability performance for practical situations? Increasing observer gains directly causes noise amplification resulting in driver discomfort. A balance should be found between driver comfort and string stability performance. Since driver comfort heavily depends on the actual vehicle, observer gains need to be tuned based on practical experience.

More importantly, simulations showed that actuator delays drastically affect CACC behaviour. The precise effect of actuator delays however, remains unstudied and is a possible topic for further research. A start can be made by re-evaluating the CACC controller design, and examining where the actuator delay enters the system. Also, the SSCS can be determined for vehicles subject to an actuator delay, such that its effect on string stability can be investigated numerically.

Even though observer-based CACC barely suffers from these actuator delays, robustness is not yet investigated thoroughly. The analysis on robustness of observer-based CACC against model and parameter inaccuracies deserves more attention. A start can be made analysing the observer-based CACC controller with a parameter inaccuracy. Since ISS can be compromised by this inaccuracy, both ISS and string stability should be considered.

Another direction for further research is the combination between observer-based CACC and degraded CACC. The resulting controller is then able to cope with communication impairments, as well as a defect, unavailable, or inaccurate sensor. Rather than relying on the communication of the estimated acceleration by the predecessor, the predecessor acceleration observer used within u-dCACC, and a-dCACC can be implemented.

Finally, in order to make the proposed CACC controllers practically adaptable, other considerations need to be taken into account. For example, gap closing manoeuvres while taking actuator limits and velocity regulations into account. Moreover, collision avoidance measures need to be taken, since string stability does not inherently exclude the possibility of collisions. The ultimate step is the application of CACC within existing traffic, which introduces numerous other challenges, such as merging traffic, non-cooperative vehicles, pedestrians, and for example traffic lights.

Bibliography

[1] I. Bae, J. Moon, and J. Seo. Toward a comfortable driving experience for a self-driving shuttle bus. *Electronics*, 8(9):943, 2019.

[2] K. Brookhuis, D. de Waard, and W. Janssen. Behavioural impacts of advanced driver assistance systems–an overview. *European Journal of Transport and Infrastructure Research*, 1(3), 2019.

[3] R. Caudill and W. Garrard. Vehicle-follower longitudinal control for automated transit vehicles. *Journal of Dynamic Systems, Measurement, and Control*, 99(4):241–248, 1977.

[4] CBS. Welke sectoren stoten broeikasgassen uit? `https://www.cbs.nl/nl-nl/dossier/dossier-broeikasgassen/hoofdcategorieen/welke-sectoren-stoten-broeikasgassen-uit-`, accessed 8 April 2020.

[5] S. Feng, Y. Zhang, S. Li, Z. Cao, H. Liu, and L. Li. String stability for vehicular platoon control: Definitions and analysis methods. *Annual Reviews in Control*, 2019.

[6] SAE International. Automated driving; levels of driving automation are defined in new sae international standard j3016, 2014.

[7] P. Ioannou and C. Chien. Autonomous intelligent cruise control. *IEEE Transactions on Vehicular technology*, 42(4):657–672, 1993.

[8] Borut Jereb, Samo Kumperščak, and Tadej Bratina. The impact of traffic flow on fuel consumption increase in the urban environment. *FME Transactions*, 46(2):278–284, 2018.

[9] P. Lambert. Cooperative adaptive cruise control of heterogeneous vehicle platoons. Master's thesis, Eindhoven University of Technology, 2019.

[10] E. Lefeber, J. Ploeg, and H. Nijmeijer. Cooperative adaptive cruise control of heterogeneous vehicle platoons. *In: Proceedings of the 21st IFAC World Congress, Berlin, Germany*, 2020.

[11] G. Marsden, M. McDonald, and M. Brackstone. Towards an understanding of adaptive cruise control. *Transportation Research Part C: Emerging Technologies*, 9(1):33–51, 2001.

[12] J. Ploeg. *Analysis and design of controllers for cooperative and automated driving*. PhD thesis, Eindhoven University of Technology, 2014.

[13] J. Ploeg. Vector, matrix, signal, and system norms. A not-so-short overview. Internal correspondence, 2018.

[14] J. Ploeg, B. Scheepers, E. van Nunen, N. van de Wouw, and H. Nijmeijer. Design and experimental evaluation of cooperative adaptive cruise control. In *14th International IEEE Conference on Intelligent Transportation Systems (ITSC)*, pages 260–265, Washington, USA, 2011. IEEE.

[15] J. Ploeg, E. Semsar-Kazerooni, G. Lijster, N. van de Wouw, and H. Nijmeijer. Graceful degradation of CACC performance subject to unreliable wireless communication. *IEEE Transactions on Intelligent Transportation Systems*, 16(1):1210–1216, 2015.

[16] J. Ploeg, N. van de Wouw, and H. Nijmeijer. Lp string stability of cascaded systems: Application to vehicle platooning. *IEEE Transactions on Control Systems Technology*, 22(2):786–793, 2013.

[17] F. Sancar, B. Fidan, J. Huissoon, and S. Waslander. MPC based collaborative adaptive cruise control with rear end collision avoidance. In *2014 IEEE Intelligent Vehicles Symposium Proceedings*, pages 516–521, Michigan, USA, 2014. IEEE.

[18] S. Shladover. Longitudinal control of automated guideway transit vehicles within platoons. *Journal of Dynamic Systems, Measurement, and Control*, 100:302–310, 1978.

[19] R. Singer. Estimating optimal tracking filter performance for manned maneuvering targets. *IEEE Transactions on Aerospace and Electronic Systems*, 6:473–483, 1970.

[20] A. Smiley and K. Brookhuis. Alcohol, drugs and traffic safety: road users and traffic safety. *Publication of: Van Gorcum & Comp BV*, 1987.

[21] R. Teetor. Speed control device for resisting operation of the accelerator, 1950. US Patent 2,519,859.

[22] UN. United Nations Paris agreement. `https://bigpicture.unfccc.int/content-the-paris-agreement`, accessed 8 April 2020.

[23] L. Wu, S. Wen, Y. He, Q. Zhou, and Z. Lu. Observer-based cooperative adaptive cruise control of vehicular platoons with random network access. In *2018 IEEE Intelligent Vehicles Symposium (IV)*, pages 232–237, Changshu, China, 2018. IEEE.

[24] Y. Zheng, S. Li, J. Wang, D. Cao, and K. Li. Stability and scalability of homogeneous vehicular platoon: Study on the influence of information flow topologies. *IEEE Transactions on Intelligent Transportation Systems*, 17(1):14–26, 2015.

[25] Y. Zhu and F. Zhu. Barrier-function-based distributed adaptive control of nonlinear cavs with parametric uncertainty and full-state constraint. *Transportation Research Part C: Emerging Technologies*, 104:249–264, 2019.

Appendices

Appendix A

Preliminaries

Preliminaries, used throughout the entirety of this thesis are summarized in this appendix.

A.1 Norms

The norm definitions as presented in [13] are used throughout this thesis.

Definition A.1. *($\mathcal{L}_p$-norm, [13]) Let $u(t)$ be a time-dependent vector signal according to $u(t) = \begin{bmatrix} u_1(t) & u_2(t) & \dots & u_n(t) \end{bmatrix}^T$. Then, the signal p-norm, or $\mathcal{L}_p$-norm, of $u(t)$ is defined as*

$$\|u(t)\|_{\mathcal{L}_p} := \left(\int_{-\infty}^{\infty} \sum_i \mid u_i(t) \mid^p dt \right)^{\frac{1}{p}}. \tag{A.1}$$

Definition A.2. *($\mathcal{H}_\infty$-norm, [13]) Consider a transfer function matrix $G(s)$ of a linear system. Then, the system infinity-norm, or $\mathcal{H}_\infty$-norm, of $G(s)$ is defined as*

$$\|G(j\omega)\|_{\mathcal{H}_\infty} := \sup_\omega \max_{u \neq 0} \frac{\|G(j\omega)u(j\omega)\|_{\mathcal{L}_2}}{\|u(j\omega)\|_{\mathcal{L}_2}}, \tag{A.2}$$

with input u_i, and the $\mathcal{L}_2$-norm as in (A.1) *for $p = 2$.*
Note that for Single-Input Single-Output (SISO) systems, (A.2) *reduces to*

$$\|G(j\omega)\|_{\mathcal{H}_\infty} = \sup_\omega \mid G(j\omega) \mid. \tag{A.3}$$

A.2 Polynomial bounds on sinusoids

Theorem A.1. *(Polynomial bounds on cosine) The cosine function can be described by its Taylor approximation*

$$\cos(x) = \sum_{n=0}^{\infty} \frac{(-1)^n}{(2n)!} x^{2n}, \tag{A.4}$$

which is an alternating convergent series. Therefore, the cosine function can be bounded by

$$\sum_{n=0}^{2N+1} \frac{(-1)^n}{(2n)!} x^{2n} \;\leq\; \cos(x) \;\leq\; \sum_{n=0}^{2N} \frac{(-1)^n}{(2n)!} x^{2n}, \quad \forall \quad N \in \mathbb{N}^+. \tag{A.5}$$

Theorem A.2. *(Polynomial bounds on sine) The sine function can be described by its Taylor approximation*

$$\sin(x) = \sum_{n=0}^{\infty} \frac{(-1)^n}{(2n+1)!} x^{2n+1}, \tag{A.6}$$

which can be written as an alternating convergent series by multiplying with x*, such that*

$$x \sin(x) = \sum_{n=0}^{\infty} \frac{(-1)^n}{(2n+1)!} x^{2n+2}. \tag{A.7}$$

Therefore, the sine function can be bounded by

$$x \sum_{n=0}^{2N+1} \frac{(-1)^n}{(2n+1)!} x^{2n+1} \ \le \ x \sin(x) \ \le \ x \sum_{n=0}^{2N} \frac{(-1)^n}{(2n+1)!} x^{2n+1}, \quad \forall \quad N \in \mathbb{N}^+. \tag{A.8}$$

A.3 Miscellaneous

Theorem A.3. *(Square root of sum) For non-negative* x, y*, the sum of square roots is larger than or equal to the square root of the sum, mathematically*

$$\sqrt{x+y} \le \sqrt{x} + \sqrt{y}, \quad \forall \quad x, y \ge 0. \tag{A.9}$$

This directly follows by writing

$$\begin{aligned} \left(\sqrt{x} + \sqrt{y}\right)^2 &= x + y + 2\sqrt{xy} \ \ge x + y, \qquad \forall \quad x, y \ge 0, \\ \Rightarrow \sqrt{x} + \sqrt{y} \ &\ge \sqrt{x+y}, \qquad \forall \quad x, y \ge 0. \end{aligned} \tag{A.10}$$

Appendix B

u-CACC in heterogeneous platoon

This appendix presents the derivation of the u-CACC control law for vehicle platoons that are heterogeneous with respect to driveline time constant τ_i, such that $\tau_i \neq \tau_{i-1}$. The derived controller only requires u_{i-1} to be communicated, whereas the controller (2.16) requires both a_{i-1}, and u_{i-1} to be communicated.

To derive this control law, the tracking error coordinates (2.10), and longitudinal vehicle model (2.1) with $\tau_i \neq \tau_{i-1}$ are used. Combining both results in the uncontrolled dynamics

$$\begin{bmatrix} \dot{e}_{i,1} \\ \dot{e}_{i,2} \\ \dot{e}_{i,3} \end{bmatrix} = \begin{bmatrix} e_{i,2} \\ e_{i,3} \\ -\frac{1}{\tau_{i-1}} \left(a_{i-1} - u_{i-1} \right) + \frac{1}{\tau_i} \left(1 - \frac{h}{\tau_i} \right) \left(a_i - u_i \right) - \frac{h}{\tau_i} \dot{u}_i \end{bmatrix}, \qquad i \in S_I. \tag{B.1}$$

Following a method similar to the one presented in Section 2.3, it is desired that $e_{i,3}$ follows

$$\dot{e}_{i,3} =: -\frac{1}{\tau_{i-1}} e_{i,3} - \frac{1}{\tau_{i-1}} \zeta_i, \qquad i \in S_I, \tag{B.2}$$

rather than the previously achieved $\dot{e}_{i,3} =: -\frac{1}{\tau_i} e_{i,3} - \frac{1}{\tau_i} \zeta_i$. Again using the same controller for the auxiliary input

$$\zeta_i := \begin{bmatrix} k_p & k_d & k_{dd} \end{bmatrix} \begin{bmatrix} e_{i,1} \\ e_{i,2} \\ e_{i,3} \end{bmatrix}, \qquad i \in S_I, \tag{B.3}$$

gives the controller

$$\begin{aligned} \dot{u}_i = &-\left(\frac{1}{h} - \frac{1}{\tau_i} + \frac{1}{\tau_{i-1}} \right) u_i + \frac{1}{h} \left(1 - \frac{\tau_{i-1}}{\tau_i} \right) \left(1 - \frac{h}{\tau_i} \right) a_i \\ &+ \frac{1}{h} \frac{\tau_i}{\tau_{i-1}} \begin{bmatrix} k_p & k_d & k_{dd} \end{bmatrix} \begin{bmatrix} e_{i,1} \\ e_{i,2} \\ e_{i,3} \end{bmatrix} + \frac{1}{h} \frac{\tau_i}{\tau_{i-1}} u_{i-1}, \qquad i \in S_I, \end{aligned} \tag{B.4}$$

which only requires u_{i-1} to be communicated. The resulting closed loop dynamics are then given as

$$\begin{bmatrix} \dot{e}_{i,1} \\ \dot{e}_{i,2} \\ \dot{e}_{i,3} \\ \dot{u}_i \end{bmatrix} = \begin{bmatrix} 0 & 1 & 0 & 0 \\ 0 & 0 & 1 & 0 \\ -\frac{k_p}{\tau_{i-1}} & -\frac{k_d}{\tau_{i-1}} & -\frac{k_{dd}+1}{\tau_{i-1}} & 0 \\ \frac{k_p \tau_i}{h \tau_{i-1}} & \frac{k_d \tau_i}{h \tau_{i-1}} & \frac{k_{dd} \tau_i}{h \tau_{i-1}} - \frac{1}{h} + \frac{\tau_{i-1}}{h \tau_i} & -\frac{1}{h} - \frac{1}{\tau_{i-1}} + \frac{\tau_{i-1}}{\tau_i^2} \end{bmatrix} \begin{bmatrix} e_{i,1} \\ e_{i,2} \\ e_{i,3} \\ u_i \end{bmatrix} + \begin{bmatrix} 0 & 0 \\ 0 & 0 \\ 0 & 0 \\ \frac{\tau_i - \tau_{i-1}}{h \tau_i} & \frac{\tau_i}{h \tau_{i-1}} \end{bmatrix} \begin{bmatrix} a_{i-1} \\ u_{i-1} \end{bmatrix}, \qquad i \in S_I. \tag{B.5}$$

A disadvantage of this approach however, is the dependency of the closed loop dynamics on the unknown parameter τ_{i-1}.

Appendix C

Degraded CACC observer tuning

This appendix presents the derivation of the continuous time Kalman filter gains, used for the u-dCACC predecessor acceleration observer. Most information is directly deducted from [19].

The controller used by u-dCACC is given as

$$\dot{u}_i = -\frac{1}{h}u_i + \frac{1}{h}\begin{bmatrix} k_p & k_d & k_{dd} \end{bmatrix}\begin{bmatrix} e_{i,1} \\ e_{i,2} \\ e_{i,3} \end{bmatrix} + \frac{1}{h}\hat{a}_{i-1}, \qquad i \in S_I, \tag{C.1}$$

with estimated state $\hat{a}_{i-1}$ as output from the observer

$$\begin{aligned} \begin{bmatrix} \dot{\hat{q}}_{i-1} \\ \dot{\hat{v}}_{i-1} \\ \dot{\hat{a}}_{i-1} \end{bmatrix} &= \underbrace{\begin{bmatrix} 0 & 1 & 0 \\ 0 & 0 & 1 \\ 0 & 0 & -\alpha \end{bmatrix}}_{=:A_s} \begin{bmatrix} \hat{q}_{i-1} \\ \hat{v}_{i-1} \\ \hat{a}_{i-1} \end{bmatrix} + \underbrace{\begin{bmatrix} l_{11} & l_{12} \\ l_{21} & l_{22} \\ l_{31} & l_{32} \end{bmatrix}}_{=:L_s} \begin{bmatrix} q_{i-1} - \hat{q}_{i-1} \\ v_{i-1} - \hat{v}_{i-1} \end{bmatrix}, \\ \begin{bmatrix} \hat{q}_{i-1} \\ \hat{v}_{i-1} \end{bmatrix} &= \underbrace{\begin{bmatrix} 1 & 0 & 0 \\ 0 & 1 & 0 \end{bmatrix}}_{=:C_s} \begin{bmatrix} \hat{q}_{i-1} \\ \hat{v}_{i-1} \\ \hat{a}_{i-1} \end{bmatrix}, \qquad i \in S_I. \end{aligned} \tag{C.2}$$

The observer gains are in [15] proposed as continuous time Kalman filter gains. This is done by following [19], starting with the statement that the predecessor acceleration is correlated in time, such that, when it is accelerating at time t, it is likely to be accelerating at time $t+\tau$ for sufficiently small τ [19]. A typical correlation function $r(\tau)$ associated with the target acceleration is

$$r(\tau) = E\{a_{i-1}(t)a_{i-1}(t+\tau)\} = \sigma_a^2 e^{-\alpha|\tau|}, \quad \alpha > 0, \tag{C.3}$$

with σ_a^2 the variance of a_{i-1}, and α the reciprocal of the maneuver time constant τ_m. Essentially, a larger α implies a more agile predecessor. The predecessor acceleration a_{i-1} is assumed to have a probability density function $p(a_{i-1})$ as presented in Figure C.1. In particular, the predecessor vehicle experiences a maximal acceleration a_{max} (or decelleration $-a_{max}$) with probability P_{max}, zero acceleration with probability P_0, and is uniformly distributed in between. From Figure C.1 it is possible to compute the mean $\mu_a = E\{a_{i-1}\}$ and variance

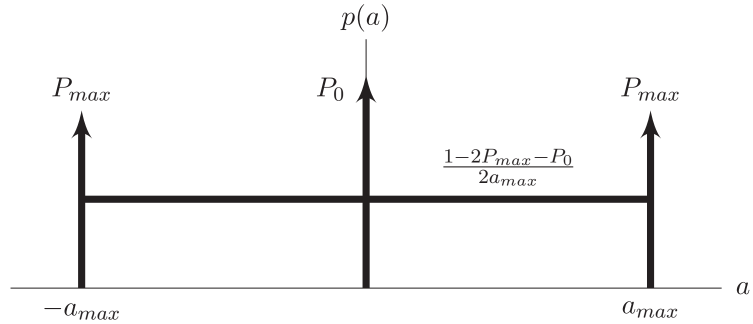

Figure C.1: Probability density function of the predecessor acceleration a_{i-1}.

$\sigma_a^2 = E\{(a_{i-1} - \mu_a)^2\}$ as

$$\begin{aligned}
\mu_a &= E\{a_{i-1}\} = \int_{-\infty}^{\infty} a_{i-1} p(a_{i-1}) da_{i-1} \\
&= -a_{max} P_{max} + a_{max} P_{max} + \frac{1 - 2P_{max} - P_0}{2a_{max}} \int_{-a_{max}}^{a_{max}} a_{i-1} da_{i-1} = 0, \\
\sigma_a^2 &= E\{(a_{i-1} - \mu_a)^2\} = \int_{-\infty}^{\infty} a_{i-1}^2 p(a_{i-1}) da_{i-1} \\
&= a_{max}^2 P_{max} + a_{max}^2 P_{max} + \frac{1 - 2P_{max} - P_0}{2a_{max}} \int_{-a_{max}}^{a_{max}} a_{i-1}^2 da_{i-1} \\
&= \frac{a_{max}^2}{3} \left(1 + 4P_{max} - P_0\right).
\end{aligned} \tag{C.4}$$

From the correlation function $r(\tau)$, it is possible to describe the acceleration a_{i-1} in terms of white noise by the Wiener-Kolmogorov whitening procedure. The Laplace transform of $r(\tau)$ can be found in standardized lists and is given as

$$r(s) = \mathcal{L}\{r(t)\} = -\frac{2\alpha\sigma_a^2}{s^2 - \alpha^2} =: H(s)H(-s)w_{i-1}(s), \tag{C.5}$$

with $H(s) = \frac{1}{s+\alpha}$ the transform of the whitening filter, and $w_{i-1}(s) = 2\alpha\sigma_a^2$ the transform of the white noise w_{i-1} causing a_{i-1}. This yields dynamics $\dot{a}_{i-1} = -\alpha a_{i-1} + w_{i-1}$, or, correspondingly

$$\begin{aligned}
\begin{bmatrix} \dot{q}_{i-1} \\ \dot{v}_{i-1} \\ \dot{a}_{i-1} \end{bmatrix} &= \underbrace{\begin{bmatrix} 0 & 1 & 0 \\ 0 & 0 & 1 \\ 0 & 0 & -\alpha \end{bmatrix}}_{=:A_s} \underbrace{\begin{bmatrix} q_{i-1} \\ v_{i-1} \\ a_{i-1} \end{bmatrix}}_{=:x_{i-1}} + \underbrace{\begin{bmatrix} 0 \\ 0 \\ 1 \end{bmatrix}}_{=:B_s} w_{i-1}, \\
\underbrace{\begin{bmatrix} q_{i-1} \\ v_{i-1} \end{bmatrix}}_{=:y_{i-1}} &= \underbrace{\begin{bmatrix} 1 & 0 & 0 \\ 0 & 1 & 0 \end{bmatrix}}_{=:C_s} \begin{bmatrix} q_{i-1} \\ v_{i-1} \\ a_{i-1} \end{bmatrix}, \qquad i \in S_I,
\end{aligned} \tag{C.6}$$

where y_{i-1} are the measurements. Note that both q_{i-1} and v_{i-1} are measured indirectly as was explained in Section 2.5. Finally, writing the dynamics (C.6) as

$$\begin{aligned} \dot{x}_{i-1} &= A_s x_{i-1} + B_s w_{i-1}, \\ y_{i-1} &= C_s x_{i-1} + \eta_{i-1}, \qquad i \in S_I, \end{aligned} \tag{C.7}$$

with measurement noise η_{i-1}, and the observer as

$$\begin{aligned} \dot{\hat{x}}_{i-1} &= A_s \hat{x}_{i-1} + LC_s \left(x_{i-1} - \hat{x}_{i-1}\right) \\ \hat{y}_{i-1} &= C_s \hat{x}_{i-1}, \qquad i \in S_I, \end{aligned} \tag{C.8}$$

allows the derivation of the process noise covariance matrix Q and measurement noise covariance matrix R as

$$\begin{aligned} Q &= B_s E\{w_{i-1} w_{i-1}^T\} B_s^T = \begin{bmatrix} 0 & 0 & 0 \\ 0 & 0 & 0 \\ 0 & 0 & 2\alpha\sigma_a^2 \end{bmatrix}, \\ R &= E\{\eta_{i-1}\eta_{i-1}^T\} = \begin{bmatrix} \sigma_q^2 & 0 \\ 0 & \sigma_v^2 \end{bmatrix}. \end{aligned} \tag{C.9}$$

Here, σ_q^2 and σ_v^2 the variance on the indirect measurements q_{i-1} and v_{i-1}, respectively. The continuous time constant Kalman gain is then computed as

$$L = PC_s^T R^{-1}, \tag{C.10}$$

where P is the solution of the continuous-time algebraic Riccati equation

$$A_s P + P A_s^T - PC_s^T {R^{-1}}^T C_s P + Q = 0. \tag{C.11}$$

Appendix D

observer-based CACC

This appendix presents the proof of the sufficient string stability condition using observer-based CACC, as was presented in Proposition 4.3. To do so, the string stability condition

$$|\Gamma(j\omega)| \leq 1, \quad \forall \quad \omega \in \mathbb{R}, \tag{D.1}$$

is used. Furthermore, the a-CACC SSCS is given as

$$\Gamma_{\mathrm{a}}^{\mathrm{CACC}}(s) = \frac{1}{H(s)} \frac{D(s)s^2 + C_a(s)}{s^2 + C_a(s)} = \frac{1}{hs+1} \frac{e^{-\theta s}s^2 + k_p + k_d s}{s^2 + k_p + k_d s}, \tag{D.2}$$

and the "observer-based CACC" SSCS is given as

$$\begin{aligned} \Gamma_o(s) &= \frac{1}{H(s)} \frac{D(s)s^2 + C_o(s)}{s^2 + C_o(s)} \\ &= \frac{1}{hs+1} \frac{e^{-\theta s}s^2 \left(1 + c_2 s^2 + (k_d c_1 + c_2)s + k_d c_2 + k_p c_1\right) + k_p + (k_d + k_p c_2)s}{s^2 \left(1 + c_2 s^2 + (k_d c_1 + c_2)s + k_d c_2 + k_p c_1\right) + k_p + (k_d + k_p) c_2 s}, \end{aligned} \tag{D.3}$$

where $c_1 := \frac{1}{l_2^e}$, and $c_2 := \frac{l_1^e}{l_2^e}$.

Proof. (Proposition 4.3) Since $h_{\min}^{\mathrm{nec}}$ is the smallest h for which a-CACC is string stable, substituting $h_{\min}^{\mathrm{nec}}$ in the SSCS (D.2) must fulfill the string stability criterion (D.1), from which follows

$$h_{\min}^{\mathrm{nec}\;2}\omega^4 + h_{\min}^{\mathrm{nec}\;2}\left(k_d^2 - 2k_p\right)\omega^2 - 2k_d \sin(\theta\omega)\omega + h_{\min}^{\mathrm{nec}\;2} k_p^2 + 2k_p\left(\cos(\theta\omega) - 1\right) \;\geq\; 0, \quad \forall \quad \omega \in \mathbb{R}. \tag{D.4}$$

Similarly, using the observer-based CACC SSCS (D.3) in the rewritten string stability condition (D.1), gives

$$\begin{aligned}
&\underbrace{\begin{aligned}&\left[c_1^2h^2\right]\omega^8+\left[h^2\left(c_1^2(k_d^2-2k_p)+c_2^2-2c_1\right)\right]\omega^6\\
&\quad+\left[h^2\left(c_1^2k_p^2+(c_2^2-2c_1)(k_d^2-2k_p)\right)\right]\omega^4+\left[2c_1(k_d+c_2k_p)\sin(\theta\omega)\right]\omega^3\\
&\quad+\left[h^2k_p^2(c_2^2-2c_1)+2\left(c_1k_p-c_2k_d-c_1k_d^2-c_2^2k_p-c_1c_2k_pk_d\right)(1-\cos(\theta\omega))\right]\omega^2\\
&\quad-2\left[(c_2^2k_pk_d+c_2k_d^2+c_1c_2k_p^2)\sin(\theta\omega)\right]\omega-2\left(c_1k_p^2+c_2k_pk_d\right)(1-\cos(\theta\omega))\end{aligned}}_{\text{Additional part caused by observer}}\\
&\quad+\underbrace{h^2\omega^4+h^2(k_d^2-2k_p)\omega^2-2k_d\sin(\theta\omega)\omega+h^2k_p^2-2k_p\left(1-\cos(\theta\omega)\right)}_{\text{Part of } a\text{-CACC}}\ \geq\ 0,\quad\forall\quad\omega\in\mathbb{R},
\end{aligned}\tag{D.5}$$

as a necessary and sufficient condition for string stability. Note that the last line is identified to be caused by a-CACC, as it is similar to the inequality (D.4) for $h=h_{\min}^{\text{nec}}$. Substituting $h^2={h_{\min}^{\text{nec}}}^2+h_{\text{saf}}^2$ in this part gives the necessary and sufficient condition for observer-based CACC string stability

$$\begin{aligned}
&\left[c_1^2h^2\right]\omega^8+\left[h^2\left(c_1^2(k_d^2-2k_p)+c_2^2-2c_1\right)\right]\omega^6+\left[h_{\text{saf}}^2+h^2\left(c_1^2k_p^2+(c_2^2-2c_1)(k_d^2-2k_p)\right)\right]\omega^4\\
&\quad+\left[2c_1(k_d+c_2k_p)\sin(\theta\omega)\right]\omega^3+\left[h_{\text{saf}}^2(k_d^2-2k_p)\right]\omega^2+\left[h^2k_p^2(c_2^2-2c_1)\dots\right.\\
&\quad\left.+2\left(c_1k_p-c_2k_d-c_1k_d^2-c_2^2k_p-c_1c_2k_pk_d\right)(1-\cos(\theta\omega))\right]\omega^2\\
&\quad-2\left[(c_2^2k_pk_d+c_2k_d^2+c_1c_2k_p^2)\sin(\theta\omega)\right]\omega+h_{\text{saf}}^2k_p^2-2\left(c_1k_p^2+c_2k_pk_d\right)(1-\cos(\theta\omega))\\
&\quad+\underbrace{{h_{\min}^{\text{nec}}}^2\omega^4+{h_{\min}^{\text{nec}}}^2(k_d^2-2k_p)\omega^2-2k_d\sin(\theta\omega)\omega+{h_{\min}^{\text{nec}}}^2k_p^2-2k_p\left(1-\cos(\theta\omega)\right)}_{\geq 0,\text{ see (D.4)}}\\
&\hspace{20em}\geq\ 0,\quad\forall\quad\omega\in\mathbb{R},
\end{aligned}\tag{D.6}$$

where the last line is positive due to the definition of $h_{\min}^{\text{nec}}$, see inequality (D.4). Bounding the sine and cosine functions in the remaining part using $1-\frac{1}{2}\theta^2\omega^2\leq\cos(\theta\omega)\leq 1$ and $\omega\left(\theta\omega-\frac{1}{6}\theta^3\omega^3\right)\leq\omega\sin(\theta\omega)\leq\theta\omega^2$ (see Appendix A.2 with $N=0$), gives

$$\begin{aligned}
&\left[c_1^2h^2\right]\omega^8+\left[h^2\left(c_1^2(k_d^2-2k_p)+c_2^2-2c_1\right)-\frac{1}{3}\left(k_pc_1c_2+k_dc_1\right)\theta^3\right]\omega^6+\left[h_{\text{saf}}^2\dots\right.\\
&\quad+h^2\left(c_1^2k_p^2+(c_2^2-2c_1)(k_d^2-2k_p)\right)+2c_1(k_d+c_2k_p)\theta-\left(c_2k_d+c_1k_d^2+c_2^2k_p\right)\theta^2\dots\\
&\quad\left.+c_1c_2k_pk_d\theta^2\right]\omega^4+\left[h_{\text{saf}}^2\left(k_d^2-2k_p\right)+h^2k_p^2\left(c_2^2-2c_1\right)-2\left(c_2^2k_pk_d+c_2k_d^2+c_1c_2k_p^2\right)\theta\dots\right.\\
&\quad\left.-\left(k_p^2c_1+c_2k_pk_d\right)\theta^2\right]\omega^2+h_{\text{saf}}^2k_p^2\\
&\quad+{h_{\min}^{\text{nec}}}^2\omega^4+{h_{\min}^{\text{nec}}}^2(k_d^2-2k_p)\omega^2-2k_d\sin(\theta\omega)\omega+{h_{\min}^{\text{nec}}}^2k_p^2-2k_p\left(1-\cos(\theta\omega)\right)\\
&=:a\omega^8+b\omega^6+c\omega^4+d\omega^2+e\\
&\quad+\underbrace{{h_{\min}^{\text{nec}}}^2\omega^4+{h_{\min}^{\text{nec}}}^2(k_d^2-2k_p)\omega^2-2k_d\sin(\theta\omega)\omega+{h_{\min}^{\text{nec}}}^2k_p^2-2k_p\left(1-\cos(\theta\omega)\right)}_{\geq 0,\text{ see (D.4)}}\ \geq\ 0\ \forall\,\omega,\in\mathbb{R},
\end{aligned}\tag{D.7}$$

as a sufficient condition for the string stability definition (D.1). In the continuation of this proof, it is shown that, for the observer gains chosen as in Proposition 4.3, the coefficients

a, b, c, d, and e are non-negative, such that $a\omega^8 + b\omega^6 + c\omega^4 + d\omega^2 + e \geq 0, \ \forall\ \omega \in \mathbb{R}$, and therefore condition (D.7) is satisfied.
It is trivial to see that $a, e > 0$ (squares of real numbers), so continue with b, c, and d.
First, $b \geq 0$ if

$$\begin{aligned} & h^2\left(c_1^2(k_d^2 - 2k_p) + c_2^2 - 2c_1\right) - \frac{1}{3}\left(k_p c_1 c_2 + k_d c_1\right)\theta^3 \geq 0, \\ \Leftrightarrow\ & h^2\left(k_d^2 - 2k_p + l_1^{e2} - 2l_2^e\right) - \frac{1}{3}\left(k_p l_1^e + k_d l_2^e\right)\theta^3 \geq 0, \\ \Leftrightarrow\ & l_1^e\left(l_1^e - \frac{1}{3}k_p\frac{\theta^3}{h^2}\right) - l_2^e\left(2 + \frac{1}{3}k_d\frac{\theta^3}{h^2}\right) + k_d^2 - 2k_p \geq 0. \end{aligned} \tag{D.8}$$

Neglecting the term $k_d^2 - 2k_p$, which is assumed to be positive, gives

$$l_1^e \geq \frac{\frac{1}{3}k_p\frac{\theta^3}{h^2} + \sqrt{\frac{1}{9}k_p^2\frac{\theta^6}{h^4} + 4\left(2 + \frac{1}{3}k_d\frac{\theta^3}{h^2}\right)l_2^e}}{2}. \tag{D.9}$$

Using $\sqrt{x+y} \leq \sqrt{x} + \sqrt{y}$ for non-negative x, y (see Appendix A.3), gives

$$l_1^e\ \geq\ \underbrace{\frac{1}{3}k_p\frac{\theta^3}{h^2}}_{=:c_{1,1}} + \underbrace{\sqrt{2 + \frac{1}{3}k_d\frac{\theta^3}{h^2}}}_{=:c_{1,2}}\sqrt{l_2^e}, \tag{D.10}$$

as a sufficient condition for l_1^e to achieve $b \geq 0$.
Second, $c \geq 0$ if

$$\begin{aligned} & h_{\text{saf}}^2 + h^2\left(c_1^2k_p^2 + (c_2^2 - 2c_1)(k_d^2 - 2k_p)\right) + 2c_1(k_d + c_2k_p)\theta \\ & \qquad - \left(c_2k_d + c_1k_d^2 + c_2^2k_p + c_1c_2k_pk_d\right)\theta^2\ \geq\ 0, \\ \Leftrightarrow\ & l_2^{e2}h_{\text{saf}}^2 + l_2^e\left(-2h^2(k_d^2 - 2k_p) + 2k_d\theta - \left(l_1^ek_d + k_d^2\right)\theta^2\right) \\ & \qquad + h^2\left(k_p^2 + l_1^{e2}(k_d^2 - 2k_p)\right) + 2l_1^ek_p\theta - \left(l_1^{e2}k_p + l_1^ek_pk_d\right)\theta^2\ \geq\ 0. \end{aligned} \tag{D.11}$$

Neglecting the positive terms $2l_1^ek_p\theta$, $2l_2^ek_d\theta$, and $h^2\left(k_p^2 + l_1^{e2}(k_d^2 - 2k_d)\right)$, and again using $\sqrt{x+y} \leq \sqrt{x} + \sqrt{y}$ for non-negative x, y, gives

$$\begin{aligned} l_2^e &\geq \underbrace{\frac{2h^2\left(k_d^2 - 2k_p\right) + k_d^2\theta^2}{h_{\text{saf}}^2}}_{=:c_{2,1}} + \frac{l_1^ek_d\theta^2 + h_{\text{saf}}\sqrt{l_1^{e2}k_p + l_1k_pk_d}\,\theta}{h_{\text{saf}}^2} \\ &= c_{2,1} + l_1^e\frac{k_d\theta^2 + h_{\text{saf}}\sqrt{k_p + \frac{k_pk_d}{l_1^e}}\,\theta}{h_{\text{saf}}^2}, \end{aligned} \tag{D.12}$$

as a sufficient condition for (D.11). Using the knowledge that $l_1^e \geq c_{1,1} + c_{1,2}\sqrt{l_2} \geq c_{1,1}$ to achieve $b \geq 0$, see condition (D.10), gives

$$l_2^e \geq c_{2,1} + l_1^e\underbrace{\frac{k_d\theta^2 + h_{\text{saf}}\sqrt{k_p + 3k_d\frac{h^2}{\theta^3}}\,\theta}{h_{\text{saf}}^2}}_{=:c_{2,2}}, \tag{D.13}$$

as a sufficient condition for (D.12), and therefore $c \geq 0$.
Third, similar to the derivation of the bound on l_2^e to achieve $c \geq 0$, a bound is posed on l_2^e such that $d \geq 0$. To do so, multiply d with l_2^{e2} and get

$$l_2^{e2}\left(k_d^2 - 2k_p\right) h_{\text{saf}}^2 - l_2^e\left(2h^2k_p^2 + 2l_1^e k_d^2\theta + (k_p^2 + l_1^e k_p k_d)\theta^2\right) + h^2k_p^2 l_1^{e2} - 2\left(l_1^{e2} k_p k_d + l_1^e k_p^2\right)\theta \geq 0. \tag{D.14}$$

Neglecting the positive term $h^2k_p^2l_1^{e2}$, using $\sqrt{x+y} \leq \sqrt{x} + \sqrt{y}$ for non-negative x, y, and using $l_1^e \geq c_{1,1} + c_{1,2}\sqrt{l_2^e} \geq c_{1,1}$ gives

$$l_2^e \geq \underbrace{\frac{\left(2h^2+\theta^2\right)k_p^2}{\left(k_d^2 - 2k_p\right)h_{\text{saf}}^2}}_{=:c_{3,1}} + l_1^e \underbrace{\frac{2k_d^2\theta + k_p k_d \theta^2 + h_{\text{saf}}\sqrt{2\left(k_d^2 - 2k_p\right)\left(k_p k_d + 3k_p\frac{h^2}{\theta^3}\right)\theta}}{\left(k_d^2 - 2k_p\right)h_{\text{saf}}^2}}_{=:c_{3,2}}, \tag{D.15}$$

as a sufficient condition for (D.14), and therefore $d \geq 0$.
Combining $b \geq 0$ (D.10), $c \geq 0$ (D.13), and $d \geq 0$ (D.15), gives the observer gain string stability conditions

$$\begin{aligned} l_1^e &\geq c_{1,1} + c_{1,2}\sqrt{l_2^e} \ \Rightarrow\ b \geq 0, \\ \wedge\ l_2^e &\geq c_{2,1} + c_{2,2}l_1^e \ \Rightarrow\ c \geq 0, \\ \wedge\ l_2^e &\geq c_{3,1} + c_{3,2}l_1^e \ \Rightarrow\ d \geq 0. \end{aligned} \tag{D.16}$$

In order to make conditions (D.16) useful, choose $l_1^e = c_{\text{saf}}\left(c_{1,1} + c_{1,2}\sqrt{l_2^e}\right)$, with a safety factor $c_{\text{saf}} \geq 1$, and substitute l_1^e in the last two lines of (D.16). Solving the resulting second order polynomial inequalities in $\sqrt{l_2^e}$ for l_2^e, gives the observer gain conditions as presented in Proposition 4.3. $\square$

Appendix E

closed loop dynamics with actuator delay

This appendix presents the derivation of the closed loop dynamics using different CACC controllers for vehicles experiencing an actuator delay. The delayed longitudinal vehicle dynamics are given as

$$\begin{bmatrix} \dot{q}_i(t) \\ \dot{v}_i(t) \\ \dot{a}_i(t) \end{bmatrix} \begin{bmatrix} 0 & 1 & 0 \\ 0 & 0 & 1 \\ 0 & 0 & -\frac{1}{\tau_i} \end{bmatrix} \begin{bmatrix} q_i(t) \\ v_i(t) \\ a_i(t) \end{bmatrix} + \begin{bmatrix} 0 \\ 0 \\ \frac{1}{\tau_i} \end{bmatrix} u_i(t-\phi), \qquad i \in S_I. \tag{E.1}$$

The closed loop dynamics using u-CACC, a-CACC, and observer-based CACC are derived in the upcoming sections. For simplicity, a homogeneous vehicle platoon is assumed.

E.1 u-CACC

The coordinate transformation used within u-CACC is given as

$$\begin{aligned} e_{i,1}(t) &:= q_{i-1}(t) - q_i(t) - hv_i(t), \\ e_{i,2}(t) &:= \dot{e}_{i,1}(t) = v_{i-1}(t) - v_i(t) - ha_i(t), \\ e_{i,3}(t) &:= \dot{e}_{i,2}(t) = a_{i-1}(t) - \left(1 - \frac{h}{\tau}\right) a_i(t) - \frac{h}{\tau} u_i(t-\phi), \qquad i \in S_I. \end{aligned} \tag{E.2}$$

Combining the coordinate transformation (E.2) with the longitudinal vehicle dynamics (E.1), and using the u-CACC controller

$$\dot{u}_i(t) = -\frac{1}{h} u_i(t) + \frac{1}{h} \begin{bmatrix} k_p & k_d & k_{dd} \end{bmatrix} \begin{bmatrix} e_{i,1}(t) \\ e_{i,2}(t) \\ e_{i,3}(t) \end{bmatrix} + \frac{1}{h} u_{i-1}(t-\theta), \qquad i \in S_I, \tag{E.3}$$

gives the closed loop dynamics

$$
\begin{aligned}
\dot{e}_{i,1}(t) &= e_{i,2}(t), \\
\dot{e}_{i,2}(t) &= e_{i,3}(t), \\
\dot{e}_{i,3}(t) &= -\frac{1}{\tau}e_{i,3}(t) - \frac{1}{\tau}\begin{bmatrix} k_p & k_d & k_{dd} \end{bmatrix} \begin{bmatrix} e_{i,1}(t-\phi) \\ e_{i,2}(t-\phi) \\ e_{i,3}(t-\phi) \end{bmatrix} + \frac{1}{\tau}\left(u_{i-1}(t-\phi) - u_{i-1}(t-\phi-\theta)\right), \\
\dot{u}_i(t) &= -\frac{1}{h}u_i(t) + \frac{1}{h}\begin{bmatrix} k_p & k_d & k_{dd} \end{bmatrix} \begin{bmatrix} e_{i,1}(t) \\ e_{i,2}(t) \\ e_{i,3}(t) \end{bmatrix} + \frac{1}{h}u_{i-1}(t-\theta), \qquad i \in S_I.
\end{aligned} \tag{E.4}
$$

From (E.4), it directly follows that the closed loop dynamics of u-CACC is disturbed by the external inputs $u_{i-1}(t-\phi) - u_{i-1}(t-\phi-\theta)$, and $u_{i-1}(t-\phi)$. Moreover, the feedback is delayed with ϕ.

E.2 a-CACC

The coordinate transformation used within a-CACC is given as

$$
\begin{aligned}
e_{i,1}(t) &:= q_{i-1}(t) - q_i(t) - hv_i(t), \\
e_{i,2}(t) &:= \dot{e}_{i,1}(t) = v_{i-1}(t) - v_i(t) - ha_i(t), \\
\varepsilon_i(t) &:= v_{i-1}(t) - v_i(t), \qquad i \in S_I.
\end{aligned} \tag{E.5}
$$

Combining the coordinate transformation (E.5) with longitudinal vehicle dynamics (E.1), and using the “alterntive CACC” controller

$$
u_i(t) = \frac{\tau}{h}\begin{bmatrix} k_p & k_d \end{bmatrix} \begin{bmatrix} e_{i,1}(t) \\ e_{i,2}(t) \end{bmatrix} + \left(1 - \frac{\tau}{h}\right) a_i(t) + \frac{\tau}{h}a_{i-1}(t-\theta), \qquad i \in S_I. \tag{E.6}
$$

gives the closed loop dynamics

$$
\begin{aligned}
\dot{e}_{i,1}(t) &= e_{i,2}(t), \\
\dot{e}_{i,2}(t) &= -\begin{bmatrix} k_p & k_d \end{bmatrix} \begin{bmatrix} e_{i,1}(t-\phi) \\ e_{i,2}(t-\phi) \end{bmatrix} + a_{i-1}(t) - a_{i-1}(t-\phi-\theta) - \left(1 - \frac{h}{\tau}\right)\left(a_i(t) - a_i(t-\phi)\right), \\
\dot{\varepsilon}_i(t) &= \frac{1}{h}e_{i,2}(t) - \frac{1}{h}\varepsilon_i(t) + a_{i-1}(t), \qquad i \in S_I.
\end{aligned} \tag{E.7}
$$

Again, the feedback is delayed with ϕ. Additionally, the disturbance acting on the closed loop of a-CACC is less synchronized. Note that for a-CACC $a_{i-1}(t-\phi-\theta)$ lags $\phi+\theta$ behind $a_{i-1}(t)$, whereas for u-CACC $u_{i-1}(t-\phi-\theta)$ lags only θ behind $u_{i-1}(t-\theta)$. Finally, due to the actuator delay ϕ, it is not possible to perfectly compensate $a_i(t)$.

E.3 observer-based CACC

Observer-based CACC uses the same tracking error coordinates (E.5) as a-CACC. Additionally, the controller is given as

$$
u_i(t) = \frac{\tau}{h}\begin{bmatrix} k_p & k_d \end{bmatrix} \begin{bmatrix} \hat{e}_{i,1}(t) \\ \hat{e}_{i,2}(t) \end{bmatrix} + \left(1 - \frac{\tau}{h}\right) \hat{a}_i(t) + \frac{\tau}{h}\hat{a}_{i-1}(t-\theta), \qquad i \in S_I, \tag{E.8}
$$

where $\hat{e}_{i,1}$, and $\hat{e}_{i,2}$ are generated by the observer

$$\begin{aligned}
\dot{\hat{e}}_{i,1}(t) &= \hat{e}_{i,2}(t) + l_1^e \left(e_{i,1}(t) - \hat{e}_{i,1}(t)\right), \\
\dot{\hat{e}}_{i,2}(t) &= -k_p \hat{e}_{i,1}(t) - k_d \hat{e}_{i,2} + l_2^e \left(e_{i,1}(t) - \hat{e}_{i,1}(t)\right), \qquad i \in S_I,
\end{aligned} \tag{E.9}$$

and $\hat{a}_i$ by the observer

$$\dot{\hat{a}}_i(t) = -\frac{1}{\tau} a_i(t) + \frac{1}{\tau} u_i(t), \qquad i \in S_I. \tag{E.10}$$

The predecessor estimated acceleration $\hat{a}_{i-1}$ is obtained via wireless inter-vehicle communication, and estimated onboard vehicle $i-1$.
Combining the tracking error coordinates (E.5), longitudinal vehicle dynamics (E.1), and controller (E.8), gives the closed loop tracking error dynamics

$$\begin{aligned}
\dot{e}_{i,1}(t) &= e_{i,2}(t), \\
\dot{e}_{i,2}(t) &= -\begin{bmatrix} k_p & k_d \end{bmatrix} \begin{bmatrix} \hat{e}_{i,1}(t-\phi) \\ \hat{e}_{i,2}(t-\phi) \end{bmatrix} + a_{i-1}(t) - \hat{a}_{i-1}(t-\phi-\theta) - \left(1 - \frac{h}{\tau}\right)\left(a_i(t) - \hat{a}_i(t-\phi)\right), \\
\dot{\varepsilon}_i(t) &= \frac{1}{h} e_{i,2}(t) - \frac{1}{h}\varepsilon_i(t) + a_{i-1}(t), \qquad i \in S_I.
\end{aligned} \tag{E.11}$$

The disturbances $a_{i-1}(t) - \hat{a}_{i-1}(t-\phi-\theta)$, and $a_i(t) - \hat{a}_i(t-\phi)$ are smaller than for a-CACC, because the estimated acceleration stays ahead of the actual acceleration. To see this, use the Laplace transform of the vehicle dynamics (E.1), and acceleration observer (E.10), and choose $\hat{a}_i(0) = 0$, such that

$$\begin{aligned}
a_i(s) &= e^{-\phi s} \frac{1}{\tau s + 1} u_i(s) + \frac{\tau}{\tau s + 1} a_i(0), \\
\hat{a}_i(s) &= \frac{1}{\tau s + 1} u_i(s), \qquad i \in S_I.
\end{aligned} \tag{E.12}$$

Using (E.12), it is possible to compute $\mathcal{L}\{a_i(t) - \hat{a}_i(t-\phi)\}$

$$\tilde{x}_i(s) := \mathcal{L}\{a_i(t) - \hat{a}_i(t-\phi)\} = \frac{\tau}{\tau s + 1} a_i(0), \qquad i \in S_I. \tag{E.13}$$

Then, using the inverse Laplace-transformation gives

$$\begin{aligned}
\tilde{x}_i(t) = a_i(t) - \hat{a}_i(t-\phi) &= \mathcal{L}^{-1}\left\{\frac{\tau}{\tau s + 1} a_i(0)\right\}, \\
&= e^{-\frac{1}{\tau}t} a_i(0), \qquad i \in S_I.
\end{aligned} \tag{E.14}$$

Due to homogeneity of the platoon, it is possible to write

$$\begin{aligned}
a_{i-1}(t) - \hat{a}_{i-1}(t-\phi-\theta) &= a_{i-1}(t) - \hat{a}_{i-1}(t-\phi) + \hat{a}_{i-1}(t-\phi) - \hat{a}_{i-1}(t-\phi-\theta) \\
&= e^{-\frac{1}{\tau}t} a_{i-1}(0) + \hat{a}_{i-1}(t-\phi) - \hat{a}_{i-1}(t-\phi-\theta), \qquad i \in S_I,
\end{aligned} \tag{E.15}$$

where the first term converges to zero, and the other terms describe the difference of estimated acceleration at times $t-\phi$ and $t-\phi-\theta$, which are only θ apart.

Technische Universiteit **Eindhoven** University of Technology

Declaration concerning the TU/e Code of Scientific Conduct for the Master's thesis

I have read the TU/e Code of Scientific Conduct[i].

I hereby declare that my Master's thesis has been carried out in accordance with the rules of the TU/e Code of Scientific Conduct

Date

31-05-2020

Name

Max Balderman

ID-number

0895067

Signature

Submit the signed declaration to the student administration of your department.

[i] See: http://www.tue.nl/en/university/about-the-university/integrity/scientific-integrity/
The Netherlands Code of Conduct for Academic Practice of the VSNU can be found here also.
More information about scientific integrity is published on the websites of TU/e and VSNU